FEASIBILITY STUDY OF TiO_2 INTERMEDIATE COATING LAYER FOR ADHESIVE STRENGTH IMPROVEMENT

MUHAMMAD FIRDAUS BIN OTHMAN

FACULTY OF ENGINEERING

UNIVERSITY OF MALAYA

KUALA LUMPUR

2013

FEASIBILITY STUDY OF TiO_2 INTERMEDIATE COATING LAYER FOR ADHESIVE STRENGTH IMPROVEMENT

MUHAMMAD FIRDAUS BIN OTHMAN

DISSERTATION SUBMITTED IN FULFILMENT OF THE REQUIREMENTS FOR THE DEGREE OF MASTER OF ENGINEERING

FACULTY OF ENGINEERING

UNIVERSITY OF MALAYA

KUALA LUMPUR

2013

UNIVERSITY OF MALAYA

ORIGINAL LITERARY WORK DECLARATION

Name of Candidate:	**Muhammad Firdaus bin Othman**
Registration/Matric No:	**KGG110002**
Name of Degree:	**Master of Engineering (Material Engineering and Technology)**
Title Thesis:	**FEASIBILITY STUDY OF TiO_2 INTERMEDIATE COATING LAYER FOR ADHESIVE STRENGTH IMPROVEMENT**
Field of Study:	**Coating Technology**

I do solemnly and sincerely declare that:

(1) I am the sole author/writer of this Work;
(2) This Work is original;
(3) Any use of any work in which copyright exists was done by way of fair dealing and for permitted purposes and any excerpt or extract from, or reference to or reproduction of any copyright work has been disclosed expressly and sufficiently and the title of the Work and its authorship have been acknowledged in this Work;
(4) I do not have any actual knowledge nor do I ought reasonably to know that the making of this work constitutes an infringement of any copyright work;
(5) I hereby assign all and every rights in the copyright to this Work to the University of Malaya ("UM"), who henceforth shall be owner of the copyright in this Work and that any reproduction or use in any form or by any means whatsoever is prohibited without the written consent of UM having been first had and obtained;
(6) I am fully aware that if in the course of making this Work I have infringed any copyright whether intentionally or otherwise, I may be subject to legal action or any other action as may be determined by UM.

Candidate's Signature Date

Subscribed and solemnly declared before,

Witness's Signature Date
Name:
Designation:

ABSTRACT

The effects of intermediate TiO_2 coating layer on the adhesion strength improvement of TiN coating were studied. Ti/TiO_2/TiN coatings were deposited by D.C magnetron sputtering on high speed steel (HSS) and stainless steel (SS) substrates. A series of dense and uniform coating films, 844.1 – 926.4 nm thickness, were deposited at discharge power of 150 W and substrate temperature ranging from 50 to 250 °C. The duration time for depositing Ti coating layer was 2400 s and for TiN and TiO_2 coating layer were 3600 s each. The as-deposited coating films were heat treated (annealed) for 1 hour at 400, 500 and 600 °C. The adhesion strength of Ti/TiO_2/TiN coatings were evaluated by scratch testing and the coating hardness values were measured using micro-hardness tester. X-ray diffraction (XRD) analysis revealed anatase TiO_2 phase. The results from the scratch test discovered that Ti/TiO_2/TiN coating exhibits higher adhesion strength compared to Ti/TiN and single layer TiN coating. The maximum adhesion strength of 1417.19 mN was observed for Ti/TiO_2/TiN coating deposited on HSS substrate. It is also observed that Ti/TiO_2/TiN coatings deposited at higher deposition temperature exhibits higher values of critical load. The adhesion strength of Ti/TiO_2/TiN coating also increases as the TiO_2 coating thickness increases. The adhesion strength of Ti/TiO_2/TiN coating deposited on HSS decreases with the increases of substrate surface roughness. It was also observed that annealing Ti/TiO_2/TiN coating at 500 °C yielded highest adhesion strength and coating hardness. The annealed coating at 600 °C revealed film delamination and exhibited lowest adhesion strength.

ABSTRAK

Kajian terhadap kesan penambahan lapisan salutan TiO_2 keatas peningkatan kekuatan lekatan lapisan TiN telah dijalankan. Lapisan Ti/TiO2/TiN dideposit keatas permukaan keluli berkelajuan tinggi (HSS) dan keluli tahan karat (SS) dengan menggunakan kaedah “DC magnetron sputtering”. Lapisan Ti/TiO_2/TiN berketebalan 844.1 – 926.4 nm dihasilkan pada kuasa D.C 150 W dan suhu substrat antara 50 sehingga 250 °C. Tempoh masa untuk penghasilan lapisan Ti adalah 2400 s dan untuk lapisan TiN dan lapisan TiO_2 adalah 3600 s setiap lapisan. Lapisan Ti/TiO_2/TiN yang dihasilkan turut menjalani rawatan haba selama 1 jam pada suhu 400, 500 dan 600 °C. Kekuatan lekatan salutan Ti/TiO_2/TiN telah dinilai dengan ujian “scratch” dan kekerasan lapisan salutan diukur dengan menggunakan mesin “micro-hardness”. Analisis Pembelauan sinar-X (XRD) menunjukkan lapisan Ti/TiO_2/TiN mengandungi ‘anatase’ TiO_2. Keputusan daripada ujian ‘scratch’ mendapati bahawa lapisan Ti/TiO_2/TiN mempamerkan kekuatan lekatan yang lebih tinggi berbanding dengan lapisan Ti/ TiN dan lapisan salutan TiN. Kekuatan lekatan maksimum 1417.19 mN diperolehi untuk lapisan Ti/TiO_2/TiN keatas substrat HSS. Lapisan Ti/TiO_2/TiN yang telah menjalani rawatan haba juga didapati mempamerkan kekuatan lekatan yang lebih tinggi. Kekuatan lekatan salutan Ti/TiO_2/TiN juga menunjukkan peningkatan apabila ketebalan salutan TiO_2 meningkat. Kekuatan lekatan salutan Ti/TiO_2/TiN diatas permukaan HSS berkurangan dengan peningkatan kekasaran permukaan HSS. Ia juga didapati bahawa rawatan haba keatas lapisan Ti/TiO_2/TiN pada suhu 500 °C menghasilkan kekuatan lekatan dan kekerasan lapisan yang paling tinggi. Rawatan haba keatas lapisan Ti/TiO_2/TiN pada suhu 600 °C menyebabkan lapisan filem tertanggal dan mempamerkan kekuatan lekatan terendah.

ACKNOWLEDGEMENT

First of all, the author would like to express his gratefulness to Dr. Bushroa Binti Abdul Razak for the supervision and guidance throughout the duration of the project. The author also would like to thanks AMMP staffs for their helps and advices. The author would like to thank IPPP UM for the necessary funds under project number PG121-2012B.

The author would like to thank lab technicians in Mechanical engineering department, especially Mrs. Hartini and Mr. Zaman for their support and valuable inputs.

Finally, the author is most grateful to his beloved mother, Jamaliah Osman for her love and care over the years. The author also thanks his lovely wife for the support and encouragement to finish the project. Lastly, the author would like to thank to those who offered assistance and help to him but unintentionally failed to mention.

CONTENTS

	Page
ORIGINAL LITERARY WORK DECLARATION	ii
ABSTRACT	iii
ABSTRAK	iv
ACKNOWLEDGEMENTS	v
CONTENTS	vi
LIST OF FIGURES	ix
LIST OF TABLES	xiv
CHAPTER 1: INTRODUCTION	
1.1 Introduction	1
1.2 Research Objectives	4
1.3 Research Outline	5
CHAPTER 2: LITERATURE REVIEW	
2.0 Introduction	6
2.1 Microstructures and adhesions of TiN coating	7
2.2 Mechanism of failure	12
2.3 Adhesion evaluation techniques	17
2.3.1 Indentation test	18
2.3.2 Laser spallation technique	21

Page

2.3.3 Scratch test 23

2.3.4 Energy description model 30

2.4 Improvement of TiN adhesion strength 32

CHAPTER 3: METHODOLOGY

3.0 Overview 36

3.1 Target preparation 36

3.2 Substrate preparation 37

3.3 Deposition process 38

3.3.1 The study of adhesion strength improvement of TiN coating by implementing Ti and TiO_2 as the interlayer. 41

3.3.2 The effect of deposition temperature on the adhesion strength of Ti/TiO_2/TiN coatings. 43

3.3.3 The effect of TiO_2 coating thickness on the adhesion strength of Ti/TiO_2/TiN coatings. 43

3.3.4 The effect of substrate surface condition on the adhesion strength of Ti/TiO_2/TiN coatings. 44

3.3.5 The effect of annealing on the mechanical properties of the substrate coating systems. 44

3.4 Evaluation and characterization

3.4.1 Film thickness 45

Page

3.4.2 Adhesion strength evaluation 49

3.4.3 Coating hardness 50

3.4.4 Morphology and chemical composition evaluation 51

CHAPTER 4: RESULTS

4.1 The effect of implementing Ti and TiO_2 as interlayer on adhesion strength improvement of TiN coating.

4.1.1 Structure and composition 53

4.1.2 Film thickness, adhesion strength and coating hardness 59

4.2 The effect of sputtering parameter on the Ti/TiO_2/TiN adhesion strength. 67

4.3 The effect of annealing on the mechanical properties of the substrate coating systems. 72

CHAPTER 5: DISCUSSIONS

5.1 The effect of implementing Ti and TiO_2 as interlayer on adhesion strength improvement of TiN coating. 76

5.2 The effect of sputtering parameter on the Ti/TiO_2/TiN adhesion strength. 80

5.3 The effect of annealing on the mechanical properties of the substrate coating systems. 81

CHAPTER 6: CONCLUSIONS AND RECOMMENDATIONS

6.1 Conclusions 82

6.2 Recommendations 83

REFERENCES 84

LIST OF FIGURES

Page

Figure 2.1: SEM micrograph of TiN coatings PVD TiN coating 8

Figure 2.2: Critical loads results against coating thickness for four different substrates hardness. 11

Figure 2.3: SEM and sketch illustration of different mode of failure: (i) brittle failure modes; (ii) ductile failure modes. 15

Figure 2.4: Schematic illustration of coating failures observed during scratch testing. 17

Figure 2.5: Schematic representation of the indentation coating adhesion test. 19

Figure 2.6: Plot of crack size, a vs. load, kg of series of indents made at different loads. 20

Figure 2.7: Fracture pattern of TiN coating as function of normal load, W and coating thickness, t as observed during the indentation test 21

Figure 2.8: Basic laser spallation set up. 23

Figure 2.9: The three main scratch modes are constant load, progressive load, and incremental load. 24

Figure 2.10: Typical scratch test data for a progressive load scratch on coated steel sample, showing the critical failure points Lc1 and Lc2. 25

Figure 2.11: Plot of acoustic emission vs. scratch distance produced from the scratch test. 26

Page

Figure 2.12: Schematic representation of scratch test apparatus used by Valli et al. (1985). 29

Figure 2.13: Acoustic and tangential friction force results obtained from scratch test of titanium nitride (TiN) coating on high speed steel substrate. (a) thick coating (b) thinner coating. 29

Figure 2.14: Adhesion strength of TiO_2, TiN, TiO_2/TiN, TiO_2/Ti/TiN and TiO_2-Ti-TiN coating deposited at room temperature, 300^0C and 400^0C. 35

Figure 3.1: Titanium target used during deposition. 37

Figure 3.2: Substrates used in the analysis (a) On the left SS and; (b) On the right HSS. 38

Figure 3.3: Schematic view of TiN/TiO_2/Ti coating system. 38

Figure 3.4: Schematic diagram of the positioning of the target and substrates during sputtering process (a) Front view of the sputtering chamber and (b) Top view of the sputtering chamber. 39

Figure 3.5: TF450 PVD magnetron sputtering system (SG Control Engineering PTE LTD, Singapore) equipped with Protec Instruments PC-500 Flow Controller. 40

Figure 3.6: Heat treatment curve during annealing treatment of deposited substrate. 45

Figure 3.7: HSS coated sample for coating thickness evaluation. 46

Figure 3.8: An image of a micro-scratch system 46

Page

Figure 3.9: A schematic diagram of a typical scratch test. 47

Figure 3.10: Coating topography scan of $Ti/TiO_2/TiN$ coating on HSS substrate 47

Figure 3.11: Cross-section with 2 µm depth created using FiB. 48

Figure 3.12: Measured values of coating layer thickness of $Ti/TiO_2/TiN$ coatings. 49

Figure 3.13: Scratch profile of TiN coating deposited onto HSS substrate and the scratch track observed using optical microscope. 50

Figure 3.14: (a) Shimadzu Microhardness tester HMV-2; (b) Indentation image using Vickers indenter at 1.961 N (HV0.2) on HSS substrate 51

Figure 4.1: X-ray diffraction pattern of $Ti/TiO_2/TiN$ samples deposited on HSS and SS substrates. 54

Figure 4.2: EDX spectrum of $Ti/TiO_2/TiN$ coating deposited onto (a) HSS and; (b) SS substrates. 55

Figure 4.3: Atomic percentage of Titanium (Ti), Nitrogen (N) and Oxygen (O) along with Ferum (Fe) for both coated HSS and SS substrates. 56

Figure 4.4: Optical microscope image of coating films deposited on high speed steel (HSS) (a) TiN coating; (b) Ti/TiN coating and; (c) $Ti/TiO_2/TiN$ coating. 57

Figure 4.5: Field emission scanning electron microscope (FESEM) images of $Ti/TiO_2/TiN$ coatings on high speed steel (HSS) and stainless steel (SS) substrates at deposition temperature of 200^0C and DC power of 58

150 kW; (a) and (b) Ti/TiO_2/TiN deposited onto HSS substrate and; (c) and (d) Ti/TiO_2/TiN coatings deposited onto SS substrate.

Figure 4.6: FESEM cross section of Ti/TiO_2/TiN coated HSS samples. 58

Figure 4.7: FiB images of samples cross-section and coating thickness measured for (a) Ti coating; (b) Ti/TiN coating and; (c) TiO_2 coating. 60

Figure 4.8: Adhesion strength of TiN, Ti/TiN and Ti/TiO_2/TiN coatings deposited onto HSS and SS at deposition temperature 200^0C and D.C power of 150 W. 62

Figure 4.9: Scratch tracks of as-deposited coatings on HSS and SS substrates; (a) TiN-HSS coatings; (b) Ti/TiN-HSS coatings; (c) Ti/TiO_2/TiN-HSS coatings; (d) TiN-SS coatings; (e) Ti/TiN-SS coatings and; (f) Ti/TiO_2/TiN-SS coatings. 63

Figure 4.10: Scratch tracks of as-deposited Ti/TiN/TiO_2 on HSS and SS substrates at higher magnification; (a) Ti/TiO_2/TiN on HSS and; (b) Ti/TiO_2/TiN on SS substrate. 64

Figure 4.11: Schematic illustration of coating failures observed during scratch testing of Ti/TiO_2/TiN coatings on HSS and SS substrate. 64

Figure 4.12: Hardness values of HSS and SS substrates and composite hardness of coating deposited at deposition temperature of 200^0C measured using Shimadzu Microhardness tester HMV2 65

Figure 4.13: Adhesion strength of Ti/TiO_2/TiN coating deposited on HSS and SS substrate at substrate temperature of 50^0C, 200^0C and 250^0C. 68

Page

Figure 4.14: Hardness values of HSS and SS substrates and composite hardness of coating deposited at different deposition temperature. 69

Figure 4.15: Critical loads and hardness of Ti/TiO_2/TiN coating deposited at 200^0C for different TiO_2 coating thickness; (a) HSS substrate and; (b) SS substrate. 70

Figure 4.16: Critical loads and hardness of Ti/TiO_2/TiN coating deposited at 200^0C on HSS substrate for different substrate surface condition (surface roughness). 72

Figure 4.17: FESEM image (top view) of Ti/TiO_2/TiN coatings deposited on HSS substrate after annealing at; (a) as-deposited; (b) 400^0C; (c) 500^0C and; (d) 600^0C. 73

Figure 4.18: XRD patterns of as-deposited and annealed Ti/TiO_2/TiN coatings deposited on HSS substrates. 74

Figure 4.19: Atomic percentages of Ti, N and O in the Ti/TiO_2/TiN coatings after annealing treatment at different anneal temperatures. 75

Figure 4.20: Critical loads and hardness values for as-deposited Ti/TiO_2/TiN coating and coating samples after annealing at 400^0C, 500^0C and 600^0C. 75

LIST OF TABLES

Page

Table 2.1: Critical loads values measured PVD TiN coating (2 μm) deposited onto high speed steel substrates having different surface roughness prior to coating treatment. 12

Table 2.2: Failure modes of thin film deposited onto different substrates. 14

Table 2.3: Available methods for coating adhesions evaluation. 18

Table 2.4: Calculated work, W of adhesion for selected material. 31

Table 3.1: Sputtering parameters and setting values. 41

Table 3.2: Summary of coating samples deposited for the analysis and the total deposition time. 42

Table 3.3: TiO_2 deposition time for Ti/TiO_2/TiN coatings deposited on HSS and SS substrates. 43

Table 3.4: Surface roughness of HSS substrate used. 44

Table 4.1: Total coating thickness measured from topography mode using micro-scratch system. 60

Table 4.2: Summary of the Ti, TiN and TiO_2 coating layer thickness measured using FiB technique. 61

Table 4.3: Critical load values for TiN, Ti/TiN and Ti/TiO_2/TiN as-deposited coatings. 62

Table 4.4: Internal stresses, σ of TiN coating layers estimated from lattice spacing and Young`s moduli for TiN, Ti/TiN and Ti/TiO_2/TiN. 66

Table 4.5: Measured surface roughness, Ra of HSS substrate. 71

CHAPTER 1

INTRODUCTION

1.1 Introduction

In advance applications of engineering materials, coatings are implemented purposely to improve the mechanical properties and durability of the materials. Such coating usually applied to the surface of industrial materials which are subjected to severe working conditions. Coatings are used to reduce the amount of friction between the materials, to improve the hardness of the substrates, to minimize the wear and to increase the corrosion resistance of the materials. Coatings are usually implemented on steel-metal working tools, high speed steel drills and mills and also on machine parts such as ball bearings. Hard coatings such as titanium (Ti) and titanium nitride (TiN) are deposited onto steels and glass substrates purposely to introduce hardness and to improve the wear resistance of the substrates.

TiN has been used as coating materials for tools steel due to its noble appearance, good adhesion to substrates, high chemical inertness, resistance to elevated temperatures, hard surfaces (2400 HV) to reduce abrasive wear, a low coefficient of friction with most work piece materials which increases lubricity and results in excellent surface finish. The used of TiN coatings onto cutting tool have increase the tool life. Study by Zhang and Zhu (1993) has reported on the improvement over 1000% in tool life for TiN coated drill bit which are used for stainless steel work pieces. Another study by Neimi et al. (1986) on the wear characteristic and properties of TiN coated gear cutting hobs showed that TiN coating reduced the wear of the hobs significantly, even though at 25% and 50% increased cutting speeds as compared to the uncoated hobs were used.

Furthermore, TiN coatings also have been used for corrosion protection for steel mostly for cutting tools. Due to its superior mechanical properties and corrosion resistance, TiN coating often used on steel substrates to protect from deteriorating environment and hence increase the service life and increase the commercial value of the products. The studies on corrosion behavior of TiN coating have been done by Chou et al. (2001).

In general, coating materials can be deposited by various techniques including chemical vapor deposition (CVD), physical vapor deposition (PVD), physical vapor chemical deposition (PCVD), plasma sprayed, sol gel technique, electroplating and salt bath immersion. PVD methods involved purely physical process to deposit materials onto a substrate by high temperature vacuum evaporation and condensation, or plasma sputter bombardment. Other type of PVD methods included electron beam physical vapor deposition, evaporative deposition, pulse laser deposition and sputter deposition. CVD methods involved chemical reactions to deposit materials onto a substrate.

TiN coating films are usually deposited onto cutting tools by physical vapor deposition (PVD) method. During PVD process, the substrate to be coated is placed in a vacuum chamber and is heated to a temperature between 400^0C and 600^0C. The coating material, Ti is vaporized and the reactive gas is introduced and ionized. TiN compound is formed and deposited onto a substrate resulting from the reaction of vaporized Ti atoms and the ionized nitrogen (Zhang and Zhu, 1993).

The studies on the TiN coatings have been done intensively in last few decades. Microstructures and mechanical properties of TiN coatings were studied for suitability for an application and also for improvements. Failure modes and mechanisms of TiN coating were also studied for better understanding of TiN coatings properties.

The expected performances or properties of the coated product can only be achieved provided that the adhesive and the intrinsic cohesion of the coating are sufficient. The adhesion strength between the substrate and coating must be sufficient enough to avoid failure at the interface and to display the desired advantages. Adhesion strength is defined as a measure of the resistance of a coating to debonding or spalling, which may result from abrasive contact with small hard particles or asperities (Laugier, 1987).

The scratch test has been widely used as the technique to evaluate the adhesion of coating since its introduction in 1950 by Heavens (Laugier, 1981). In this method, a loaded probe with a smoothly rounded point (stylus) is drawn across the coating surface and the load is progressively increased until the removal of the coating occurs. Since it's introductory, improvements have been done by previous researcher on the scratch testing for improve accuracy in measuring adhesion strength.

Good adhesion properties can be achieved by one of the following three mechanisms; (i) intermediate phase formation, (ii) new bonding configurations at the interface, (iii) lowering off the interfacial energy between the material. The adhesion strength of TiN coating system can be increases by the inclusion of other metallic coating layer such as Ti deposited in between TiN coating layer and a substrate. Helmersson et al. (1985), in their study of adhesion of titanium nitride coatings on high-speed steels have proved the beneficial effect of Ti interlayer on the adhesion of coatings. The use of an intermediate layer of pure titanium increases the adhesion for TiN films deposited. Gerth and Wiklund (2008) also performed a study on the improvement of TiN adhesion strength by analyzing metallic coating as interlayer. Their study claimed that adhesion of TiN coating improved with the used of Ti and Cr interlayer.

To enhance the adhesion of coatings deposited by PVD process, it is a promising technique to use an interface layer. An interface layer is considered as a mixing of transition layers. Both chemical and mechanical bonding between coating layers are expected to be improved by having composition change in the interface transition region (Kusano et al., 1998a).

There is also possibility of using oxide metal as the intermediate layer for adhesion strength improvement. The metal oxide layer may enhance the adhesion strength by creating strong intermediate or inter diffusion layer at coating layer interfaces. The adhesion strengths of TiN coating are expected to increase with the presence of Ti and TiO_2 interlayer coatings.

On the basis of this hypothesis, the present of both Ti and TiO_2 coating layers in existing TiN coating may improve the adhesion strength by forming strong bonds at the interface. For example, by having Ti/TiO_2/TiN compositional gradient coatings instead of Ti/TiN or TiN coating alone are expected to provide better adhesion strength.

1.2 Research Objectives

The objective and aims of the study are as follows;

i. To improve the adhesion strength of TiN coating by implementing Ti and TiO_2 as the interlayer.
ii. To analyze the effects of substrate temperature on the adhesion strengths of the coating systems.
iii. To investigate the contributions of TiO_2 coating thickness on the adhesion strength of the coating systems.
iv. To investigate the effects of different substrate pretreatment methods (surface roughness) on the adhesion strength.

v. To analyze the effects of annealing on the mechanical properties of the substrate coating systems.

1.3 Research Outline

In the present study, Ti/TiO_2/TiN coatings were produced by using D.C magnetron sputtering method. Each coating layers were deposited in sequences. Ti coating layer was deposited first followed by TiO_2 coating and lastly TiN coating layer. Substrates used for the study were high speed steel (HSS) and stainless steel (SS). Investigations of the produced Ti/TiO_2/TiN coatings were conducted by several methods. The mechanical properties of the coating were evaluated in terms of adhesion strength by applying micro-scratch test and coating hardness by micro-hardness tester. Field emission scanning electron microscopy (FESEM), an optical microscope and X-ray diffraction analysis were used to observe surface morphologies and to determine phase composition of Ti/TiO_2/TiN coatings, respectively. Energy dispersive X-ray spectroscopy (EDX) was used for qualitative determination of the elements which are present on the sample surface.

CHAPTER 2

LITERATURE REVIEW

2.0 Introduction

The studies on the coating/substrate systems have been performed and developed since 1950's with the works on single layer of coatings deposited onto numbers of different substrates such as steels and glasses concentrating on the improvement of the mechanical properties and the adhesion strength (Laugier, 1981). The trends were progressed with the study of multilayer coating and the effect on the adhesion strength of the substrate-coating systems (Wang et al., 1995; Helmersson et al., 1985; Valli et al., 1985; Gerth and Wiklund, 2008; Kusano et al., 1998b). More recently, works on the new development of new coating materials and new method of adhesion strength evaluations have been conducted (Jaworski et al., 2008; Gupta et al., 1992; Wang et al., 2004). Studies on the effectiveness of the coatings on the substrates have been done intensively to analyze the performance of the coatings and the problems that might be associated with specific type of coating and substrate systems (Stebut et al., 1989; Bull, 1991).

This particular study will concentrate on the adhesion strength improvement of titanium nitride (TiN) coating by depositing titanium (Ti) and titanium dioxide (TiO_2) interlayer for adhesion enhancement. TiN coating are often employed for improving tribology performance of tools and machine parts in industrial applications due to their mechanical properties including high hardness and high wear resistance. The coatings must adhere well to the substrates in order to achieve the desired performance.

The inclusion of Ti interlayer has proven to increase the adhesion strength of TiN coatings system. Helmersson et al. (1985), in their study of adhesion of titanium nitride coatings on high-speed steels proved the beneficial effect of Ti interlayer on the adhesion of TiN-HSS coating substrate system. Perry (1983) also reported on the interlayer coating which can be utilized on adhesion strength improvement. A metallic interlayer of titanium is most effective on titanium alloy steel and oxide or nitrides containing interlayer are effective on steel or super alloy.

This chapter will provide comprehensive review on the coating deposition techniques available and method which will be used in this particular study. The methods used to evaluate the adhesion strengths, namely; the indentation test, laser spallation technique and scratch test are also reviewed. Adhesion strengths of TiN coatings as well as the failure modes and mechanisms of coating failure will also be reviewed. Factors which affect the adhesion strength of coating-substrate systems will also be discussed.

2.1 Microstructures and adhesions of TiN coating

For tooling applications, the most important properties of the coatings require are the coating thickness, density, hardness, adhesion, temperature resistance, wear, corrosion and oxidation resistance. TiN coatings are widely used in cutting tools and wear parts due to high hardness and strength, high wear resistance a well as high temperature stability (Laugier, 1987).

The coating thickness of TiN film on tool steels is generally between 2 and 10 μm. The PVD TiN coatings are thinner between 3 to 5 μm (Zhang and Zhu, 1993). The TiN coating hardness apparently increases with increasing film thickness (Chou, 2002). Thus, thicker coating thickness may provide longer tool life.

The microstructures of TiN coatings are depends on the deposition process. TiN films deposited by the PVD method can be characterized as being entirely columnar, with grains generally extending through the coating thickness (Laugier, 1987).

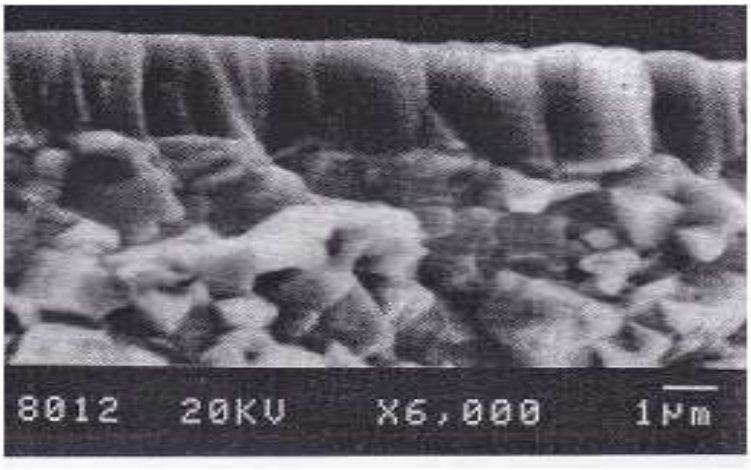

Figure 2.1: SEM micrograph of TiN coatings PVD TiN coating (Laugier, 1987).

Figure 2.1 shows the microstructure of TiN coating deposited on cemented carbide substrates by PVD method showing the columnar structures of the coating with the grains extending through the coating thickness.

The adhesion strength of the PVD coating was significantly poor compared to coating deposited by other method such as CVD. The PVD coating tended to spall suddenly at critical load of 1.2 kgf. The poorer adhesion strength of PVD TiN coating can be explained probably due to columnar morphology which in turn resulting in low toughness and also no interfacial bonding layer are observed in the coating. The adhesion strength of a coating depends on both chemical and physical interaction between the coating and the substrate materials and also the microstructure of the interface region. Poor adhesion of coatings may be attributed to the low degree of chemical bonding and poor interfacial contact between the coating and substrates.

The adhesion strengths of coating-substrate system usually represented by the values of critical load measured by scratch testing. The critical load depends on several parameters

related to the testing conditions and to the coating-substrate system. Juhani Valli and Mäkelä (1987) discussed on the factors affecting scratch test results in their work on TiN coated HSS which are surface roughness as well as friction between coating and indenter. For substrate surface roughness, the surface roughness should not exceed 0.25 μm in order to eliminate the effect on the scratch test results. Poor surface finish decrease the critical normal force, showing worse adhesion value compared to polished surface. Their works also mentioned on the influence of lubricants on the critical normal forces. The use of a thin ion-plated silver overlay will increase the critical normal force remarkably and also enhance the repeatability of the testing.

Perry (1993) reported on the effect of coating thickness and the substrate hardness of the TiN coatings deposited onto steels and cemented carbides by ion-plating PVD method. Their observations show that the critical load increases with both increasing coating thickness and increasing substrate hardness. For hard coatings deposited onto steel, the critical value of TiN coating increases with the coating thickness up to certain thickness value. At larger thickness, the critical loads may become constant, independent of the coating thickness. In contrast, for hard coating deposited onto cemented carbide, the critical loads are nearly independent of coating thickness.

In contrast, Chopra (1969), in his work on the adhesive strengths of gold deposited onto glass and other substrates by sputtering and evaporation observed that the critical loads applied during scratch test increased rapidly with increasing coating thickness and with increasing substrate hardness. The increases in the critical load as the substrate hardness increases can be explained by the amount of load required to plastically deform tougher substrates increases compare with soft substrate. Softer substrates can easily plastically deform and there is a sharp change in the shear stress distribution at the coating substrate interface. As the substrate become tougher, the shear stress at the interface is less at the same stylus load.

Helmersson et al. (1985) studied the effect of substrate temperature and pretreatment on the adhesion of TiN coatings. The adhesion of the films increased with substrate temperature, reaching a maximum between 400 and 500 °C. Substrate pretreatment such as sputter etching prior to deposition also improves the film adhesion even though a complete removal of the oxide layer is not achieved.

Steinmann and Hintermann (1985) also confirmed the work done in other studies on the effects of hardness of the substrates and coating thickness on the critical load of the coating-substrate system. Their work confirmed on the linear relationship between critical load and substrate hardness as shown in Figure 2.2. From the figure, it can be seen that as the coating thickness increases, the value of the critical load increases in linearly fashion. The hardened and tempered samples show higher value of critical loads compared to annealed sample. Higher adhesion strength between coating and substrate can be achieved by using substrate with high hardness.

Schulz et al. (1991) demonstrated on the influence of alternating sequences of heating and deposition on the coating adhesion. Using an electron beam, a localized heat treatment of the sample can be applied whereby the heating rate and final temperature can be chosen over a wide range. The growth and stoichiometry of the coatings can be influenced by alternating sequences of heating and deposition. Preheating prior to deposition process might well increase the adhesion of coating.

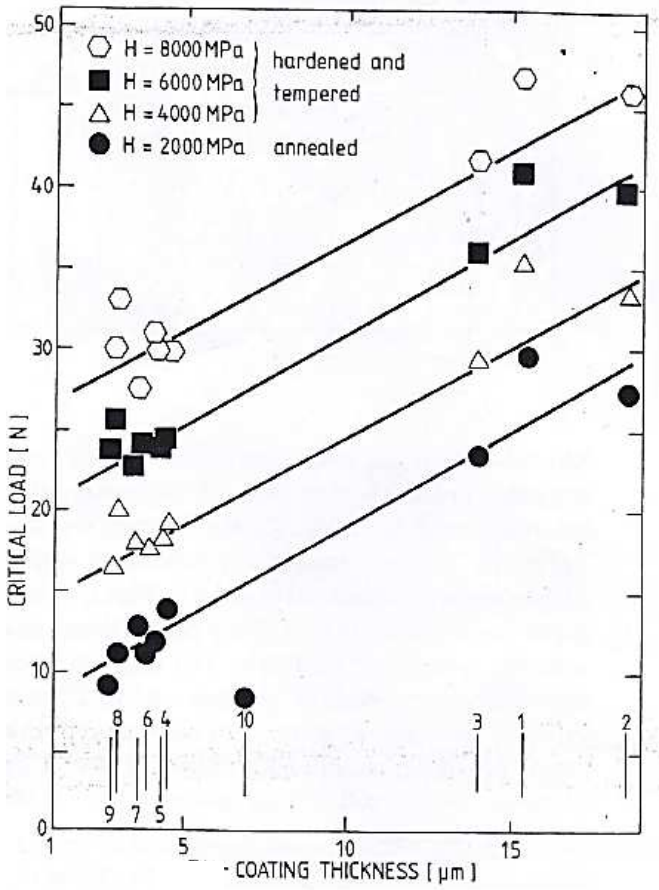

Figure 2.2: Critical loads results against coating thickness for four different substrates hardness (Steinmann and Hintermann, 1985).

Other factor that might contribute on the adhesion strength of the coating is the influence of the substrate roughness prior to coating deposition. Steinmann et al. (1987) suggested that the critical load of the coating depends on the substrate roughness. Table 2.1 summarized the values of critical load of TiN coating deposited onto HSS substrate with different surface roughness prior to coating process. The critical values of TiN coating clearly dependence on the substrate surface roughness. Substrates with smooth contact surface with average roughness less than 0.1 µm tend to produce higher adhesion to the coating. It is believed that although all the substrates were coated during the same treatment, the adhesive properties can vary since the efficiency of the cleaning operation is influenced by the surface roughness.

Table 2.1: Critical loads values measured PVD TiN coating (2 μm) deposited onto high speed steel substrates having different surface roughness prior to coating treatment.(Steinmann et al., 1987).

Sample	Surface preparation	Average roughness, R_a (μm)	Total roughness R_t (μm)	Critical load (N)
1	Polishing (600 grit paper)	0.03	0.40	56
2	Rectification	0.05	1.00	56
3	Polishing (alumina)	0.07	0.60	54
4	Shot peenin	0.40	4.65	40
5	Milling	1.75	12.5	27
6	Shot blasting	7.00	70.0	13

2.2 Mechanism of failure

The study of the mechanisms and modes of failure are essential in order to understand the behavior of the coating system under certain loading conditions. Brittle coatings behave in different manner compared with ductile coating deposited on the same substrates when subjected to a loading condition in scratch test. Perry (1983) reported on the mechanisms of coating failure for brittle and ductile coatings where the brittle films can be remove completely but ductile film subjected to gradually thinning (sideway extrusion).

Bull (1991) reported that TiN coatings deposited onto a range of different substrates from soft nickel to hard cemented carbide, summarized that the failure of coating-substrate systems fall into two general groups, depending on whether the substrates behave in brittle or ductile manner during scratch test.

Brittle failure modes in scratch testing can be classified into: (1) gross spallation; (2) spallation ahead of the indenter; (3) recovery spallation behind the indenter; (4) hertzian cracking and; (5) tensile cracking. Large area spallation or gross spallation occur when the adhesion is poor or if the residual stress level in the coating is high. Spallation is also another common failure mode in which the coating is detached to minimize the amount of elastic

energy stored by the large compressive stresses ahead of the moving stylus during scratch test. Hertzian ring cracks occur when the tensile radial stresses at the edge of the diamond contact generate a ring crack which propagates from the surface through the coating into the substrate. Several of these cracks intersect and cause a crack network along the edge of the crack track. Tensile cracks form from the cracks which form at the rear of diamond contact.

Ductile failure modes in scratch testing can be classified into: (1) spallation; (2) buckling; (3) conformal cracking and; (4) tensile cracking. The spallation and buckling modes are very similar to the spallation mode for brittle failure except the magnitude of failure is smaller and generally confined within scratch track. Conformal cracks occur when there is through-thickness cracking at the front and sides of the indenter. This is due to the partial ring cracks which occur ahead of the indenter and then passes over and pushed into scratch track. Tensile cracking occurs at the rear of diamond contact due to the tensile stress generated on sliding as observed for the brittle materials. Figure 2.3 shows the sketch and scanning electron microscope details on the brittle and ductile failure modes in scratch testing.

For ductile failure, the area of uncovered substrate is small and within the scratch track. For brittle failure the area is more extensive and often extends beyond the limit of the scratch track. Table 2.2 shows the failure mode of thin film deposited onto different substrate (ductile or brittle) depending whether the applied stresses are compressive or tensile. For ductile substrates, interface failure can occurs for both tensile and compressive stress provided that interfacial adhesion is poor. If adhesion is good, failure tends to occur within the coating. For brittle substrates, interface failure again can occur for both tensile and compressive stress if adhesion is poor and possibility of interfacial cracking for tensile stress.

Table 2.2: Failure modes of thin film deposited onto different substrates (Bull, 1991).

Stress	Film	Substrate	Interface bonding	Decohesion mechanism(s)
Tensile	Brittle	Ductile	Good	Film cracking (no decohesion)
			Poor	Film cracking (interface decohesion)
Compressive	Brittle	Ductile	Good	Buckling propagation in film
			Poor	Buckling propagation at interface
Tensile	Brittle	Brittle	Good	Film cracking and interface decohesion
			Poor	Edge decohesion at interface
Compressive	Brittle	Brittle	Good	Substrate splitting
			Poor	Buckling propagation at interface

There are also some other works conducted on thin film coating to study the failure mode of thin coating. Hedenqvist et al. (1990) studied the failure mode of TiN coating on high speed steel. Failure mode of TiN coatings were studied based on scratch tests performed on a TiN coated on high speed steel substrates with various coating thickness and substrate hardness. In their report, four groups of coating damage and detachment mechanisms were recognized: (1) deformation; (2) crack formation; (3) chip formation and; (4) flaking. The scratch mechanisms were observed on two different conditions: scratch mechanisms below the critical normal force and above the critical normal force. At normal force value which is close to zero, no visible surface damage observed due to elastic deformation of the coating substrate system. With increasing normal force, the plastic deformation extends through the coating into the substrate. The degree of plastic deformation increases with increasing normal force.

During scratching, transverse surface cracks were often observed due to tensile stresses generated behind the moving diamond tips which then resulting in internal transverse cracking. Internal transverse cracks increase with increasing normal force. External transverse cracking may also appear at higher normal force values.

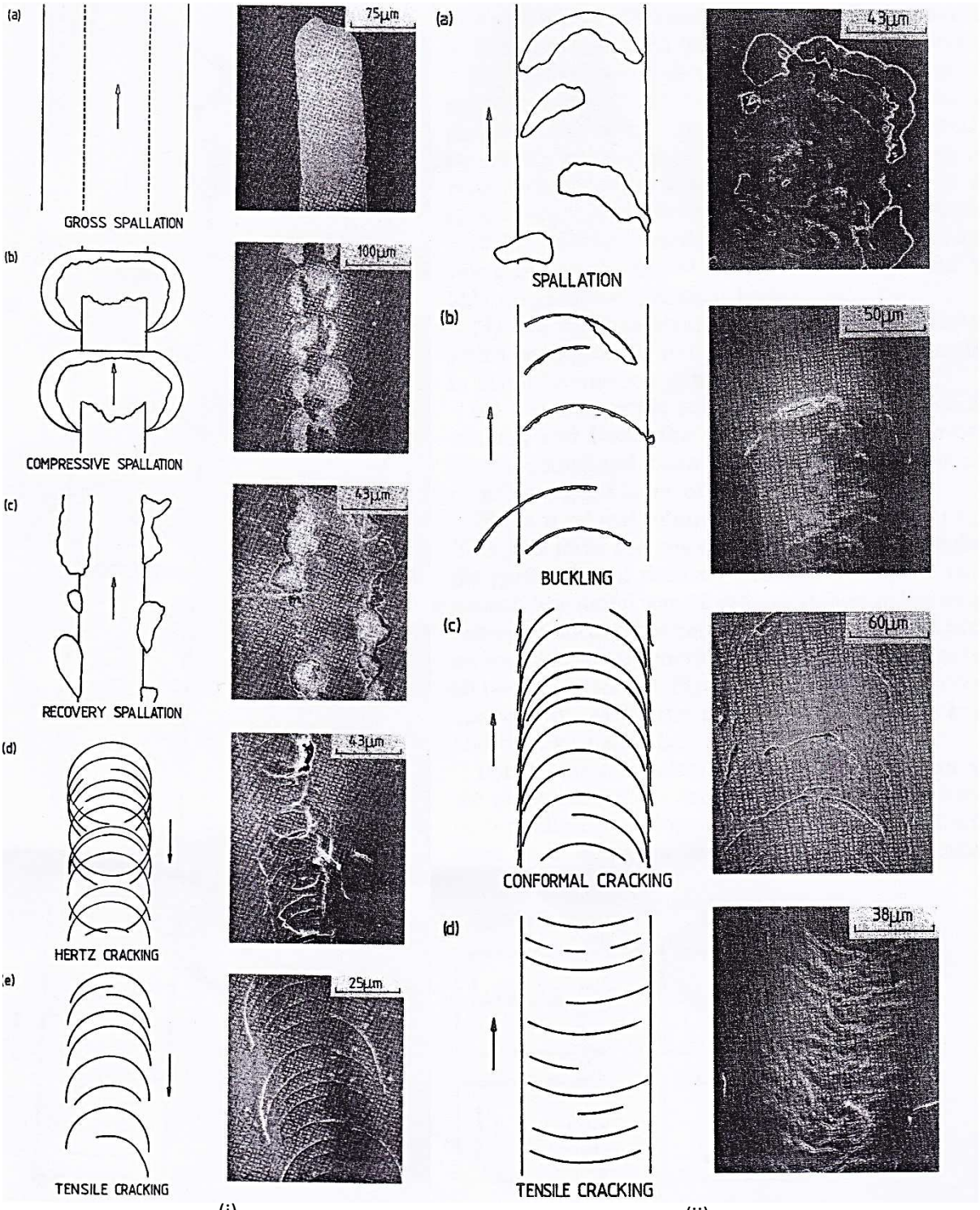

Figure 2.3: SEM and sketch illustration of different mode of failure: (i) brittle failure modes; (ii) ductile failure modes (Bull, 1991).

Above the critical normal force, chip formation and flaking occurred. The substrate material is being exposed in the scratch bottom by a discontinuous chip removal mechanism. The

detached chips consist of heavily deformed coating-substrate materials. Flaking predominantly occurs outside the scratch track due to high frictional force values.

Similar work has been done by Stebut et al. (1989) on major damage mechanism during scratch testing of TiN coated high speed steel substrate. Scratch testing damage starts by tensile type cracking nucleation behind the trailing edge of diamond indenter. Tensile type crack pattern include partial ring crack prior to spalling and envelope cracks parallel to sliding direction. However, for hard coatings on hard substrates, no conformal cracking generated ahead of the indenter leading edge are observed which is contradicted to Bull (1991) findings where conformal cracking is the major spalling initiator.

Larsson et al. (2000) also studied the mechanism of coating failure as demonstrated by scratch and indentation testing of TiN coated high speed steel. During scratch test, six different coating failure mechanisms could be identified (see Figure 2.4): (1) cracks parallel with the scratch channel; (2) semicircular cracks within the scratch channel; (3) external transverse cracks; (4) cohesive chipping; (5) adhesive spalling and; (6) complete breakthrough of the coating within the scratch channel. During indentation, there are four different type of coating failures which have been distinguished: (1) circular crack within the indentation; (2) radial cracks outside the indentation; (3) cohesive chipping and; (4) adhesive spalling. The mechanism of parallel cracking in scratch testing is due to deflection of the coating into the physically deformed underlying substrate material. External transverse cracking initiated during or after unloading due to high residual stresses generated in the coating. The cohesive and adhesive coating failures occur during unloading behind the diamond stylus.

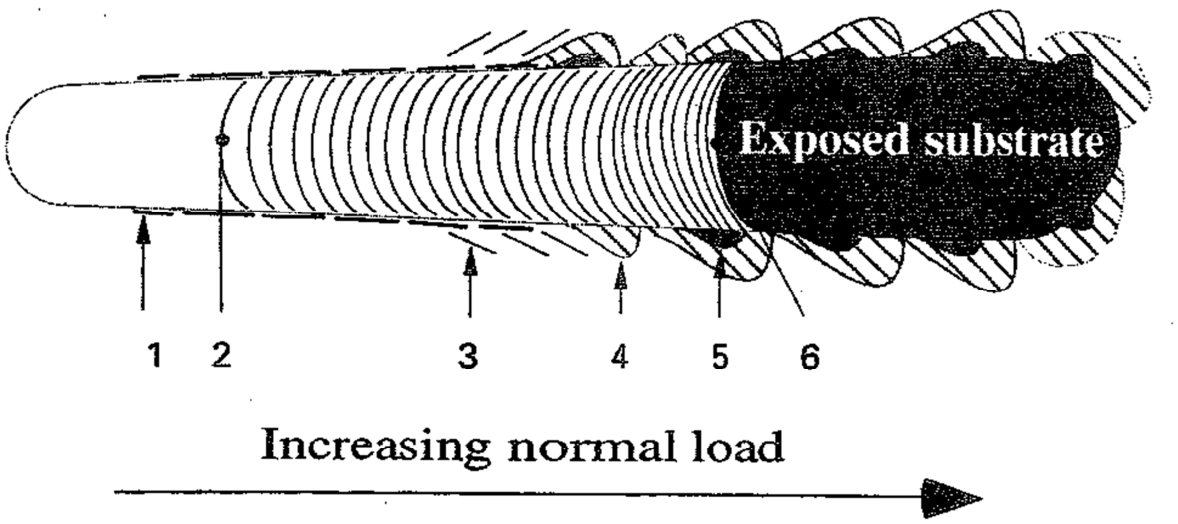

Figure 2.4: Schematic illustration of coating failures observed during scratch testing: 1: parallel cracks; 2: semicircular cracks; 3: external transverse cracks; 4: coating chipping; 5: coating spalling; 6: coating breakthrough (Larsson et al. (2000).

2.3 Adhesion evaluation techniques

The adhesion between the coating and substrate is a measure value to quantify the performance and reliability of coated materials for engineering applications. Methods which have been developed for evaluating substrate-coating adhesion often have its own advantages and disadvantages depending on the specific coating-substrate systems.

The measurement of experimental adhesion can be determined in two ways: (1) by defining the force of adhesion as the maximum force per unit area exerted when two materials are separated; (2) by defining the work of adhesion as the work done in separating two materials from one another (Chalker et al., 1991).

Table 2.3 shows some of the methods developed to measure the adhesion of thin films that have been reported in literatures. The methods can be classified into qualitative and quantitative methods, mechanical and non-mechanical methods. The mechanical methods are

of more practical interests. Tape test is the simplest and most widely used method to evaluate coating adhesion. The indentation, laser spallation and scratch adhesion test are the most practical methods to be used and widely been used for the analysis of coating adhesions.

In this section, a compressive review on the indentation, laser spallation and scratch test are presented. Details explanations on each technique are made and advantages as well as limitations of each are also presented.

Table 2.3: Available methods for coating adhesions evaluation (Chalker et al., 1991).

Qualitative	Quantitative
Mechanical methods	
Abrasion test	Scratch test
Bend and scratch test	Laser spallation technique
Scotch tape test	Indentation test
	Direct pull-off method
Non-mechanical methods	
X-ray diffraction	Thermal method
	Nucleation test

2.3.1 Indentation test

The indentation adhesion test was done by introducing a stable crack into the coating-substrate interface by the used of conventional indentation procedures using either Brale or Vickers indenters (Chalker et al., 1991). In indentation test, it is assumed that the interface within the vicinity of the plastic zone created during indentation has a lower toughness than either the film or substrate materials and consequently will be area of preferential lateral crack formations. Figure 2.5 shows the schematic view of indentation test showing the crack size induced resulting from the indenter loads. The coating removal mechanisms obtained from the indentation test were studied and the values of critical normal loads at the event of

complete removal of coating from the substrate usually refer as the adhesion of coating-substrate systems.

Figure 2.6 shows the results of a series of indents made at different loads in the indentation test conducted by Jindal et al. (1987). During the test, the average change in lateral cracking is monitored as a function of load and the interfacial fracture toughness K_{Ii} is derived from the linear portion of the indentation load vs. lateral crack length plot according to

$$K_{Ii} = \left(\frac{G_{Ii}E_c}{1-{v_c}^2}\right)^{\frac{1}{2}} \tag{2.1}$$

where, A is a constant and E_c and v_c are Young`s modulus and Poisson`s ratio of the coating respectively. It is also observed that in this technique, the indentation adhesion parameters P_c and K_{Ii} are relatively insensitive to the substrate hardness.

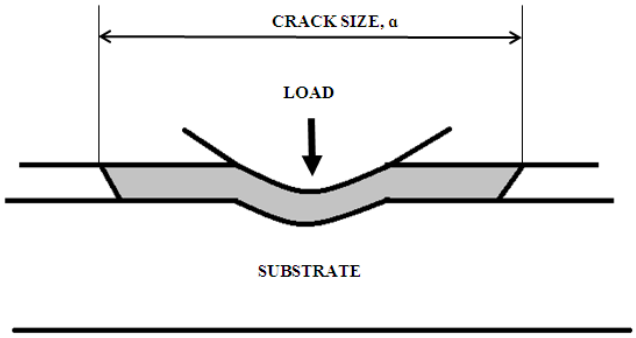

Figure 2.5: Schematic representation of the indentation coating adhesion test.

In the indentation test, different types of coating failures were observed depend on the amount of loads applied during the test. In the analysis of coating failure in TiN coated high speed steels by Larsson et al. (2000), four different types of coating failure were observed. At relatively low normal load (5-25 N), only circular cracks at the rim and inside the indentation were found. At loads above 60-130 N, radial cracks propagating perpendicular to the rim of

circular indentation were found. At loads above 600 N, small cohesive and large adhesive failures outside the indentation were seen.

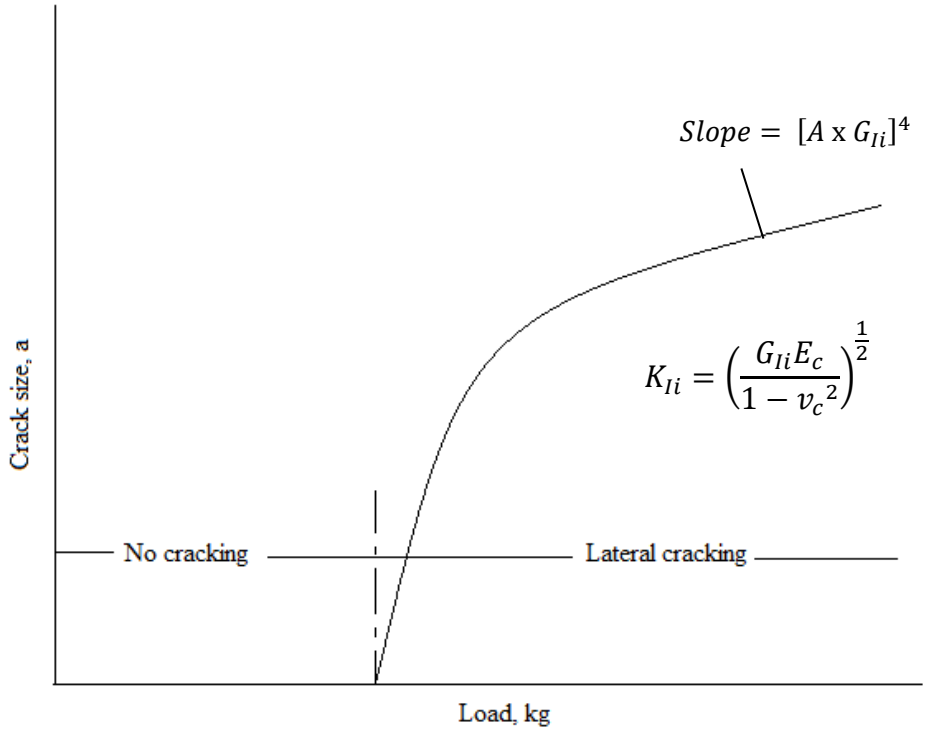

Figure 2.6: Plot of crack size, a vs. load, kg of series of indents made at different loads. (Jindal et al., 1987).

Another indentation test carried out by Diao et al. (1994) in ceramic coatings observed different fracture patterns at different normal loads. From their observation, two types of coating removal mechanisms were observed in the indentation tests. One mechanism was chipping caused by generation of ring cracks (blunt indenter) and the second mechanism was spalling caused by the generation of lateral cracks at the interface (sharp indenter).

Figure 2.7 shows the fracture patterns of different thickness TiN coating observed during the indentation test. At higher coating thickness, no cracks are observed at normal load, W up to 3000 N. At lower coating thickness, ring cracks are observed at normal load above 1000 N. The results obtained also suggest that as the coating thickness increases, the resistance of the

coating to crack or fail also increases. Thus, the adhesions of the coating are increases with the higher coating thickness

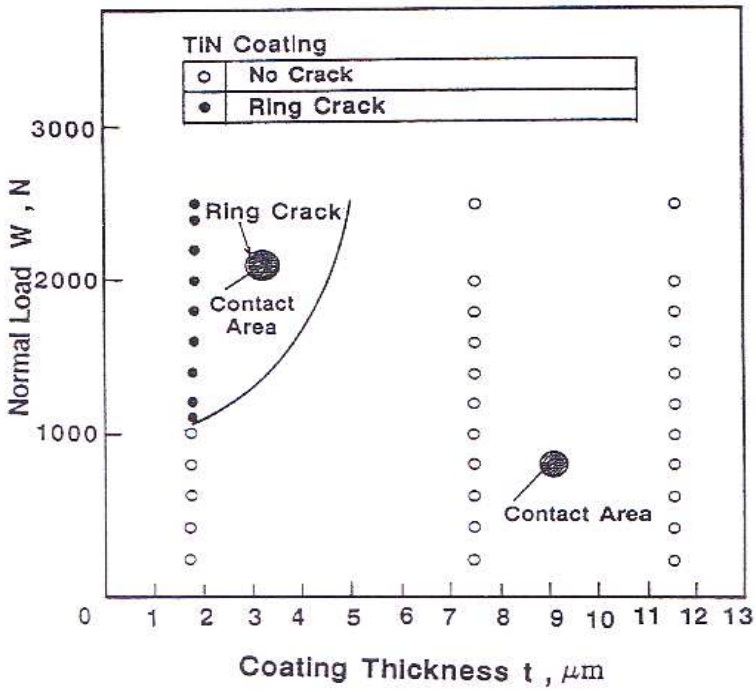

Figure 2.7: Fracture pattern of TiN coating as function of normal load, W and coating thickness, t as observed during the indentation test by Diao (1994).

The limitation of this method for adhesion strength evaluation is that only fracture patterns of the coating at specific indent loads can be determined. The mechanism or fracture patterns of the coating prior to critical loads cannot be observed. The static indentation test should be used to evaluate the fracture resistance and coating-substrate adhesion, while dynamic scratch testing can preferably be used for evaluating the load carrying capacity of the coating-substrate composite.

2.3.2 Laser spallation technique

Laser spallation was established as a method to quantify the tensile strength of interface between engineering substrates and thin ceramic, polymeric, or metallic coating. Gupta et al.

(1992) have developed laser spallation experiment to measure the strength of planar interfaces between a substrate and a thin coating (in the thickness range of 0.3–3 μm).

In basic laser spallation test (see Figure 2.8), a 2.5 ns Nd:YAG laser pulse is focused to an area 3 mm in diameter on a 0.5-mm thick aluminum film. The film is sandwiched between the back surface of a substrate and a 50 to 100 mm thick layer of solid water glass. The induced expansion of aluminum generates a compressive stress pulse (with 1 ns rise time) directed toward the coating which is deposited on the substrate's front surface. The compressive stress wave reflects into a tensile pulse from the coating's free surface and leads to its complete removal at a sufficiently high amplitude which referred to as spallation.

The critical stress at the interface is calculated by measuring the transient displacement history of the coating's free surface (induced during pulse reflection) by using an optical interferometer with a resolution of 0.2 ns in the single shot mode. The measured free surface velocity (or displacements) is related to the maximum interfacial tensile stress that is generated by the reflecting stress wave by using a wave mechanics based simulation. The peak value of this interface tensile stress at the onset of interface separation is taken as the interface strength (Hagerman et al., 2007).

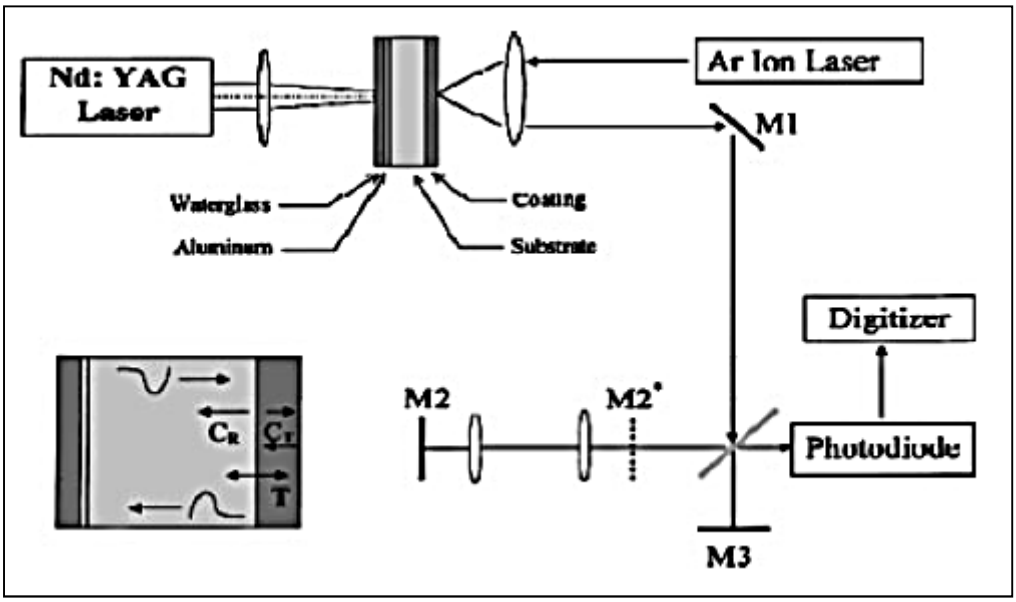

Figure 2.8: Basic laser spallation set up. (Gupta, 1994)

The laser spallation technique is expedient than other test methods to measure and analyze the failure strength of coatings and interface strength due to its relatively simple setup. However, the limitations of this technique are on the sample film thickness and hardness. The preliminary spallation tests need to be conducted to determine whether complete separation of coating area from substrate occurs or not. The sample with large film thickness did not result in the complete separation of coating area from substrate due to large film thickness and high hardness. This was because the ends of the interfacial crack formed at interface did not have enough energy to break through the hard thick coating to form a free spall. Thus, these particular methods can be successfully used on thin coatings. Modification can be done on the samples by making the coated area small (within 3 mm diameter) so that, the laser pulse can be directly focus on that area and complete separation of the coating area can be obtained.

2.3.3 Scratch test

The scratch test has been widely used as the technique to evaluate the adhesion of coating since its introduction in 1950 by Heavens (Laugier, 1981). In scratch testing, a diamond stylus

of defined geometry is drawn across the surface of a coated sample at a constant speed with a defined normal force over a defined distance. The normal force can be set constant, progressively increase, or incrementally increase depends on the model of analysis (see Figure 2.9). In constant-load scratch testing, the normal force is maintained at a constant level while scratching the sample. By increasing the load for each subsequent scratch, a scratch map can be generated to determine the critical load corresponding to a specified damage. In progressive-load scratch testing, the stylus is drawn along the sample while the normal force is linearly increased to a maximum predetermined value. The critical load is recorded as the normal force at which the damage is first observed. Incremental-load scratch testing consists of incrementally increasing constant load scratch segments, and is very useful if space is limited on the sample.

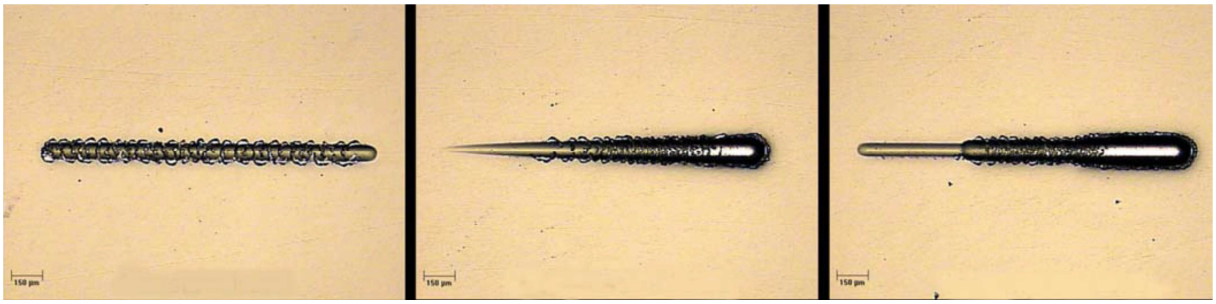

Figure 2.9: The three main scratch modes are constant load, progressive load, and incremental load (from left to right).

The diamond stylus used in scratch test typically has Rockwell C geometry with an angle of 120 degrees and a spherical tip radius of 200 μm. The normal force at the event of coating detachment is called the critical load, Lc. The critical load Lc is defined as the load that corresponds to the failure event. This load is related to the practical adhesion strength and the damage resistance of the coating/substrate system. After completion of the test, the scratch track was microscopically analyzed for specific, well-defined damage such as cracking, deformation, buckling, spallation, or delamination of the coating.

Figure 2.10 shows the typical scratch test data for a progressive load scratch test on high speed steel sample coated with TiN. The loading rate is 4 mN/s and the scratch length of 900 μm. From the figure, the critical failure points L_{c1} and L_{c2} are 900 mN and 1050 mN respectively. The first critical load (L_{c1}) is 900 mN, and it corresponds to the point at which first damage is observed. This first damage has the shape of an interfacial shell-shaped spallation. The second critical load (L_{c2}) is 1050 mN, and it is the point at which the damage becomes continuous and complete delamination of the coating starts.

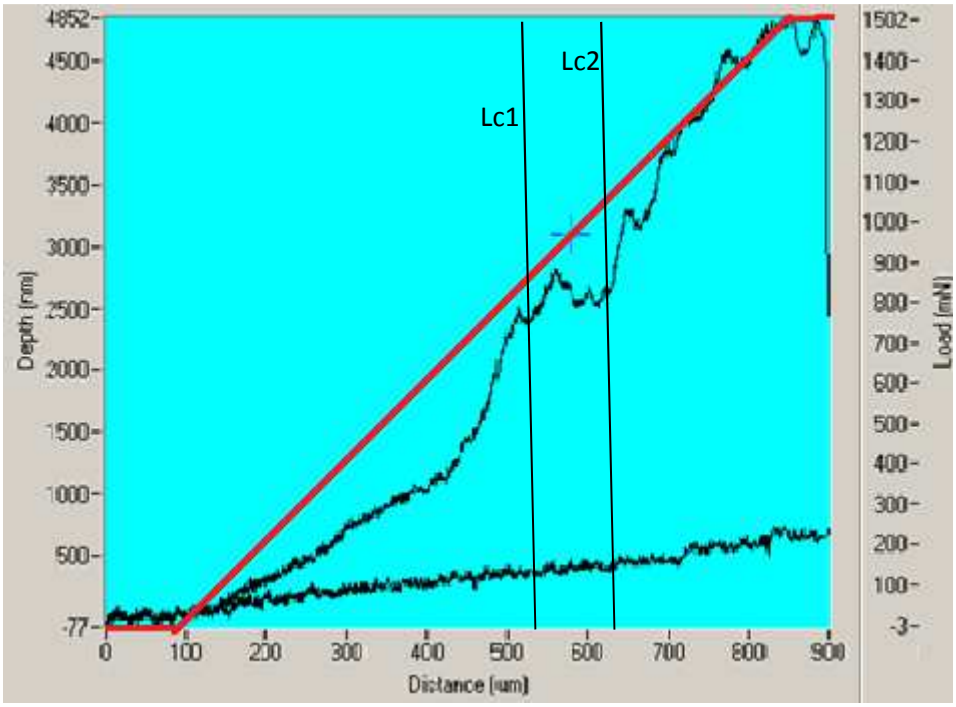

Figure 2.10: Typical scratch test data for a progressive load scratch on coated steel sample, showing the critical failure points Lc1 and Lc2.

Since its inception, the developments of the scratch test technique for measuring coating adhesion have been done. Instead of having only the data of normal force and penetration depths from the scratch test results, acoustic emission equipment has been used to provide secondary data for coating detachment analysis. The acoustic emission (AE) equipment or sensor is used to provide traceable signals whenever coating detachments present during the

scratch tests. The signals can be used to compare results from different samples and may avoid some subjectivity of measurement made by eyes.

Figure 2.11 represents the plot of acoustic emission vs. scratch distance obtained from typical scratch test equipped with AE sensor. Figure 2.11 can be understood that the coating detachment start to observe when there is a sudden jump in the AE signal. L_{c1} represents the first critical points of coating detachment which is referred to cohesive failure of the coating. L_{c2} represents the 2nd critical points of coating detachment where complete fails of the coating starting to occur. L_{c2} is the critical load of the coating failure and also represent the value of coating adhesions.

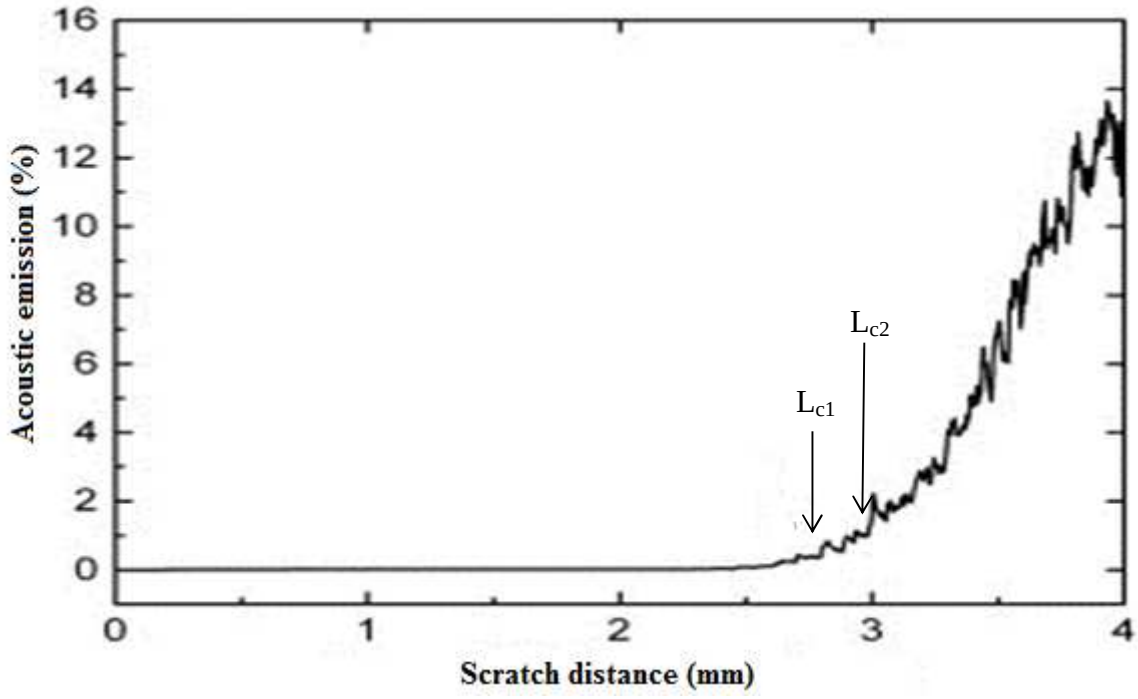

Figure 2.11: Plot of acoustic emission vs. scratch distance produced from the scratch test.

Bull (1991) have carried out used scratch test analyses on the adhesion of titanium nitride coatings deposited onto a range of different substrates from soft nickel to a hard cemented carbide and to identify the failure modes which occur during the test with the assistance of AE probe. The scratch test was performed using a Rockwell C diamond stylus with the tip radius

of 200 µm. The tester was equipped with acoustic emission monitoring equipment in order to determine the coating failure.

Another work done by Je et al. (1986) also implemented the scratch testing with AE equipment in their assay on the reactively sputtered TiN coatings on a soft substrate. From the work, they found that the critical load of a thicker coating (approximately 1.5 µm), cracking and also loss of the coating were observed with an increase in acoustic emission. However, at the critical loads of thinner coatings (1.2 µm or less), coating loss was not observed even though there is an increase in the emission and coating cracking did occurred. Their findings suggested that the AE emission can provide accurate information on the occurrence of coating failure but limited to certain level of coating thickness. For example in their work, coating thickness of 1.2 µm or less, the AE emission still showing increases in the signal but microscopic observation on the coating clearly do not indicated any failure.

Yamamoto et al. (1992) on their study of the acoustic emission behavior at scratch test for TiN coating concentrated on the relationships between the AE behavior and the intrinsic properties of deposited TiN films, and also to evaluate the mechanical strength of the coatings by analyzing the AE intensity. They concluded that the AE intensity of the coatings measured by the scratch test depends not only on the adhesion of a coating-substrate interface but also on the intrinsic properties of a deposited film. The substrate hardness has little effect on AE intensity. However, the internal stress and toughness of the coated film strongly affect the AE intensity. The critical load correlates with AE intensity which is determined by the toughness and the internal stress. AE intensity increases with decreasing the toughness and the internal stress of coated films. They also suggested that an analysis of AE behavior at the scratch test can qualitatively evaluate the toughness of coatings.

With the limitation of the AE emission assessment technique as mentioned above, Valli et al. (1985) have developed the scratch test method of adhesion assessment by recording the tangential friction force between the indenter and coating rather than the acoustic emission which has previously been used to detect the critical load. Figure 2.12 represents the scratch test apparatus arrangement. A direct correlation was detected between changes in friction force and acoustic emission. They also concluded that the friction force monitoring can provide advantages over acoustic emission detection of coating failure in scratch test. The acoustic emissions provide good indicating of coating failure when the coating thickness was above 1.5 μm. Below this value, the interpretation became difficult and no meaningful acoustic emission normally detected at coating thickness below 0.5 μm. Conversely, measurement of tangential force enabled the determination of critical load in all case down to a coating thickness of 0.3 μm. Comparison values produced by this method with the values recorded by other authors using acoustic emission were within the defined band for given substrate condition and test parameters. The main advantage of the extension is that relatively thin (less than 1 μm) coatings can be studied and still have the possibility of continuously recording the test results in addition to the optical microscopy studies. Addition to that, the coatings of the same color as the substrate can easily be studied.

Figure 2.13 shows the AE emission and tangential force signals detected on thick and very thin of TiN coating on HSS substrate (less than 1 μm). The coating failure could be detected only by a change in the frictional force. No meaningful acoustic emission could be detected from thinner coating.

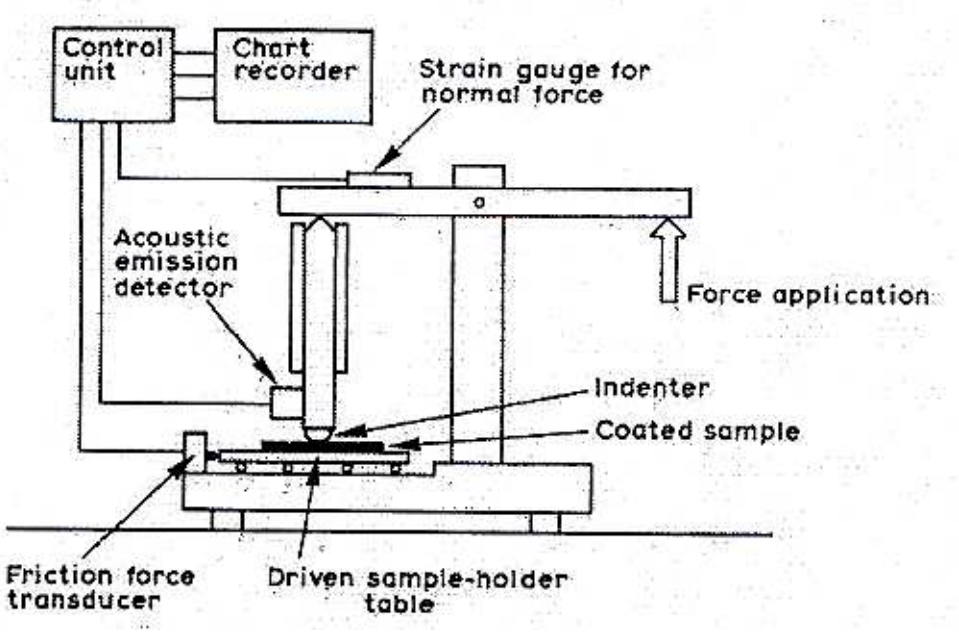

Figure 2.12: Schematic representation of scratch test apparatus used by Valli et al. (1985).

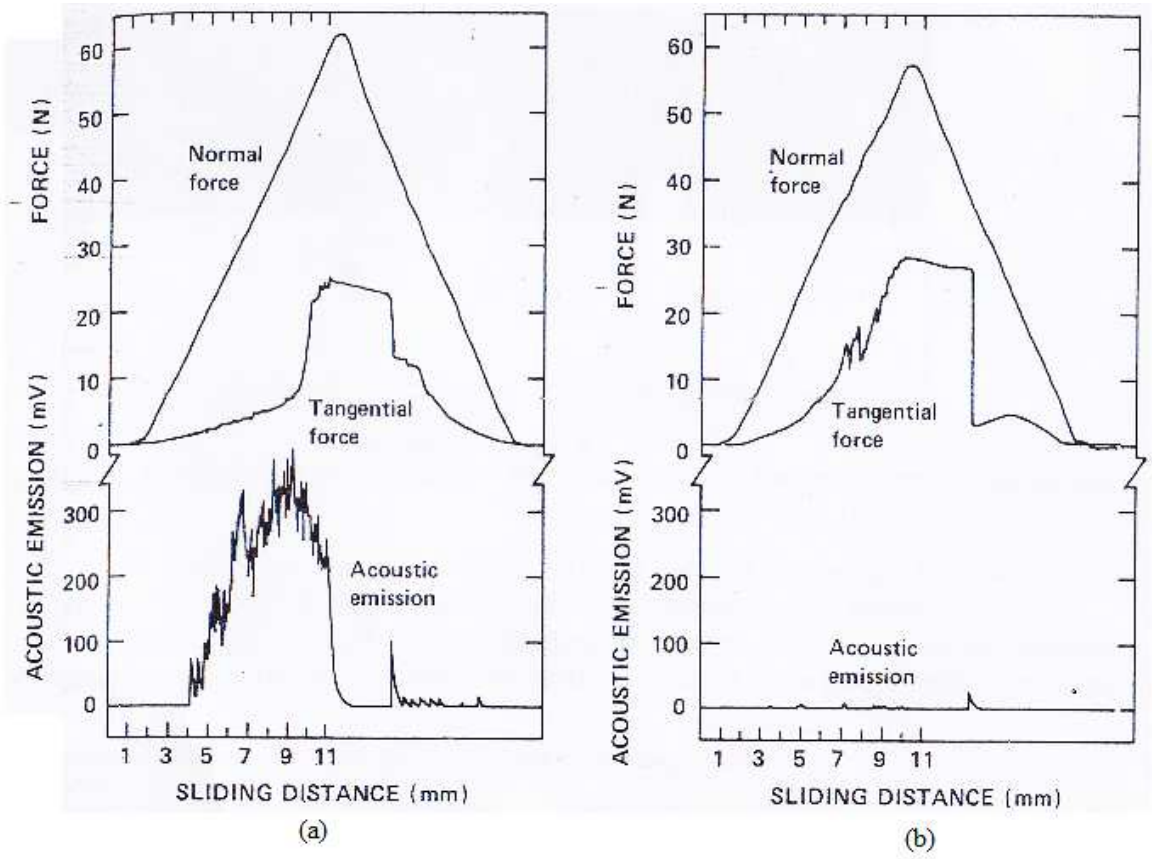

Figure 2.13: Acoustic and tangential friction force results obtained from scratch test of titanium nitride (TiN) coating on high speed steel substrate. (a) thick coating (b) thinner coating (Valli et al., 1985).

2.3.4 Energy description model

Another technique of scratch test assessment has been suggested by Laugier (1984). He has introduced an energy description model of coating removal by scratch test. He suggested that the adhesion behavior can be modeled in terms of the strain energy released during removal of coating. In the model, the compressively stressed coating in the region ahead of the indenter is considered to reduce its stored energy by peeling or spalling from the substrate at a critical applied load. The approach is applicable to ductile and brittle coatings. The adhesion force calculated from the basic scratch test typically in an order of magnitude lower than estimate based on condensation energy measurement.

He suggested a simple energy balance criterion in which stored elastic energy in the coating ahead of the indenter is considered to be released to form new surfaces when the critical normal load is reached. Table 4 summarized the calculated work, W of adhesion for selected material using the formula by Laugier (1984).

$$W = \frac{1\{\sigma(x)\}^2}{2\,E}\,h \tag{2.2}$$

where, E is the young`s modulus of the coating, h is the coating thickness and σ(x) is the stress in the coating, which is considered to be constant throughout the thickness. The coating stress, σ(x) is calculated from $\sigma(x) = \sigma_{appl}(x) + \sigma_{int}(x)$, where $\sigma_{appl}(x)$ is the applied stress and $\sigma_{int}(x)$ is the internal stress. The internal stress, $\sigma_{int}(x)$ is found to be almost constant in all materials. The applied stress, $\sigma_{appl}(x)$ resulting from the sliding indenter is not decrease significantly throughout the coating thickness if a > h, where a is the radius of contact circle and h is the coating thickness.

From Table 2.4, the applied stress, $\sigma_{appl}(x)$ has been used for the calculation of W when $\sigma_{int}(x)$ is not available. The values of $\sigma_{appl}(x)$ have been calculated for f = 0.3. It is also noted that the

critical load increases with time (the values quoted are for as-deposited aluminum and for aging periods of 400 h (for aluminum) and 200 h (for iron)).

Table 2.4: Calculated work, W of adhesion for selected material (Laugier, 1984).

Material	Critical load P **($\times 10^{-3}$ kgf)**	Stress ($\times 10^3$ MPa)			Adhesion energy **W (J m^{-2})**	Condensation energy from critical condensation experiments **(J m^{-2})**
		$\sigma_{appl}(x)^n$	$\sigma_{int}(x)$	$\sigma(x) = \sigma_{appl}(x) + \sigma_{int}(x)$		
Ag	5	0.79	-0.01	0.78	0.40	0.24
Au	2	0.58	-0.08	0.50	0.16	
Al[b]	5	0.79	0.07	0.72	0.38	0.72
Al[b]	70	1.90			2.40	
Fe[b]	100	2.10	-0.96	1.14	0.38	
Fe[b]	500	3.60			3.80	

The scratch testing has proved to be reliable method to determine the adhesion of coating-substrate system. However, there are several variables that affecting the scratch test results which are need to be considered and understood. Valli and Mäkelä (1987) have listed several factors which might well affecting the scratch test results. The influence of lubrication and surface roughness on the scratch test result should be understood. Frictions are the dominant factor affecting the test results. The use of thin ion-plated silver overlay increases the critical normal force remarkably. The use of oils can even enhance the repeatability of testing for example in the case of hard coatings on high strength substrates. Addition to that, performance of a coating might be affected by the poor surface quality. The surface roughness R_a value should not exceed 0.25 µm if reproducible results are required. A poor surface finish decreases the critical normal force reading compared to a polished surfaced.

In addition to the extrinsic factors listed above, a number of intrinsic parameters also have an importance influence on the derived value of critical loads. Some of the parameters are loading rate, scratching speed, indenter tip radius and indenter wear which have been reviewed by Steinmann et al. (1987).

The scratch adhesion test appears to be the only available practical methods to study the adhesion of coatings. However, care is needed in performing the test and in the interpretation of the results if reliable results are to be drawn on coating-substrate adhesions. The intrinsic and extrinsic factors must be given full attention of their influence on the value of the critical loads. Although scratch test is very quick test and simple to perform, an underestimate of the practical adhesion in any application can still be occurs for example in the case where catastrophic failure occurs at the first sufficiently large flaw.

2.4 Improvement of TiN adhesion strength

The improvements on the adhesion strengths of TiN coating are needed due to tribology nature of the tooling applications. TiN coatings are proved to be useful in providing better wear resistance and hence improving the tool life of the cutting tools. Good adhesion strength are required for desired properties to be achieved. In tooling applications, current development in TiN coating technology focusing on the lower temperature processes and good adhesion strengths between coatings and substrates. However, lower deposition process temperature tend to produce lower adhesion. The adhesion strengths of TiN coating can be enhanced by method of processing, composition and the stucture of the coatings.

In order to enhance the adhesion strength of TiN coating, new methods of coating deposition have been introduced by other reseacher. PVD methods are more prefered in toolong applications due to environmental reasons, greater productivity and the possibility of multiple coatings. Thus, previous researchers have been working on the deposition processes that

operate at low processing temperature but at the same time provide better adhesion. Plasma-enhanced chemical vapor deposition (PECVD) or plasma assisted chemical vapor deposition (PACVD) is a combinatation of CVD and PVD process (zhang & zhu, 1993). The working principle of PECVD is that the CVD is operated with a plasma and the energy required for reaction being supplied by electricity, raising the ions to high temperature and thus reducing the need of thermal energy to be supplied. Hence, high working temperature are no longer required. The advantages of this deposition process beside the low operating temperature are the simplicity of the apparatus and good adhesion strength of the coatings.

Modification of the composition of the TiN coating is another solutions to the adhesion strength and property improvement of TiN coatings. Wang et al. (1995) studied the effects of aluminum (Al) inclusion on the microstructure and properties of (Ti,AL)N coating on high speed steel (HSS). Analysis on the interface microsturcture between coating and substrate showed that there was a transition layer between the (Ti,Al)N and the HSS substrate. The treansition layer was composed of α-Ti phase and FeTi phase. The α-Ti phase was formed at the beginning of deposition when Ti was first deposited on the surface of the substrate. The FeTi phase was formed when the α-Ti phase diffused into the substrate with increasing substrate temperature. The presents of these transition phase was believed to increase the adhesion between coating and substrate. It is also observed that the wear of the substrate in the form of adhesion abrasion also improved with (Ti,Al)N coating. The aluminium atoms are small (r = 1.43Å), thus, it has ability to fit into the TiN cystal structure at substitutional sites or interstitial sites. As a results, more denser coating structure can be achieved.

In structure of the coatings, TiN adhesion strength can be improved by introducing a metallic interlayer such as Ti between the TiN coating and the substrate. Helmersson et al. (1985) reported on the adhesion of the films increased with the use of an intermediate layer of pure titanium between TiN coating and substrates. The use of 0.1μm intermediate layer of pure

titanium increases the adhesion for films deposited at temperatures below 400 °C. Above this temperature a thin TiC layer is formed in the titanium–steel interface result in reduction of the adhesion. In contrast with Helmersson et al. findings, Valli et al. (1985) reported on the decrease of the coating adhesion when 0.3 μm Ti interlayer deposited between TiN and HSS substrate. The different in observations might indicate that an optimum should be determined for such interlayers for maximum adhesion. Gerth and Wiklund (2008) also performed a study on the improvement of TiN adhesion strength by analyzing metallic coating as interlayer. In their study, W, Mo, Nb, Cr, Ti, Ag and Al, have been evaluated with respect to their influence on the adhesion of PVD TiN coatings deposited onto polished high-speed steel. The results showed that Tin coating with Ti and Cr interlayers both give the best adhesion compared to other metallic interlayers.

The adhesion strength improvement with the presence of Ti interlayer can be explained on the basis of better bonding between the titanium interlayer and the substrate and also better bonding between the titanium layer and the TiN coating. It is suggested by some researcher that the Ti interlayer acts as a graded interface that can evades the abrupt change in composition at the sharp interface between a coating and metal substrate.

There is also possibility of adhesion strength enhancement by using multi-compositional coatings has been done by Kusano et al. (1998b). In their assay, the adhesion of compositional gradient TiO_2/Ti/TiN, ZrO_2/Zr/ZrN, and TiO_2/Ti/Zr/ZrN coatings were studied. Figure 2.14 shows the adhesion strength of TiO_2, TiN, TiO_2/TiN, TiO_2/Ti/TiN and TiO_2-Ti-TiN coating deposited at room temperature, 300^0C and 400^0C. The results showed that the adhesion strength of TiN coating deposited at room temperature were increases with the present of TiO_2/Ti layer (TiO_2/Ti/TiN coatings). At substrate temperature 300^0C and 400^0C, TiO_2 /Ti/TiN and TiO_2/TiN shows a good adhesion strengths while TiO_2/Ti/TiN coatings show superior adhesion compared to TiN coating at substrate temperature of 400^0C. The good

adhesion strength observed can be explained by the basis that by making a compositional change in the interface transition region gradient and smooth, both chemical and mechanical bonding are expected to be improved.

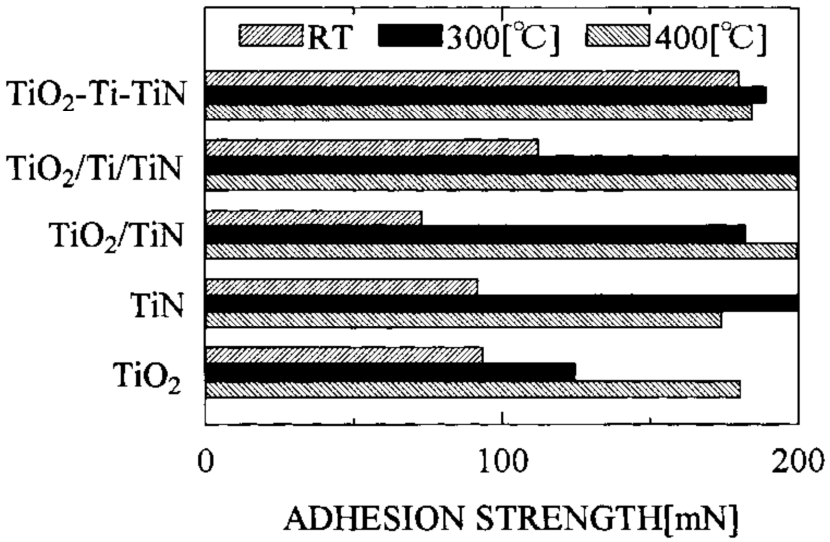

Figure 2.14: Adhesion strength of TiO_2, TiN, TiO_2/TiN, TiO_2/Ti/TiN and TiO_2-Ti-TiN coating deposited at room temperature, 300^0C and 400^0C.(Kusano et al., 1998b).

CHAPTER 3

METHODOLOGY

3.0 Overview

In the present study, two-interesting sets of studies were conducted separately. The first part is to analyze the adhesion strength and hardness of Ti/TiO_2/TiN coating deposited onto high speed steel substrate and stainless steel substrate. The second part of the study is to analyze the effect of substrate temperature, TiO_2 coating thickness and the substrate surface condition on the adhesion strength. The effects of annealing on the coating adhesion strength were also studied. Details of target preparation, substrates preparation, experimental parameters, characterization and evaluation of coated samples are detailed in the following sections.

3.1 Target preparation

A commercially available titanium target (purity 99.995%), 4 inch diameter x 3 mm thickness, was used in this study. The target was ultrasonically clean in acetone for 20 minutes while being heated at 50^0C at the same time in ultrasonic bath to remove dirt, grease and residues from machining processes. It was then rinsed in ethanol and distilled water to ensure that the target was free from surface contaminants and acetone residues. After cleaning process, the titanium target was sputtered in an argon atmosphere for an hour in order to remove oxide layers.

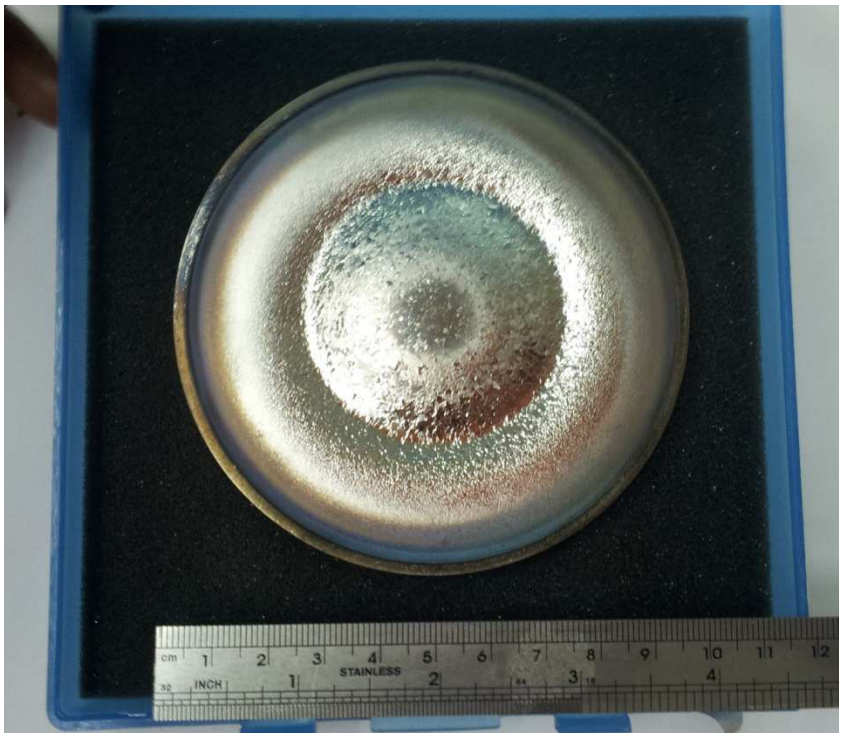

Figure 3.1: Titanium target used during deposition.

3.2 Substrate preparation

Two types of substrate materials were used in the experiments. The coatings were deposited onto high speed steel (HSS) and stainless steel (SS) substrates. The HSS substrates used are 10 x 10 x 5 mm in dimension. Stainless steel substrates used were coupon shape SUS304 Stainless Steel with dimension 10mm (diameter) x 3mm (thickness) and clockwise polished supplied by NovaScientific Resource (M) Sdn. Bhd.

Both type of substrates were abraded and polished using silica paper. The mean surface roughness was measured at Ra = 0.02 μm and Ra = 0.03 μm for HSS and SS respectively. The substrate materials were ultrasonically cleaned at 50 °C in acetone for 25 minutes to remove residues followed by rinsing in ethanol to remove acetone and the remaining residues from substrates. Eventually, the substrates were then rinsed with distilled water. Finally, the substrates are dry by blowing dry nitrogen. Prior to deposition, both substrates were framed to

provide the formation of step in the coating for the purpose of the film thickness measurement.

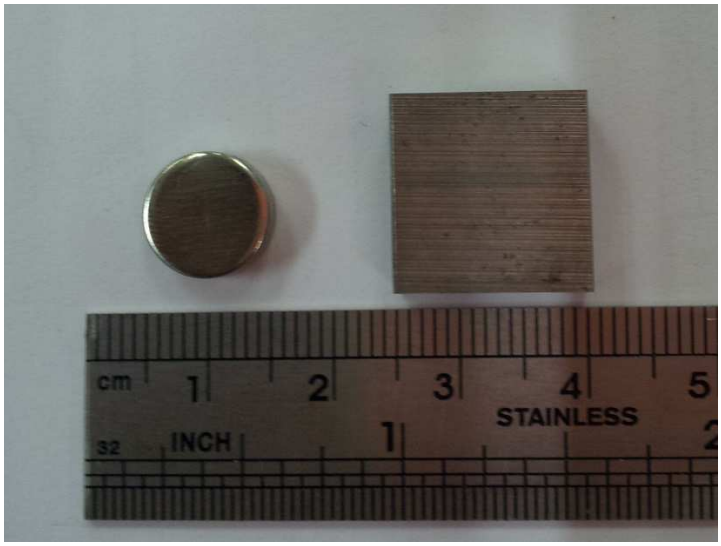

Figure 3.2: Substrates used in the analysis (a) On the left SS and; (b) On the right HSS.

3.3 Deposition process

The depositions of Ti/TiO_2/TiN coating were performed using a TF450 PVD magnetron sputtering system (SG Control Engineering PTE LTD, Singapore). Titanium, Ti layer was first deposited onto substrates followed by Titanium dioxide, TiO_2 layer and thin layer of Titanium nitride, TiN (see Figure 3.3 for coating layer orientation).

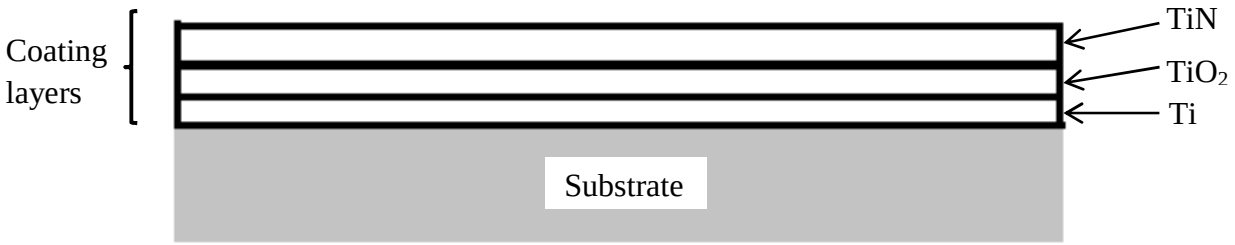

Figure 3.3: Schematic view of TiN/TiO_2/Ti coating system.

The Ti target was placed in parallel to substrate holder. The distance from the target to substrate holder was about 150 mm. A schematic diagram of the positioning of the target and the substrates during sputtering process is shown in Figure 3.4.

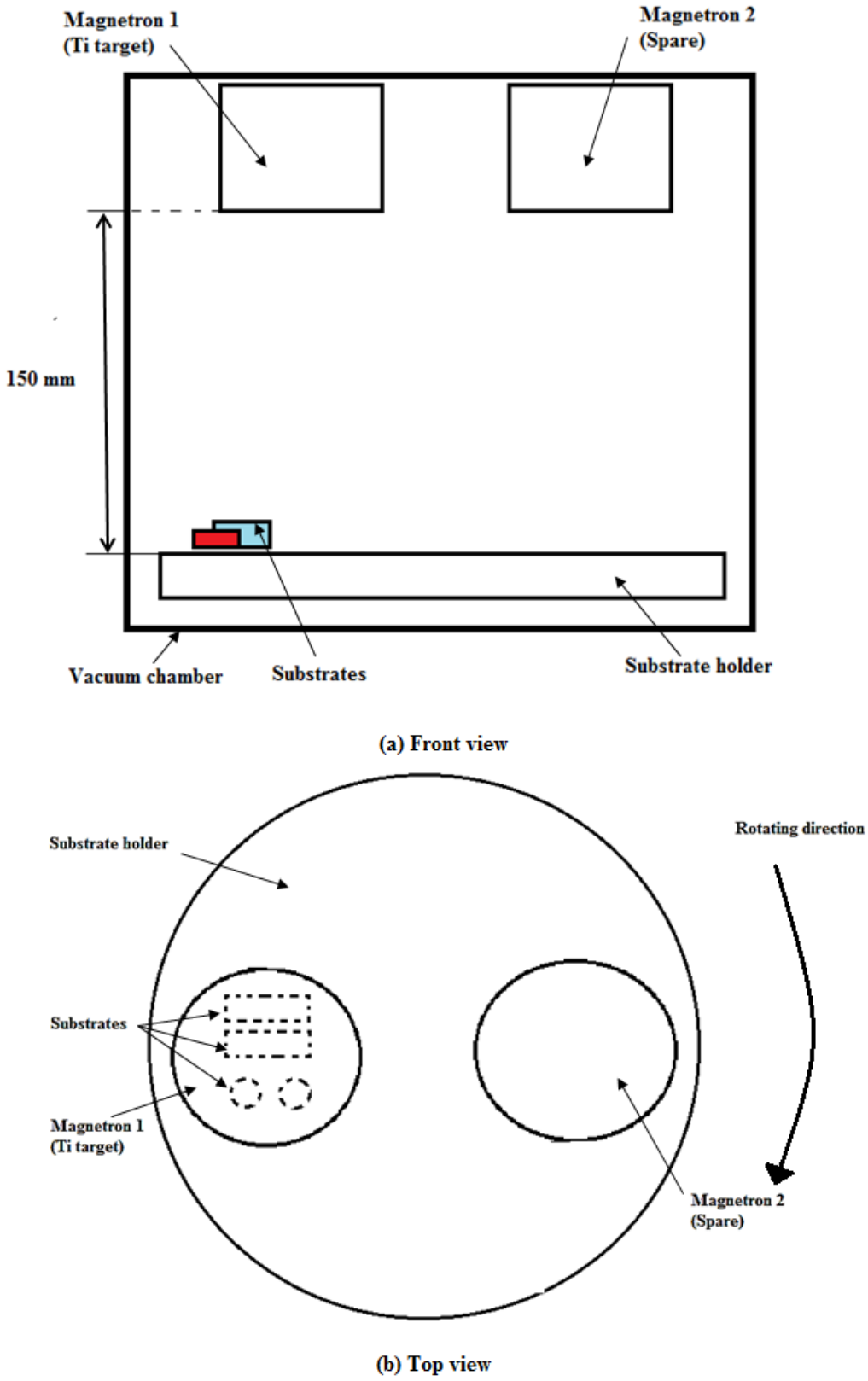

Figure 3.4: Schematic diagram of the positioning of the target and substrates during sputtering process (a) Front view of the sputtering chamber and (b) Top view of the sputtering chamber.

With the shutter closed, the process was initiated by pre-sputtering the Ti target for 5 minutes to clean and remove any contaminant from the target. The substrate holder was set to rotate at 4 rpm to ensure uniform deposition.

The coating layers were deposited using DC magnetron sputtering method. The deposition apparatus used is shown in Figure 3.5. The deposit system is stainless-steel vacuum chamber. The base pressure in process chamber was 2.5 x 10^{-5} Torr. The working gasses were Ar (99.999%), O_2 (99.995%), and N_2 (99.99%) and were used as sputtering and reactive gases respectively. Titanium target (purity 99.995%) was used and powered by DC generator. Prior to each deposition, the titanium target was pre-sputtered in an argon atmosphere in order to remove oxide layers. The substrate holder was rotated during the deposition process to improve coating uniformity.

Figure 3.5: TF450 PVD magnetron sputtering system (SG Control Engineering PTE LTD, Singapore) equipped with Protec Instruments PC-500 Flow Controller (enlarge picture).

To isolate and to study every single interface and also to analyse the effect of TiO_2 inclusion on the adhesion strength of TiN coating system, it is necessary to prepare base samples; TiN coating and Ti/TiN coating for comparison purposes. Table 3.1 summarised the experimental conditions of the sputtering process. The parameters for depositing TiN, TiO_2 and Ti coating layer were chosen based on literature review (Bushroa et al., 2011; Carradò et al., 2010; Nsongo and Gillet, 1995). For Ti coating, the sputtering was carried out at an argon pressure of 4.9 x 10^{-3} Torr with argon flow rate of 40 sccm for 40 minutes in order to obtain coating layer of 500 nm. For TiN and TiO_2 coating layer, the deposition was carried out for 60 minutes respectively to obtain coating thickness of 100 – 200 nm. For deposition of TiN, the ratio of argon and nitrogen gasses used was 3:2 ($Ar:N_2$) and for TiO_2, the ration of argon and oxygen gasses was 5:1 ($Ar:O_2$).

Table 3.1: Sputtering parameters and setting values.

Parameters	TiN deposition	TiO_2 deposition	Ti deposition
Pre-sputtering	10 minutes	10 minutes	10 minutes
Flow gas (sccm*)	14:8.4($Ar:N_2$)	40:8($Ar:O_2$)	40 (Ar)
P(Torr) x 10^{-3}	8.4	5.8	4.9
P (W)	150	150	150
Deposition temperature (^{0}C)	200	200	200
Deposition time (s)	3600	3600	2400

*sccm = standard cubic centimetre per minute

3.3.1 The study of adhesion strength improvement of TiN coating by implementing Ti and TiO_2 as the interlayer.

In this study, 4 sets of coated samples were prepared separately as summarized in Table 3.2. All coatings were deposited on high speed steel (HSS) and stainless steel (SS) substrates respectively at deposition temperature of 200 ^{0}C. The sputtering process was done at 150 W

discharge power levels while the remaining coating parameters were set according to parameters mentioned earlier.

Each of individual coating-substrate systems were then subjected to adhesion strength evaluation by scratch test method. The adhesion strength of each coating systems were compared to determine any adhesion strength improvement. Each coating was subjected to hardness test in order to determine the hardness of each coating using micro-hardness tester. The coating thicknesses of each coating-substrate system were measured using topography measurement method and Focus Ion Beam (FiB) method. The composition, cross-section and the microstructures of the coatings were analyzed using EDAX and FESEM analysis.

Table 3.2: Summary of coating samples deposited for the analysis and the total deposition time.

Sample No.	**Coatings***	**Substrates****	**Total Deposition Time*****
1	Ti	HSS	2400 s
		SS	2400 s
2	TiN	HSS	3600 s
		SS	3600 s
3	Ti/TiN	HSS	6000 s
		SS	6000 s
4	Ti/TiO_2/TiN	HSS	9600 s
		SS	9600 s

*coating layers are deposited according to designated sequences. For example, Ti was first deposited followed by TiO_2 and lastly TiN layer for Ti/TiO_2/TiN coating-substrate systems.

**surface roughness of HSS and SS substrates were Ra = 0.02 μm and Ra = 0.03 μm respectively.

***Total deposition time was calculated from the each layer deposition time.

3.3.2 The effect of deposition temperature on the adhesion strength of $Ti/TiO_2/TiN$ coatings.

To study the effect of substrate temperature on the adhesion of the coating systems, samples with different substrate temperature are prepared while keeping the other parameters at same values. The multilayer coating systems $TiN/TiO_2/Ti$ are deposited onto stainless steel and HSS substrates at substrate temperature 50, 200 and 250 °C respectively. Scratch test and hardness test were conducted on each sample.

3.3.3 The effect of TiO_2 coating thickness on the adhesion strength of $Ti/TiO_2/TiN$ coatings.

To study the effect of TiO_2 coating thickness on the adhesion strength of the coating systems, the thickness of the TiO_2 coating layer was varied by varying the deposition time of TiO_2 coating layer (see Table 3.3). 3 sets of sample were prepared with vary TiO_2 coating layer thickness at deposition temperature of 200 °C. Other parameters for deposition of TiN and Ti and the coating thickness are kept constant. The coatings are deposited onto stainless steel and HSS substrate.

Table 3.3: TiO_2 deposition time for $Ti/TiO_2/TiN$ coatings deposited on HSS and SS substrates.

Sample No.	**Coatings**	**Substrates**	**TiO_2 deposition time**
1	$Ti/TiO_2/TiN$	HSS SS	1800 s
2	$Ti/TiO_2/TiN$	HSS SS	3600 s
3	$Ti/TiO_2/TiN$	HSS SS	5400 s

3.3.4 The effect of substrate surface condition on the adhesion strength of Ti/TiO_2/TiN coatings.

To study the effect of substrate surface condition on the adhesion strength of the coating systems, different substrates with different surface roughness were used for coating deposition. Different surface roughness values were achieved by using different grade of silica paper during polishing process. Parameters for deposition of TiN, Ti and TiO_2 coatings are kept constant as in Table 3.1. Substrate used in this analysis was high speed steel (HSS). Surface roughness of the substrate was summarized in Table 3.4.

Table 3.4: Surface roughness of HSS substrate used.

No	**Sample**	**Roughness (Ra)**			
		Reading 1 (μm)	Reading 2 (μm)	Reading 3 (μm)	Average (μm)
1	HSS-S1	0.02	0.03	0.03	0.03
2	HSS-S2	0.30	0.27	0.25	0.27
3	HSS-S3	1.13	1.21	1.25	1.20

3.3.5 The effect of annealing on the mechanical properties of the substrate coating systems.

Three Ti/TiO_2/TiN coated HSS substrates were put in the sputtering chamber. The sputtering process was done at deposition temperature 200 °C at 150 W discharge power levels while the remaining coating parameters were kept constant as in Table 3.1. The deposited substrates were heated to 400, 500 and 600 °C annealed temperatures at heating rate of 7.5 °C/min. Each substrate was annealed for an hour. The heating process was performed using Elite Thermal System Limited chamber furnace. Figure 3.6 shows the heating curve for each substrate at different anneal temperature.

The heat treated and unheated HSS substrates were then subjected to adhesion strength evaluation and hardness test. The microstructures of the annealed samples were observed using optical microscope.

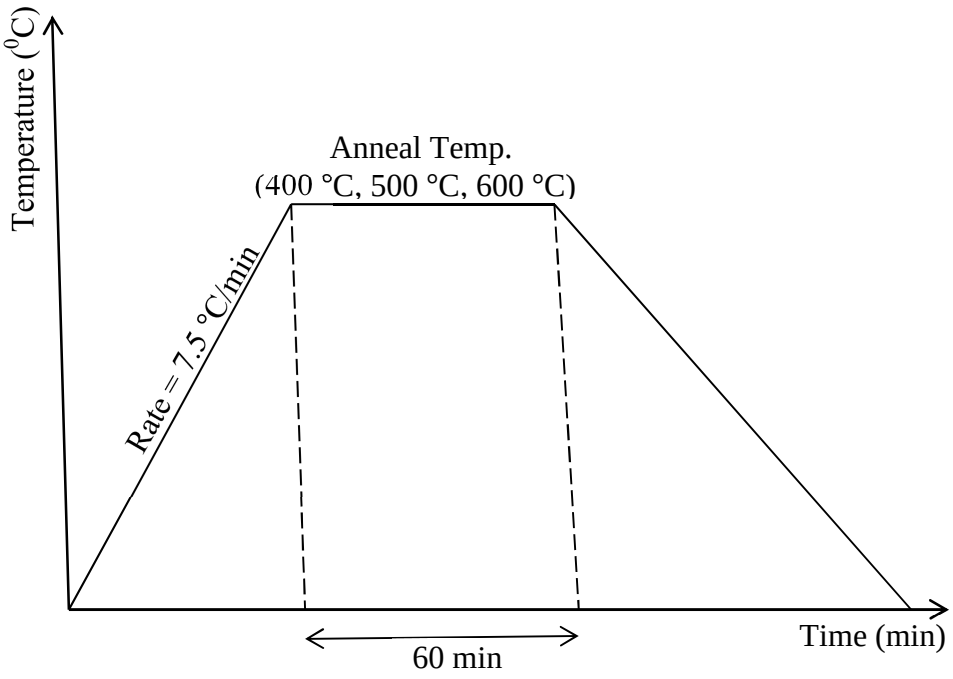

Figure 3.6: Heat treatment curve during annealing treatment of deposited substrate.

3.4 Evaluation and characterization

3.4.1 Film thickness

The film thickness of the coating films on the HSS and SS substrates were measured using a Micro Material Nano Test (Wrexam, UK) micro-scratch system with a diamond probe and also using Focused Ion Beams (FiB) technique.

To measure the film thickness using micro-scratch system, each coating layer was deposited individually onto HSS substrate in order to evaluate each coating layer. Before deposition, tape was attached on the substrate surface to create framed surface in order to evaluate the coating thickness (see Figure 3.7).

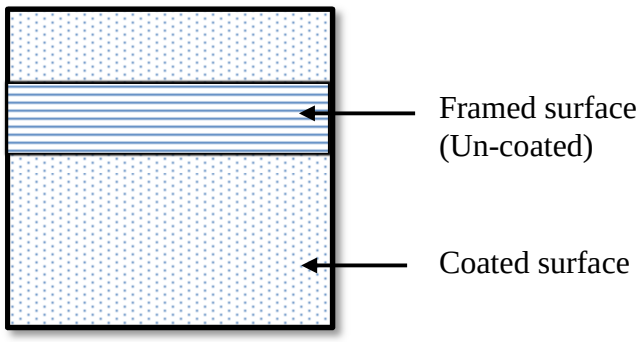

Figure 3.7: HSS coated sample for coating thickness evaluation.

Three HSS substrates with polished surface were used with Ti, TiO_2 and TiN coatings deposited on each substrate. Figure 3.8 shows the set-up of a micro-scratch system while Figure 3.9 is the schematic diagram.

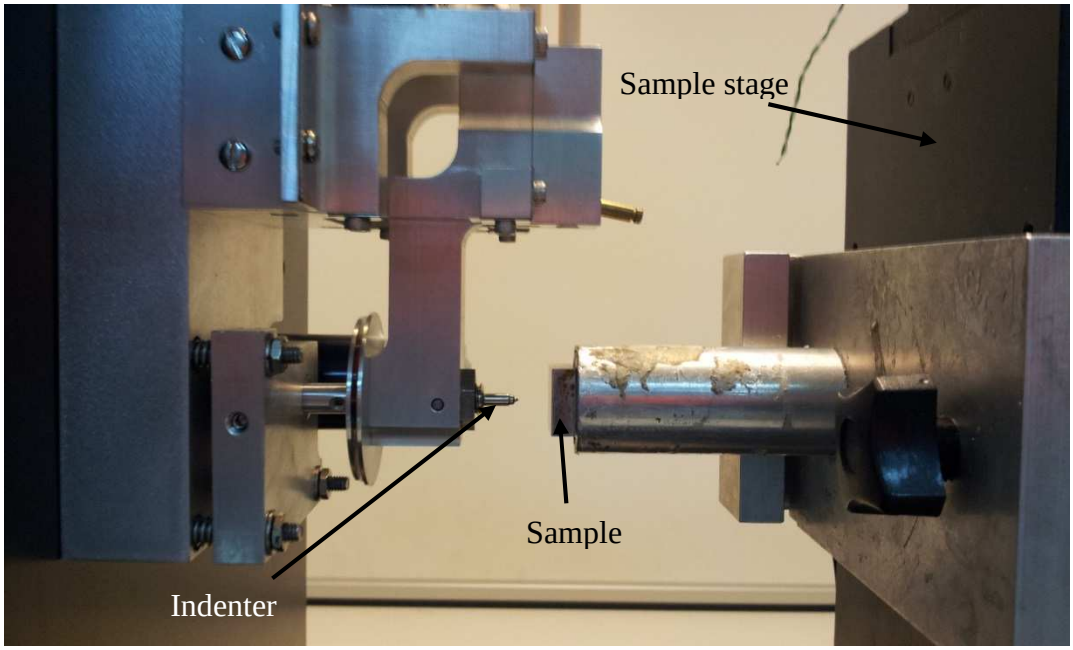

Figure 3.8: An image of a micro-scratch system.

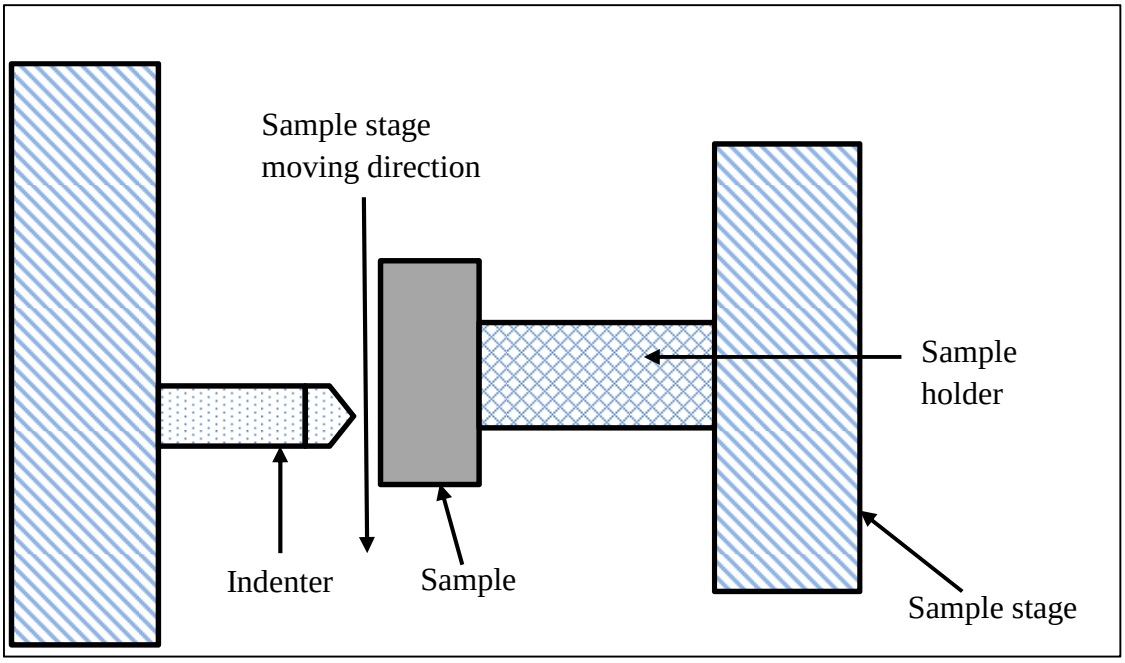

Figure 3.9: A schematic diagram of a typical scratch test.

In measuring coating layer thickness using micro-scratch system, a single pass topography scan at 1 mN load and a scanning length of approximately 220 µm was applied starting from the coating surface and ending at the framed surface. Figure 3.10 shows a typical topography scan for measuring coating thickness.

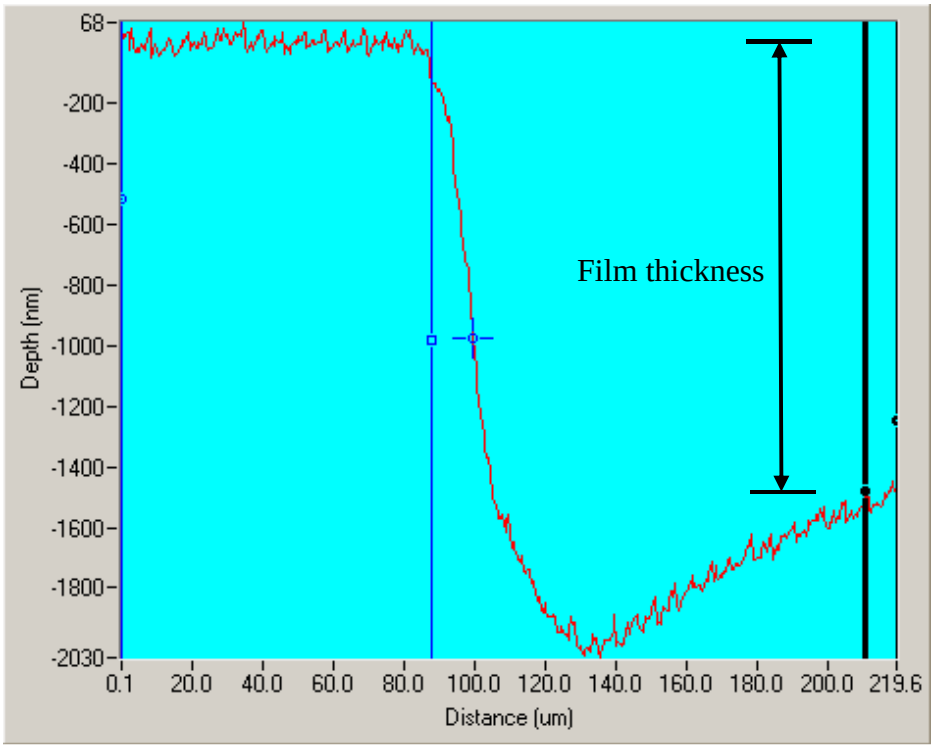

Figure 3.10: Coating topography scan of Ti/TiO_2/TiN coating on HSS substrate.

Coating thickness measurement using micro-scratch system only can be used for measuring thickness of single coating layer and total thickness of multiple coating. Thus for this particular study, Focused Ion Beams (FiB) method is used to evaluate the thickness of each layer of Ti/TiO_2/TiN coating, FiB systems operate in similar principle with scanning electron microscope (SEM). However, FiB systems use a finely focused ion beams (usually gallium) instead of electrons beam used in SEM. FiB systems frequently used as a micro- and nano-machining tool, to modify or machine work pieces in micro- and nano- scale. In this study, FiB system was used to evaluate the coating layer thickness of Ti/TiO_2/TiN. A cross section of 2 µm depth was created using FiB technique with milling voltage of 2.0 kV. The thickness of each coating layer was measured in SEM mode. Figure 3.11 and Figure 3.12 show the cross-section created using FiB technique and the measured values of each coating layer thickness for Ti/TiO_2/TiN coating deposited onto HSS substrate.

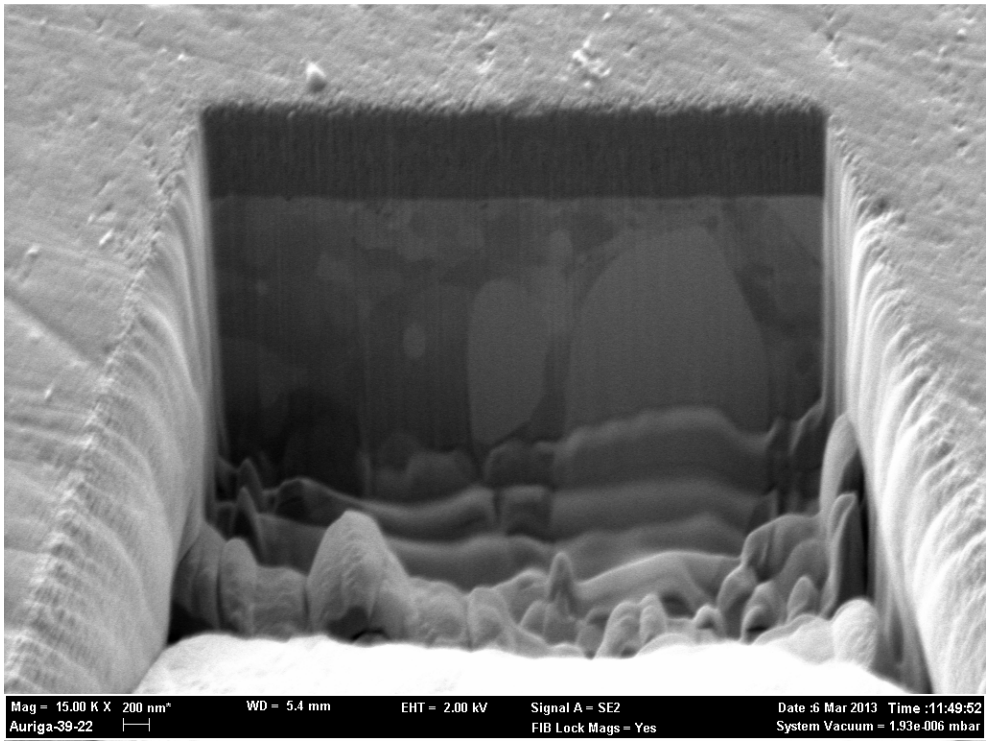

Figure 3.11: Cross-section with 2 µm depth created using FiB.

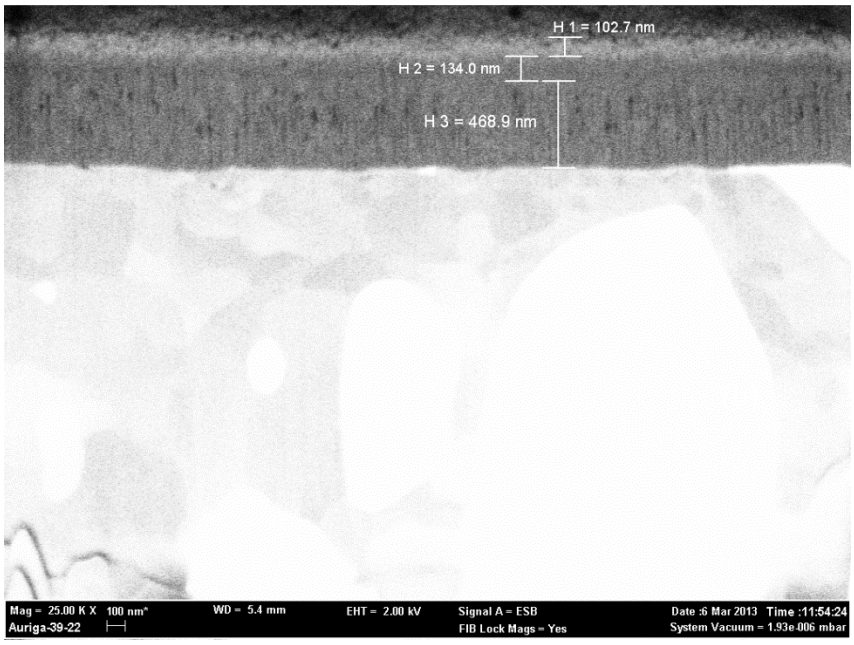

Figure 3.12: Measured values of coating layer thickness of Ti/TiO_2/TiN coatings.

3.4.2 Adhesion strength evaluation

To evaluate the adhesion of coatings on HSS and SS substrates, the scratch test been used. In this method a loaded spherical tip is drawn across the coating surface. The load is increased step by step until coating failure occurs. The minimum load at which adhesive failure occurs (critical load) is taken as a measure of the film adhesion.

In this work, Micro Material Nano Test (Wrexam, UK) micro-scratch system with a diamond probe been used. Multi-pass wear experiment was performed on each sample to evaluate topography of the coating before scratch, during scratch and after scratching. Each sample were scratch at least 3 times using a scan speed, scanning length, loading rate and maximum load of 2 μm/sec, 900 μm, 4.0 mN/sec and 1500 mN, respectively. The critical load was recorded when a sign of failure either cohesion or adhesion was detected. The scratch paths were then analyzed using optical microscope to conform the present of failure. Figure 3.13

shows the typical scratch profile of TiN coating on HSS substrate and the scratch track observed using optical microscope.

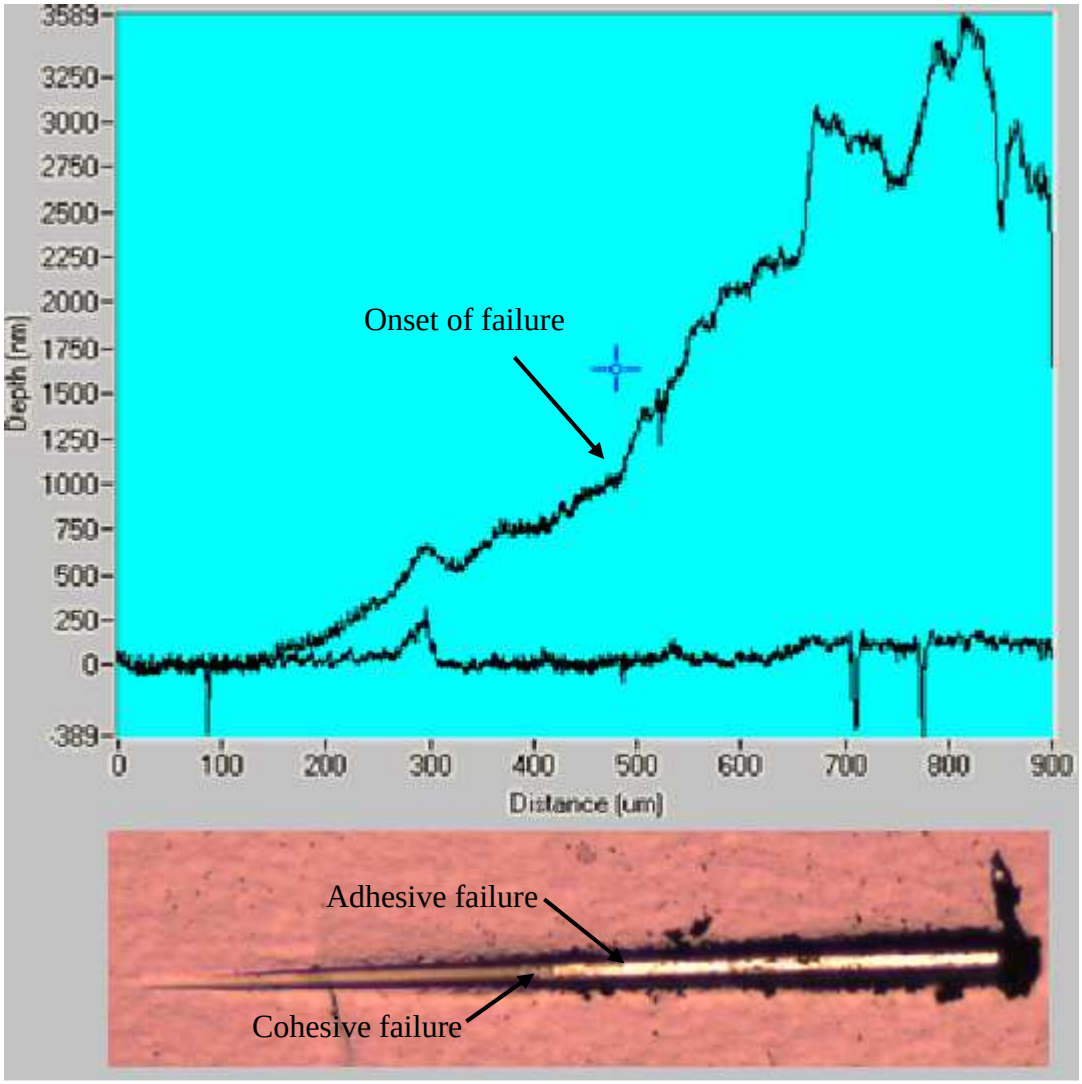

Figure 3.13: Scratch profile of TiN coating deposited onto HSS substrate and the scratch track observed using optical microscope.

3.4.3 Coating hardness

The composite microhardness of the uncoated and Ti/TiO_2/TiN coated HSS and SS samples, at different deposition parameters (substrate temperature, coating thickness, surface condition) and annealed samples were measured using Shimadzu Microhardness tester HMV-2 (see Figure 3.14) with Vickers indenter. The load was 1.961 N (HV0.2) with a dwell time of 5

seconds. The hardness of each samples were measured at least three times and the average hardness values were calculated. The hardness values of coated samples were then compared with uncoated samples to conclude any discrepancies.

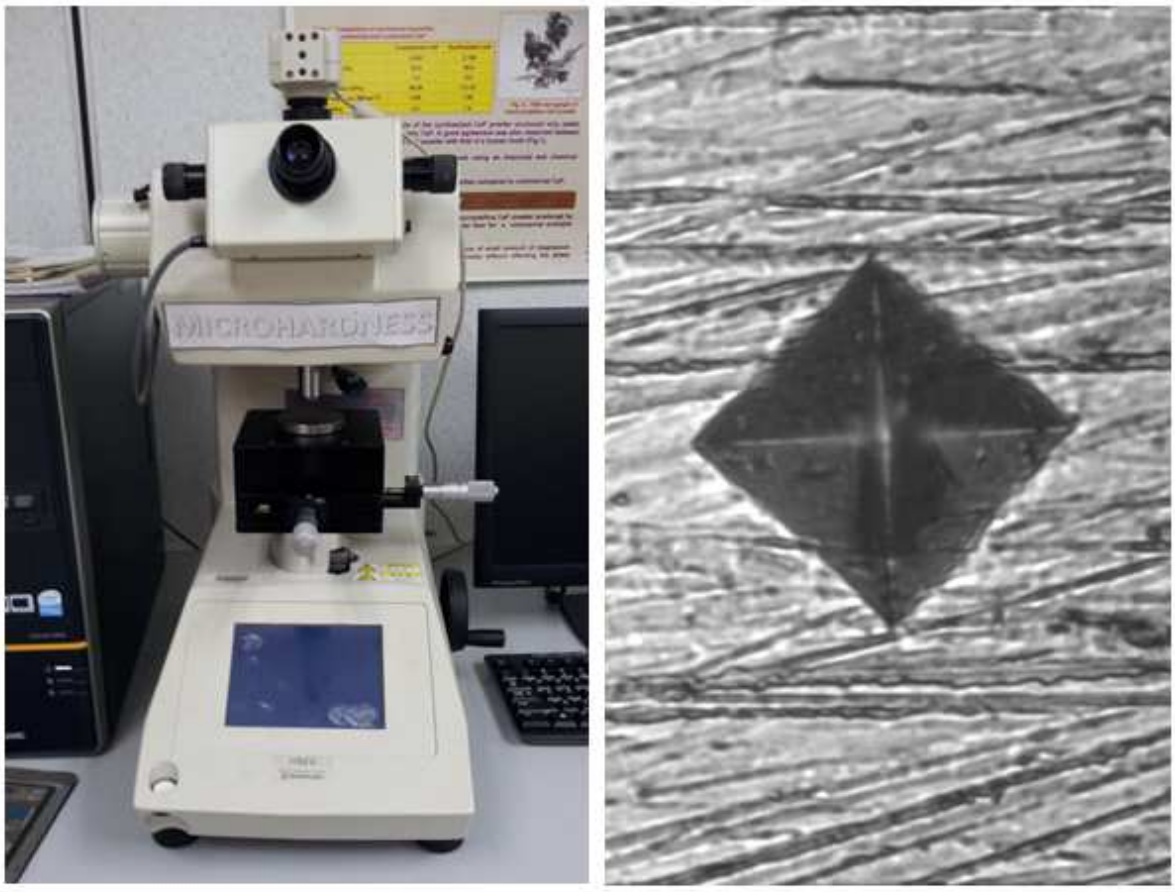

(a) (b)

Figure 3.14: (a) Shimadzu Microhardness tester HMV-2; (b) Indentation image using Vickers indenter at 1.961 N (HV0.2) on HSS substrate.

3.4.4 Morphology and chemical composition evaluation

Surface morphologies of the coated samples were investigated using a field emission scanning electron microscope (FESEM) Auriga Zeiss. The chemical compositions of the coatings were assessed using SEM XL40 EDAX analysis, three spots in each sample. The hardness of the coated and uncoated samples was measured using Shimadzu HMV-2 Micro-hardness tester. In order to check the crystallinity of the as-deposited coatings, X-ray diffraction (XRD) analysis was carried out with a Empyrean PANalytical diffractometer using Cu $K\alpha_1$

(0.154060 nm) radiation at 40 mA and 45 kV. The coatings were scanned in the standard $\theta - 2\theta$ geometry from 20 to 120 with a 0.0260 step size. Surface image after scratch test were analyzed using a light optical microscope to the scratch pattern of coated samples.

CHAPTER 4

RESULTS

4.1 The effect of implementing Ti and TiO_2 as interlayer on adhesion strength improvement of TiN coating.

4.1.1 Structure and composition

X-ray diffraction patterns (XRD) for Ti/TiO_2/TiN coating deposited onto HSS and SS samples revealed that the coatings is initially amorphous and developed into crystalline structure. The XRD patterns show a number of peaks which indicates the presence of TiN, TiO_2, Ti and Fe phases. In Figure 4.1, XRD patterns exhibited strong diffraction peaks at $2\theta = 42.5^0$ indicating TiN phase oriented along (2 0 0) plane for both coating deposited on both substrate. TiO_2 peaks were detected at $2\theta = 36.9^0$ for both substrates and belong to (1 0 3) plane. Similar results were reported by Kasetsart (2008). TiO_2 structure observed was polycrystalline having anatase phase only which in agreement with that compile in the Joint Committee on Powder Diffraction Standards (JCPDS) 84-1286 file. Ti peak was observed at $2\theta = 40^0$ and strongly oriented in (1 0 1) direction. Fe peak was detected at $2\theta = 44.7^0$ oriented along (1 0 1) plane belonging to the substrate which was visible to all coatings. The intensity of TiO_2 phase was significantly low for coating deposited on SS substrate.

The crystallite dimension D, is estimating according using Debye-Scherrer's formula given by following equation.

$$D = \frac{0.9\,\lambda}{B\cos\theta} \qquad (4.1)$$

Where λ is the X-ray ($K\alpha_1$) wavelength ($\lambda = 1.5406\,nm$), θ is the Bragg diffraction angle and *B* is the line width at half-maximum height (FWHM). The crystallite size obtained using this formula is 16.3 nm for anatase TiO_2, 28.8 nm for Ti and 38.7 nm for TiN.

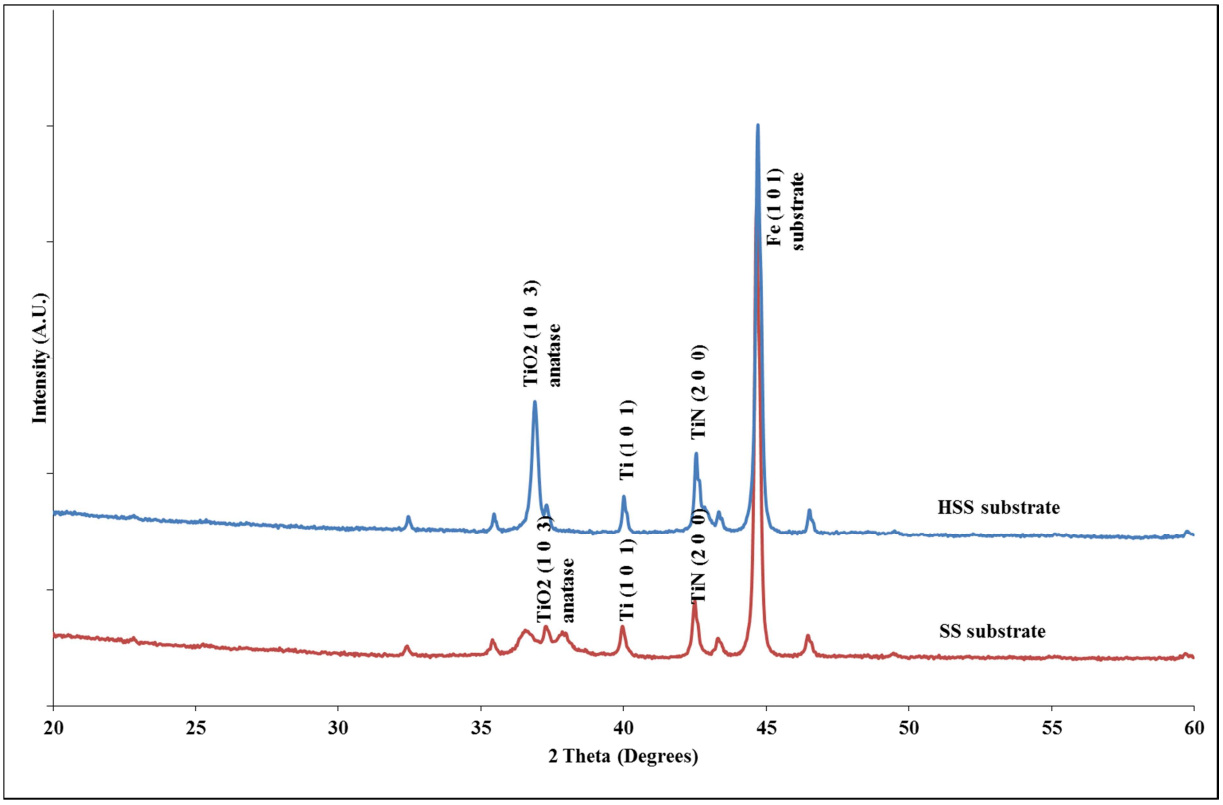

Figure 4.1: X-ray diffraction pattern of Ti/TiO_2/TiN samples deposited on HSS and SS substrates.

The present of Ti, TiO_2 and TiN phase in Ti/TiO_2/TiN coating systems were confirmed with energy dispersive X-ray spectroscopy (EDX) analysis on HSS and SS samples. Figure 4.2 (a) and (b) show the EDX spectrum of the coatings deposited on HSS and SS coatings. The analysis revealed the coating samples are comprised of Titanium (Ti), Oxygen (O), Nitrogen (N), Ferum , Manganese (Mn), Copper and Zinc (Zn). Fe, Mn, Cu and Zn are the contribution from the substrates. Ti phase in both samples show higher intensity compared to nitrogen and oxygen due to higher thickness of Ti coating layer. The traces of nitrogen and oxygen in the analysis confirmed the present of TiN and TiO_2 coating layer in the coating-substrate systems.

The composition of Ti, oxygen and nitrogen on the coated film for both substrates can be summarized in Figure 4.3. For HSS coated substrate, the composition of coating films were Titanium (17.02 At%), Nitrogen (51.84 At%) and Oxygen (8.91 At%) along with the traces of Fe (20.3 At%). For SS coated substrate, the composition of coating films were Titanium (16.25 At%), Nitrogen (37.88 At%) and Oxygen (16.2 At%) along with the traces of Fe (25.58 At%).

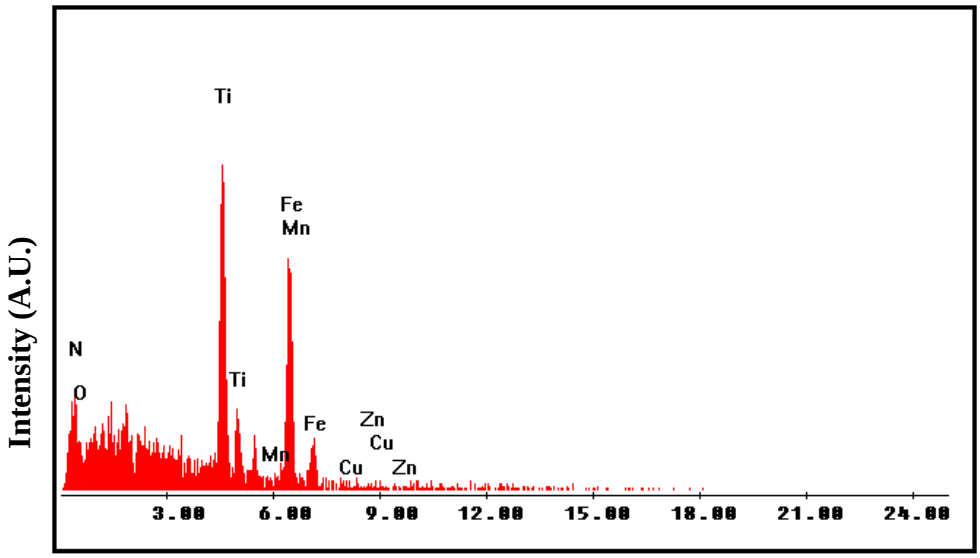

(a)

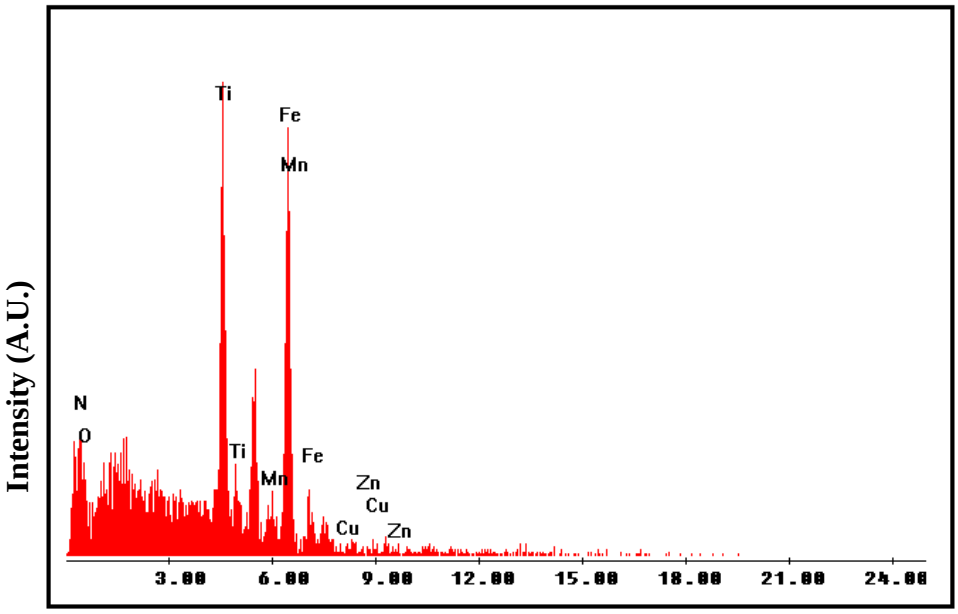

(b)

Figure 4.2: EDX spectrum of Ti/TiO_2/TiN coating deposited onto (a) HSS and; (b) SS substrates.

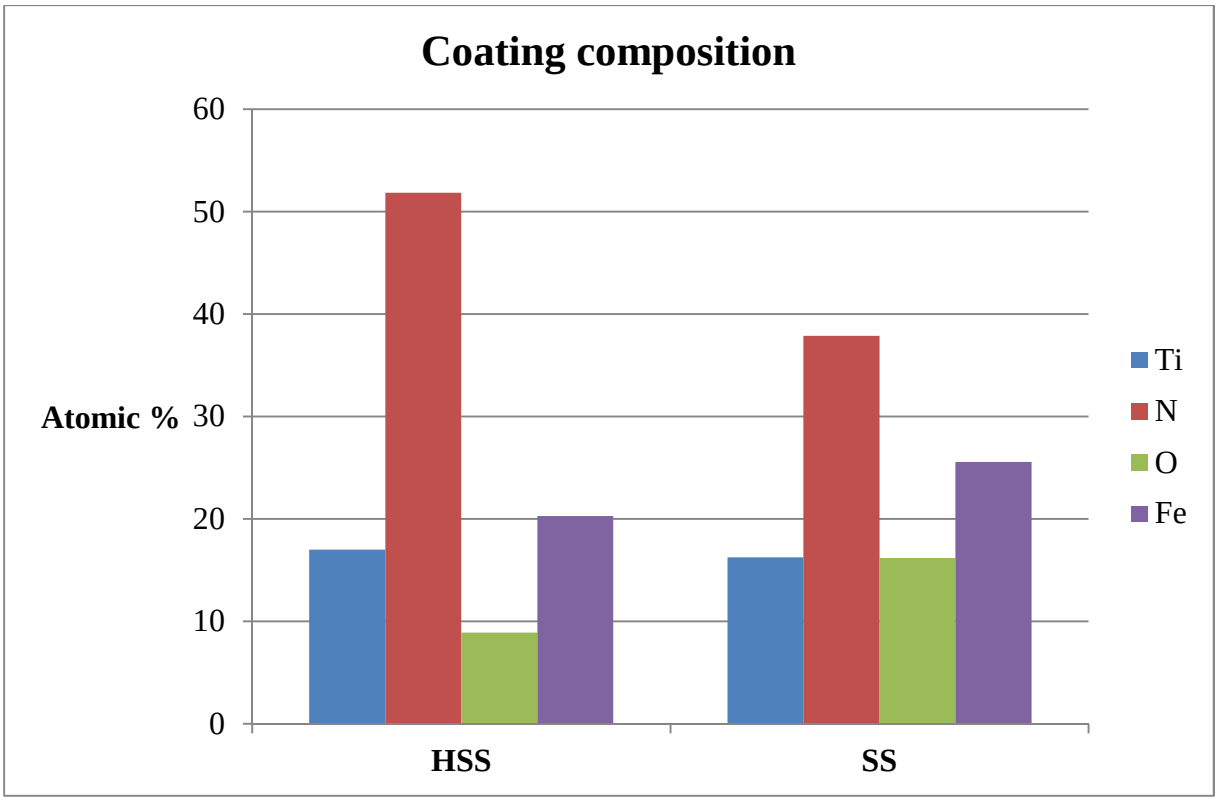

Figure 4.3: Atomic percentage of Titanium (Ti), Nitrogen (N) and Oxygen (O) along with Ferum (Fe) for both coated HSS and SS substrates.

Figure 4.4 shows optical images of coating surfaces on HSS substrate. All coating layers were deposited at substrate temperature 200 °C and D.C power of 150 W. Deposition time for TiN and TiO_2 coating layers were 3600 s. Ti coating layer was deposited for duration of 2400 s. Other parameters for deposition process were summarized in Table 3.1. The deposited coatings had non-transparently uniform and dense films, no sign of cracks and delamination were observed. The colors of the coatings depend on the ratio of nitrogen and oxygen gas used through the deposition process. For TiN coating, golden bronze color was observed which is a typical color for TiN. The present of intermediate Ti coating layer does change the coating color to dark bronze color. The color of single layer Ti coating observed was silver. The addition of TiO_2 coating layer into Ti/TiN changed the coating color to violet bronze color.

Similar optical microscope results were observed for coating deposited on SS substrate. The coating also had non-transparently and dense film and no sign of cracks as well as delamination observed. In terms of coating uniformity, coatings deposited on SS seem to be varied in thickness. This may be due to rougher SS surface compared to HSS.

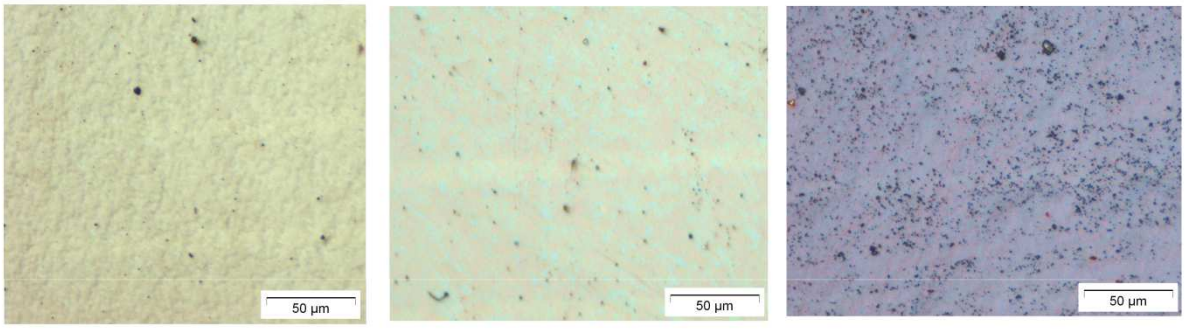

(a) (b) (c)

Figure 4.4: Optical microscope image of coating films deposited on high speed steel (HSS) (a) TiN coating; (b) Ti/TiN coating and; (c) Ti/TiO_2/TiN coating.

Figure 4.5 shows field emission scanning electron microscope (FESEM) images of Ti/TiO_2/TiN coatings on high speed steel (HSS) and stainless steel (SS) substrates. From the figure, it can be observed that coatings were more uniformly distributed on HSS substrate as compared to SS substrate. Figure 4.5 (a) and (b) show the microstructure (FESEM top view) of Ti/TiO_2/TiN coating on HSS substrate. It can be seen that the coating layer is made of small grains of hexagonal crystallite of approximately 38.7 nm size which represent TiN coating.

As shown in FESEM cross-section of Ti/TiO_2/TiN coated samples (Figure 4.6), the complete growth of coating-substrate system produced flakes that are overlapped, arranged as in network which may contribute to enhancement of adhesion strength.

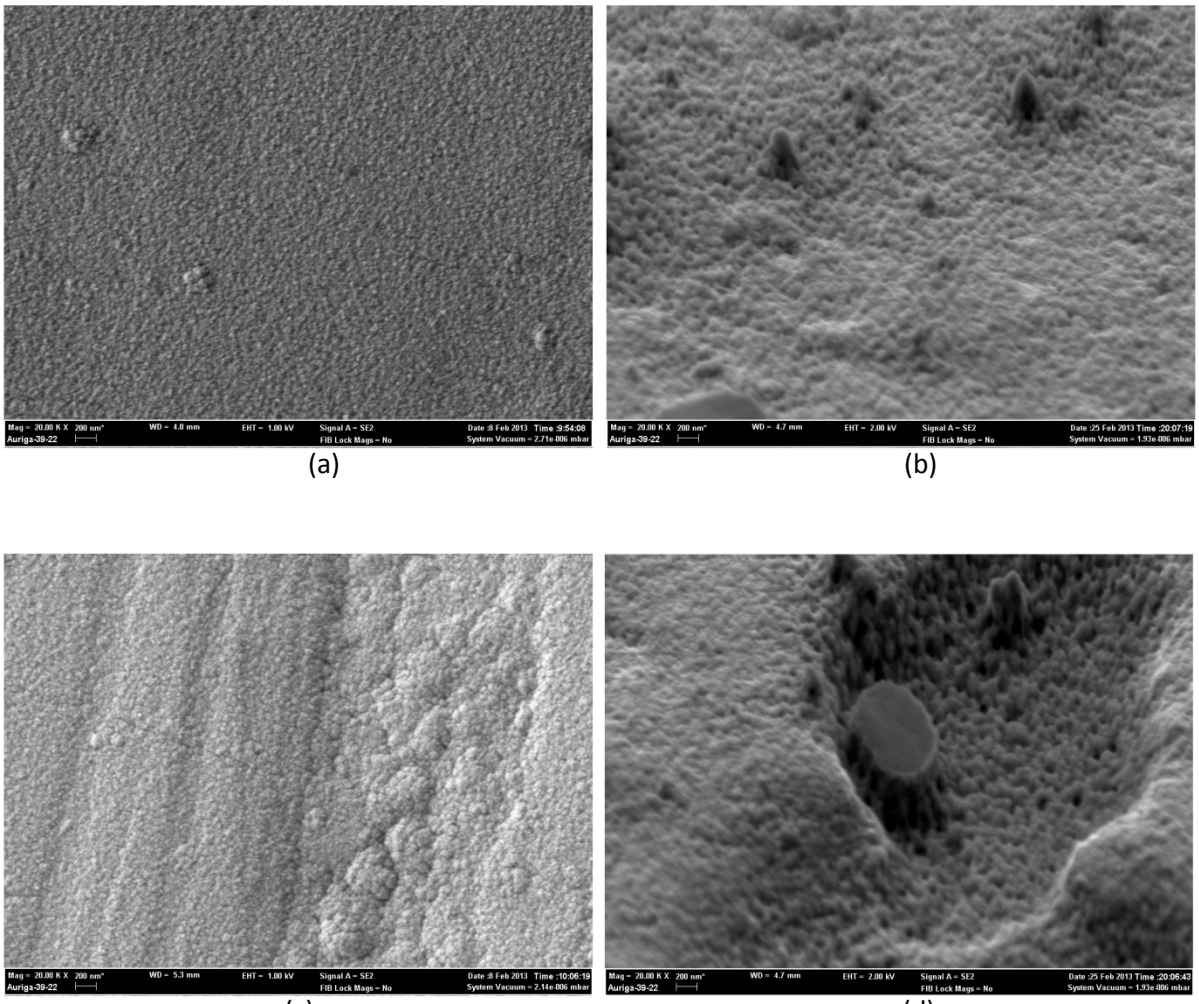

Figure 4.5: Field emission scanning electron microscope (FESEM) images of $Ti/TiO_2/TiN$ coatings on high speed steel (HSS) and stainless steel (SS) substrates at deposition temperature of 200^0C and DC power of 150 kW; (a) and (b) $Ti/TiO_2/TiN$ deposited onto HSS substrate and; (c) and (d) $Ti/TiO_2/TiN$ coatings deposited onto SS substrate.

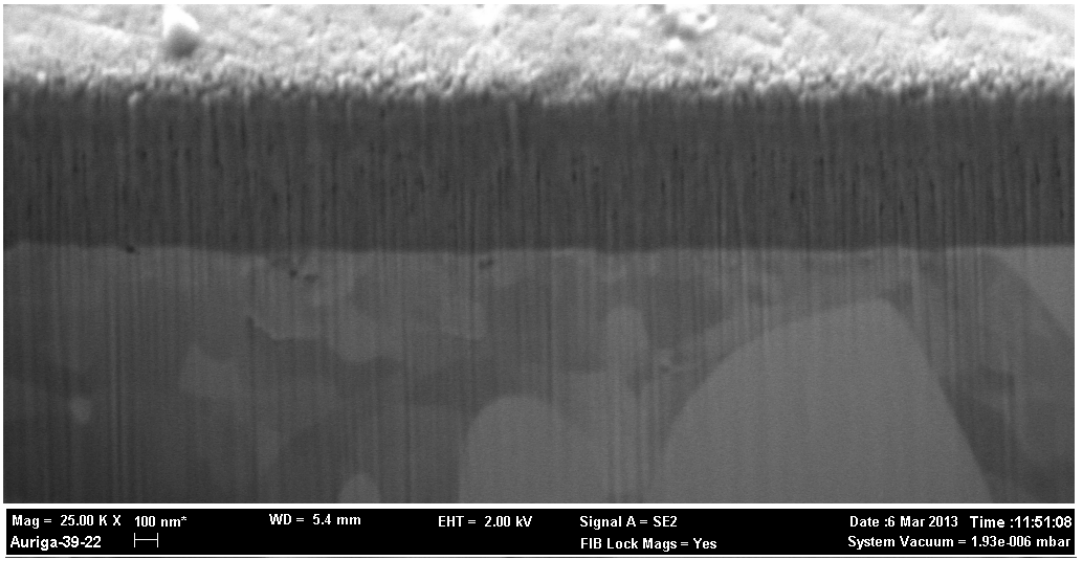

Figure 4.6: FESEM cross section of $Ti/TiO_2/TiN$ coated HSS samples.

4.1.2 Film thickness, adhesion strength and coating hardness

The thickness of Ti/TiO_2/TiN coatings was measured using micro-scratch system and focus ion beam (FiB) method. Due to limitation of micro-scratch system in measuring each coating layer thickness, FiB method was used to evaluate the each coating layers thickness. Micro-scratch system was used to measure the total coating thickness for each coating-substrate systems as summarized in Table 4.1. For single layer Ti coatings, the total thickness measured was 511.15 nm and 532.25 nm for coated HSS and SS respectively. The result was confirmed with FiB method (see Figure 4.7). The thickness of Ti coating layer found to be 504.7 nm. The Ti coating deposition rate was 12.62 nm/min for deposition time of 2400 s, D.C power of 150 W and Argon (Ar) gas flow of 40 sccm. The Ti coating layer thickness was similar with the Ti thickness found by Bushroa et al. (2011) for deposition Ti interlayer of Ti/TiSiN coating system by D.C magnetron sputtering method at deposition time of 2400 s, D.C power of 100 W and Ar gas flow of 40 sccm. The results obtained in this work suggested that the increase of sputtering power from 100 W to 150 W has marginal effect on the deposition rate of the coating.

The thickness of TiN coating measured by micro-scratch system was found to be 185.30 nm and 178.45 nm for coated HSS and SS, respectively. The TiN coating thickness evaluated using FiB method was 174.2 nm with the deposition rate of 2.90 nm/minute. The deposition of TiN coating was done for duration of 3600 s, D.C power of 150 W and gas flow ratio of 14:8.4 (Ar:N_2) sccm.

The thickness of TiO_2 coating was measured as 165.2 nm using FiB method. The total thickness of Ti/TiN coating system measured by micro-scratch system was found to be 712.10 nm and 686.20 nm for coated HSS and SS substrate, respectively. The total thickness of Ti/TiO_2/TiN coating was 852.50 nm and 825.45 nm for HSS and SS, respectively. The

deposition rate for each coating layers were calculated from the coating thickness and deposition time. Deposition rate for TiO_2 coating was 165.2 nm/min. The parameters used for deposition and the coating thickness of Ti, TiN and TiO_2 coating were summarized in Table 4.2.

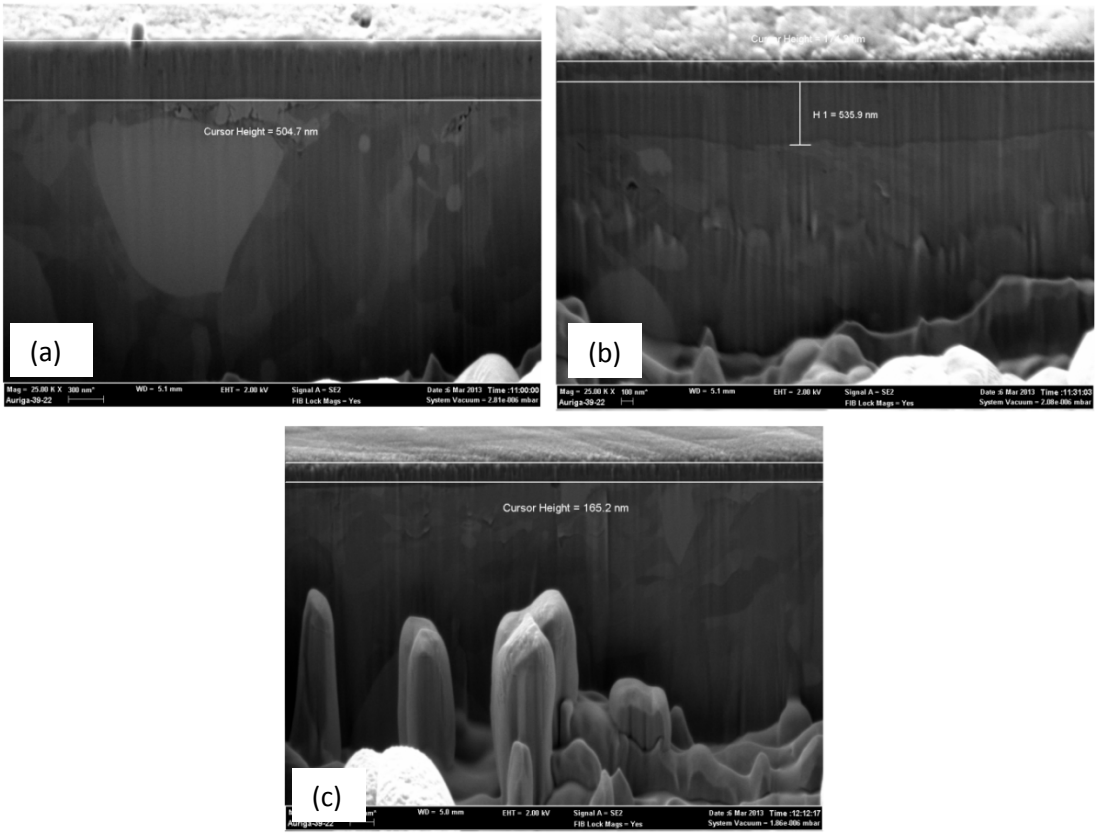

Figure 4.7: FiB images of samples cross-section and coating thickness measured for (a) Ti coating; (b) Ti/TiN coating and; (c) TiO_2 coating.

Table 4.1: Total coating thickness measured from topography mode using micro-scratch system.

Sample No.	Coatings*	Substrates	Total Deposition Time	Total thickness (nm)
1	Ti	HSS	2400 s	511.15
		SS	2400 s	532.25
2	TiN	HSS	3600 s	185.30
		SS	3600 s	178.45
3	Ti/TiN	HSS	6000 s	712.10
		SS	6000 s	686.20
4	Ti/TiO_2/TiN	HSS	9600 s	852.50
		SS	9600 s	825.45

Table 4.2: Summary of the Ti, TiN and TiO_2 coating layer thickness measured using FiB technique.

Parameters	TiN coating	TiO_2 coating	Ti coating
Flow gas (sccm)	14:8.4(Ar:N_2)	40:8(Ar:O_2)	40 (Ar)
D.C power, *P* (W)	150	150	150
Deposition temperature (^{0}C)	200	200	200
Deposition time (s)	3600	3600	2400
Thickness (nm)	174.2	165.2	504.7
Deposition rate (nm/min)	2.90	2.75	12.62

The critical load of the studied Ti/TiO_2/TiN coating was determined by the micro-scratch tests combined with the observation of the scratch tracks under the optical microscope. Three different micro-scratch tests were performed for each deposited substrates at substrate temperatures of 200 °C and all the tests give consistent results. Figure 4.8 shows the adhesion strength of TiN, Ti/TiN and Ti/TiO_2/TiN coating deposited on HSS and SS substrate. Ti/TiN coatings show good adhesion compared to TiN for both HSS and SS substrate. The adhesion strength improvement proved that Ti interlayer has beneficial effect on the adhesion strength of single layer TiN coating. The results were in agreement with the findings by Helmersson et al. (1985) on the adhesion of the films increased with the use of an intermediate layer of pure titanium in between TiN coating and substrates. Further improvement on the adhesion strength can be observed with the use of TiO_2 as intermediate layer deposited in between TiN and Ti coating layer. The adhesion strengths of Ti/TiO_2/TiN coatings were 1417.19 mN and 1264.46 mN for HSS and SS substrates, respectively. It is also observed that Ti/TiO_2/TiN coatings deposited on SS substrate exhibited higher adhesion strength compared to coatings on HSS substrate. Table 4.3 summarized the critical loads and respective scratch distance measured with optical microscope.

Optical micrographs of the scratch scars on TiN, Ti/TiN and Ti/TiO_2/TiN are shown in Figure 4.9. It is observed that each scratch track gets wider uniformly with progressively increasing load. From the analysis of the scratched samples, the scratch track for each coating-substrate

systems revealed cohesive (coating is destroyed within the coating itself) and adhesive failure (coating is removed from the substrate).

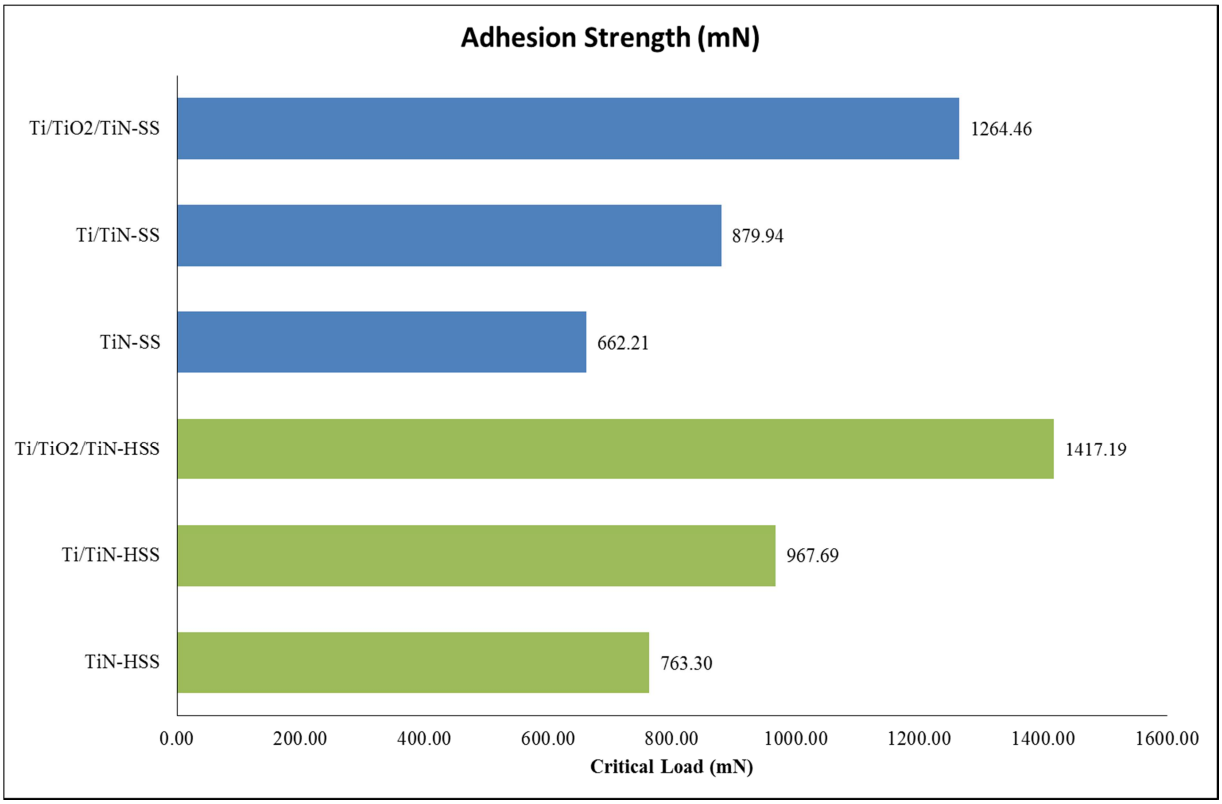

Figure 4.8: Adhesion strength of TiN, Ti/TiN and Ti/TiO_2/TiN coatings deposited onto HSS and SS at deposition temperature 200^0C and D.C power of 150 W.

Table 4.3: Critical load values for TiN, Ti/TiN and Ti/TiO_2/TiN as-deposited coatings.

No.	Sample Name	Substrate	Coating	Critical Load (mN)	Scratch distance (µm)
1	TiN-HSS	HSS	TiN	763.30	479.23
2	Ti/TiN-HSS	HSS	Ti/TiN	967.69	578.89
3	Ti/TiO2/TiN-HSS	HSS	Ti/TiO2/TiN	1417.19	797.92
4	TiN-SS	SS	TiN	662.21	420.50
5	Ti/TiN-SS	SS	Ti/TiN	879.94	533.70
6	Ti/TiO2/TiN-SS	SS	Ti/TiO2/TiN	1264.46	721.22

Figure 4.9 illustrates the coating failure for TiN, Ti/TiN and Ti/TiO_2/TiN coating deposited on HSS and SS substrates, respectively. From the figure, it is observed that the coatings exhibit cohesive failure followed by complete delamination of the coating (adhesive failure).

The cohesive failure of a coating is mainly accompanied by partial conical cracks and some debris at the side of the scratch tracks. The complete delamination of films is due to the interfacial failure at the coating-substrate interface.

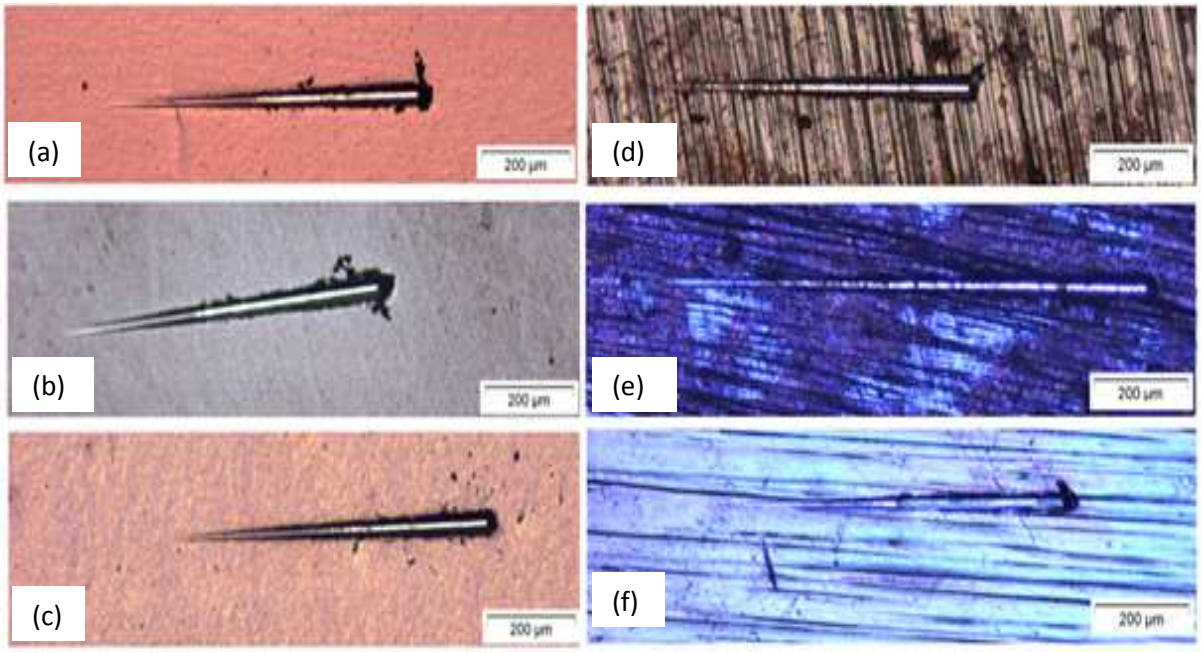

Figure 4.9: Scratch tracks of as-deposited coatings on HSS and SS substrates; (a) TiN-HSS coatings; (b) Ti/TiN-HSS coatings; (c) Ti/TiO_2/TiN-HSS coatings; (d) TiN-SS coatings; (e) Ti/TiN-SS coatings and; (f) Ti/TiO_2/TiN-SS coatings.

Figure 4.10 shows scratch track of as-deposited Ti/TiN/TiO_2 coatings on HSS and SS substrates. It can be seen from figure, both coated substrates undergone similar mechanism of failure. As the normal load increases, parallel cracks starting to occur followed by semicircular cracks. As normal load increases further, external transverse cracks and coating chipping were observed. Prior to complete removal of coating (adhesive failure), coating spalling was developed. Figure 4.11 shows the schematic illustration of coating failure observed during scratch test on Ti/TiO_2/TiN coating deposited onto HSS and SS substrate.

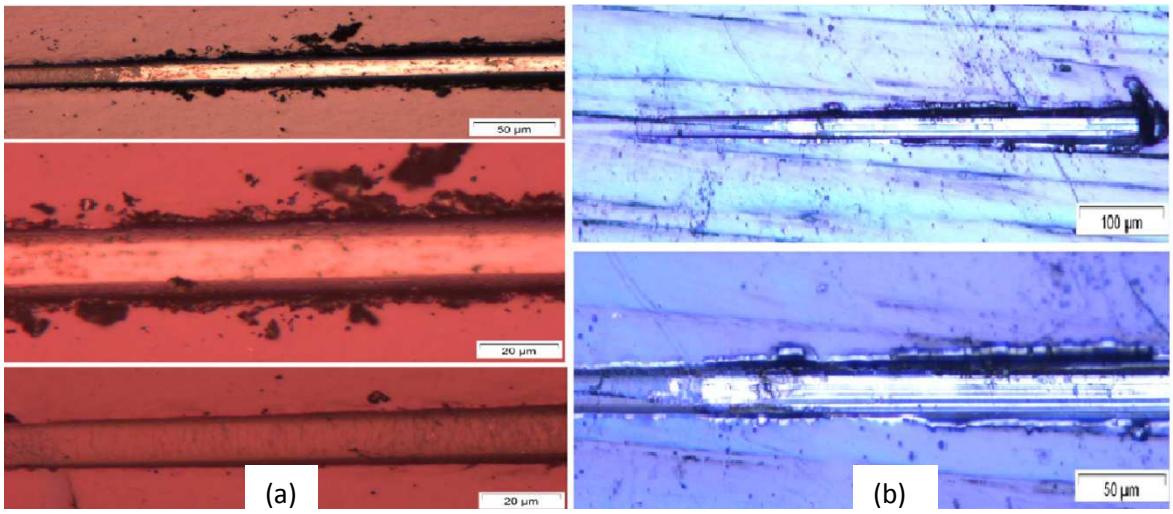

Figure 4.10: Scratch tracks of as-deposited Ti/TiN/TiO_2 on HSS and SS substrates at higher magnification; (a) Ti/TiO_2/TiN on HSS and; (b) Ti/TiO_2/TiN on SS substrate.

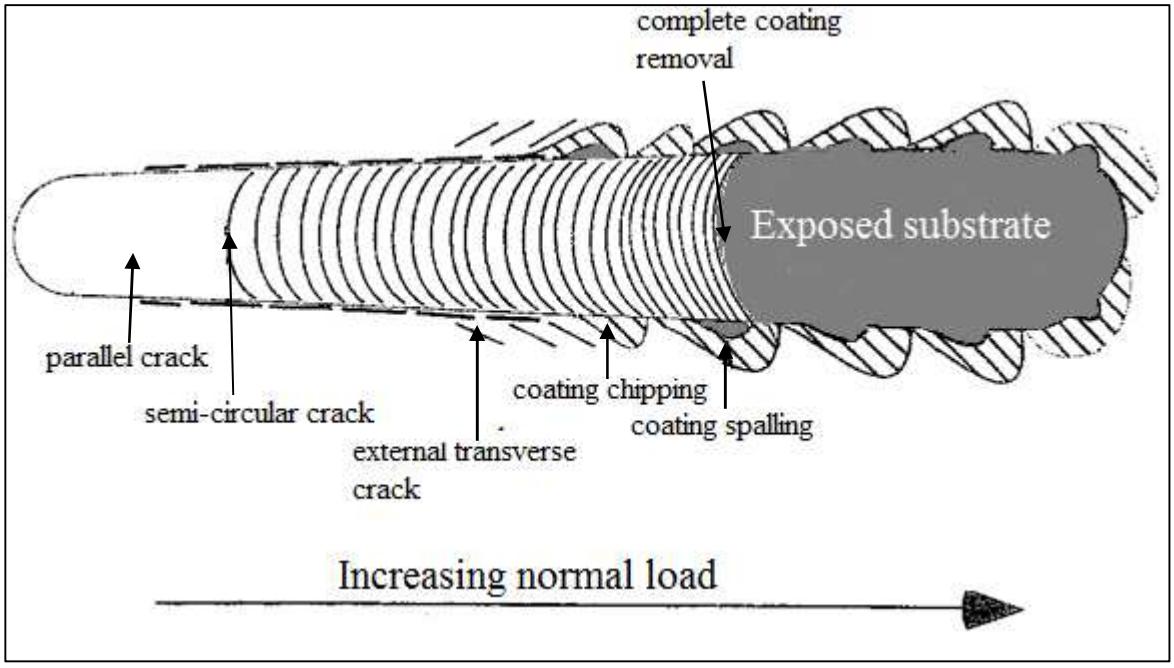

Figure 4.11: Schematic illustration of coating failures observed during scratch testing of Ti/TiO_2/TiN coatings on HSS and SS substrate.

The hardness of TiN, Ti/TiN, Ti/TiO_2/TiN coatings and the substrate are shown in Figure 4.12. For HSS substrate, single layer TiN coating and Ti/TiN coating show high hardness compared to the substrate. The highest hardness of 2790 MPa was obtained for single layer

TiN coating. A slight decrease in hardness value was observed for Ti/TiN coatings. The hardness value obtained for Ti/TiO_2/TiN coating was 2628 MPa which is lower than TiN coating.

For SS substrate, the hardness value for Ti/TiO_2/TiN and TiN coating were 3401 MPa and 3464 MPa, respectively. A significant decrease in hardness value was observed for Ti/TiN coating. The hardness value for Ti/TiN coating was 3164 MPa. The results show that the inclusion of Ti and TiO_2 interlayer coating deposited at 200 °C does not improve the hardness of TiN coating-substrate systems.

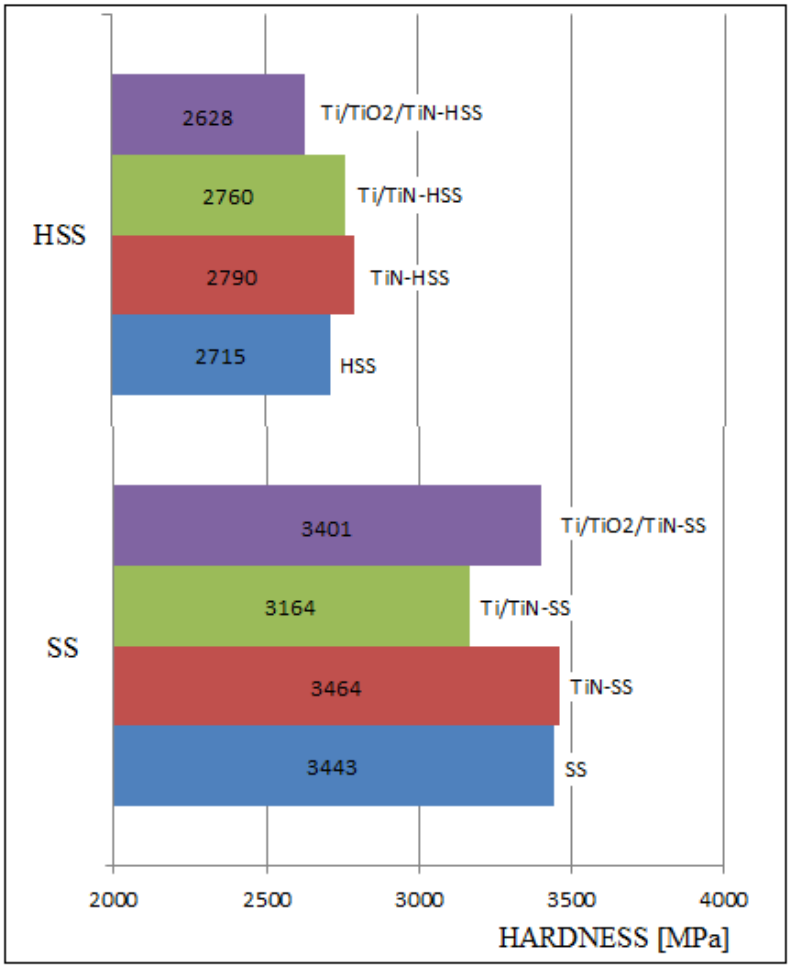

Figure 4.12: Hardness values of HSS and SS substrates and composite hardness of coating deposited at deposition temperature of 200 °C measured using Shimadzu Microhardness tester HMV2.

The internal stress, σ of the coating was estimated by using the following equation;

$$\sigma = \frac{E}{2\nu} \text{ x } \frac{d_0 - d}{d_0} \quad (4.2)$$

Where *E* is Young`s moduli, *d* is a measured lattice spacing, $d_0$ is an unstressed lattice spacing obtained from JCPDS data for TiN and *v* is the Poisson`s ratio. The Poisson`s ratio used in the calculation was $\nu$ = 0.3, cited from the value obtained from the bulk TiN (Kusano et al., 1998b). Young`s moduli of the coating were determined from the unloading portion of the applied force-penetration depth curves of the nano-indentation test. In Table 4.4, internal stress of the TiN, Ti/TiN and Ti/TiO_2/TiN coating are shown based on the lattice spacing and Young`s moduli.

Table 4.4: Internal stresses, σ of TiN coating layers estimated from lattice spacing and Young`s moduli for TiN, Ti/TiN and Ti/TiO_2/TiN.

Sample	Young`s moduli (GPa)	*d* value (nm)	d_o value (nm)	Internal stress, σ (GPa)
TiN-HSS	360	2.12795	2.121	-1.97
Ti/TiN-HSS	380	2.12675	2.121	-1.72
Ti/TiO_2/TiN-HSS	451	2.12538	2.121	-1.55

From estimation of internal stresses, single layer TiN coating provided highest value of stress where σ = 1.97 GPa. The value of internal stress decreased with the existence of Ti and TiO_2 interlayer. The internal stress values for Ti/TiN and Ti/TiO_2/TiN coatings were 1.72 GPa and 1.55 GPa, respectively. All the stresses were compressive.

4.2 The effect of sputtering parameter on the $Ti/TiO_2/TiN$ adhesion strength.

The adhesion strengths of coating-substrate system depend on some other parameters. Some of the sputtering parameters were identified by previous researcher which effect the critical loads of coating-substrate systems and hence the adhesion strength. The parameters included sputtering power, substrate temperature, coating thickness and substrate surface condition. In the present study, the effect of substrate temperature, coating thickness and substrate surface condition on the adhesion strength of $Ti/TiO_2/TiN$ coatings were studied.

Figure 4.13 shows the adhesion strength of $Ti/TiO_2/TiN$ coating deposited on HSS and SS substrate at deposition temperature of 50, 200 and 250 °C. From the figure, it can be seen that $Ti/TiO_2/TiN$ coatings deposited at higher deposition temperature exhibit higher value of critical load. Maximum adhesion strength of 1417.19 mN was observed for coating deposited at 200 °C. Lowest adhesion strength of 1056.16 mN was evaluated for coating deposited at 50 °C. Similar observations were observed for coating deposited on SS substrate. Maximum adhesion strength of 1264.46 mN was observed for coating deposited at temperature 200 °C. Thus, it can be concluded that the optimum adhesion strength of $Ti/TiO_2/TiN$ coatings can be obtained at temperature of 200 °C.

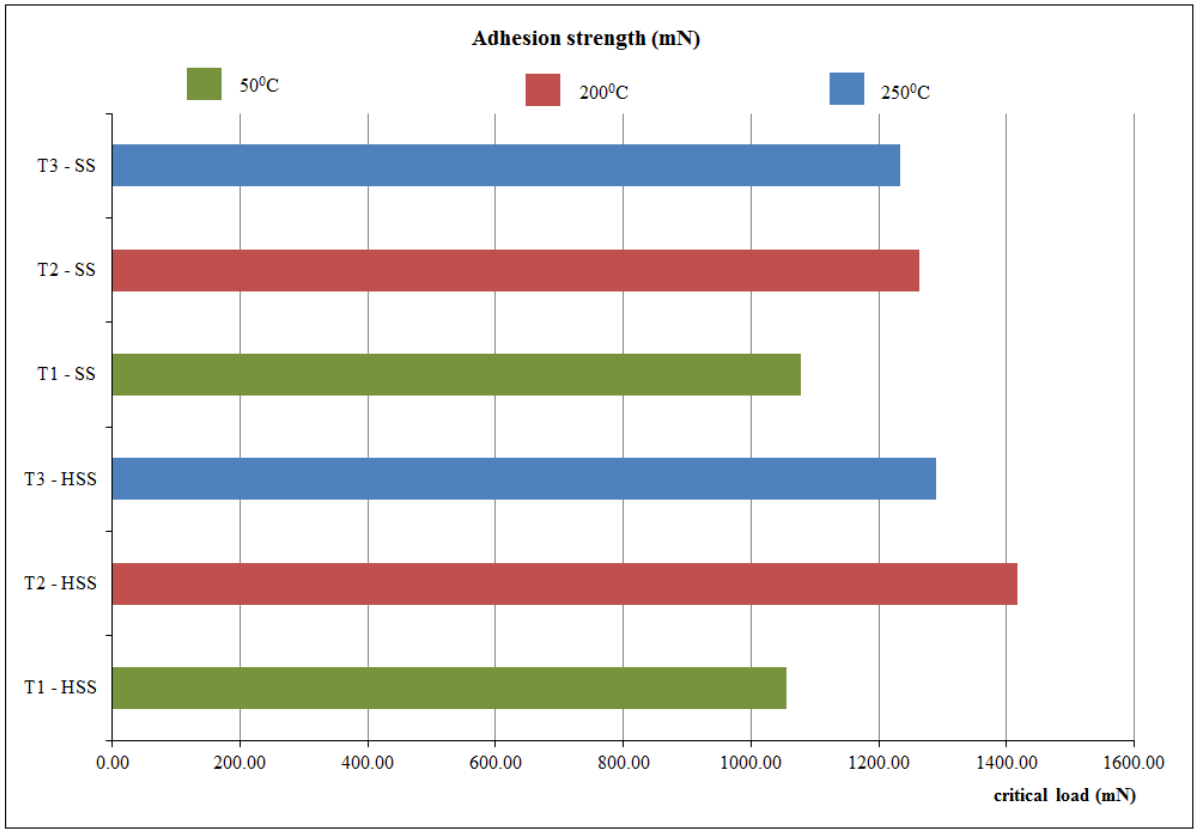

Figure 4.13: Adhesion strength of Ti/TiO_2/TiN coating deposited on HSS and SS substrate at substrate temperature of 50, 200 and 250 °C.

The hardness of Ti/TiO_2/TiN coating deposited at different deposition temperatures are shown in Figure 4.14. The results were compared with the hardness of single layer TiN coating. It can be noticed that, for Ti/TiO_2/TiN deposited HSS substrate, the hardness of the coating increases as the deposition temperature increases from 200 to 250 °C. The hardness was 2969 MPa compared to 2790 MPa for single layer TiN coating. However, different observations were obtained for deposited SS substrate. Maximum coating hardness of 3486 MPa was determined for coating deposited at deposition temperature of 50 °C which is slightly higher that the hardness of single layer TiN coating.

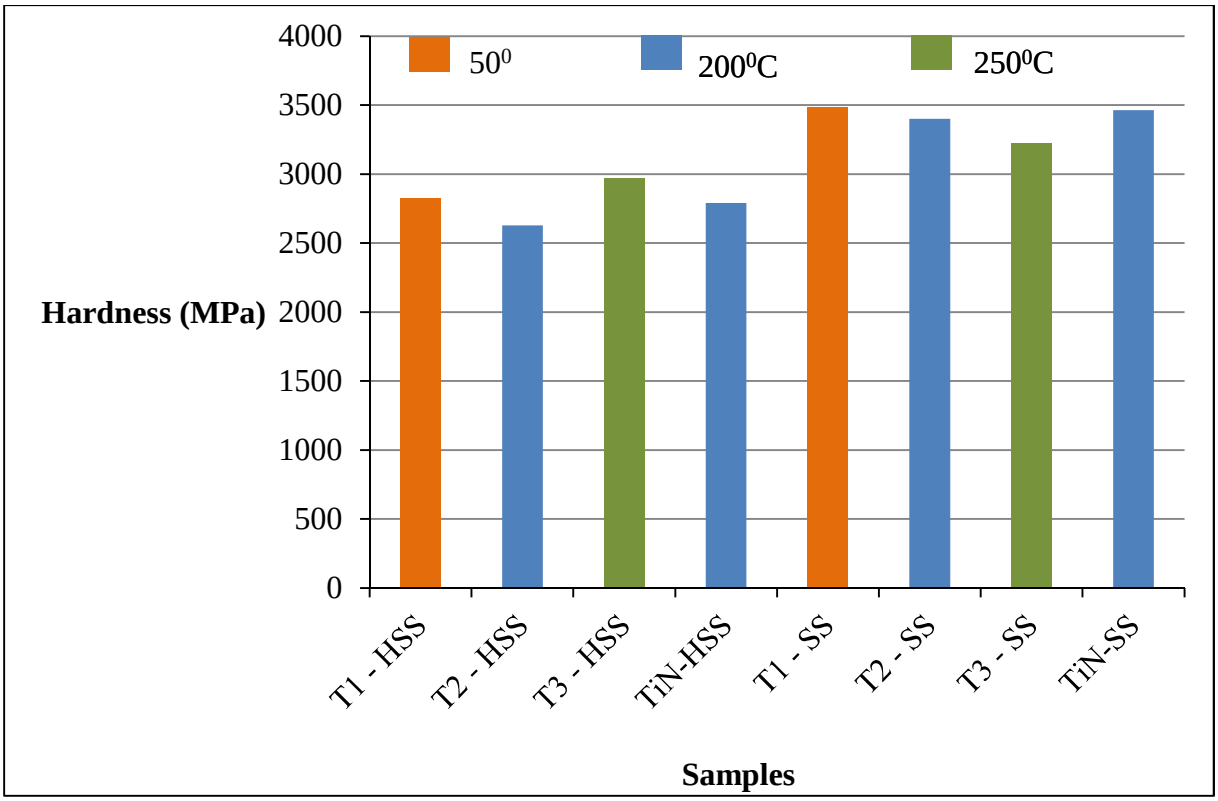

Figure 4.14: Hardness values of HSS and SS substrates and composite hardness of coating deposited at different deposition temperature.

The effects of TiO_2 coating thickness on the adhesion strength and hardness of Ti/TiO_2/TiN coating were illustrated in Figure 4.15. Three different thickness of TiO_2 coating layer were deposited on HSS and SS substrates. The thickness measured was 82.5, 165.2 and 247.5 nm. The adhesion strength of Ti/TiO_2/TiN coating increases as TiO_2 coating thickness increases. The values of critical load measured were 977.08, 1417.19 and 1539.78 mN for 82.5, 165.2 and 247.5 nm TiO_2 coating thickness, respectively. A similar pattern was observed for coating deposited on SS substrate. As the TiO_2 increases, the measured critical load was increases. The measured critical load for coating deposited on SS substrate were 1114.46, 1264.46 and 1366.51 mN for 82.5, 165.2 and 247.5 nm TiO_2 coating thickness, respectively.

For measured coating hardness, the maximum hardness value of 2918 MPa was obtained for coated HSS substrate with 247.5 nm TiO_2 coating thickness. For SS substrate, a maximum

hardness value of 3486 MPa was measured for coating with 165.2 nm thick of TiO_2 coating layer.

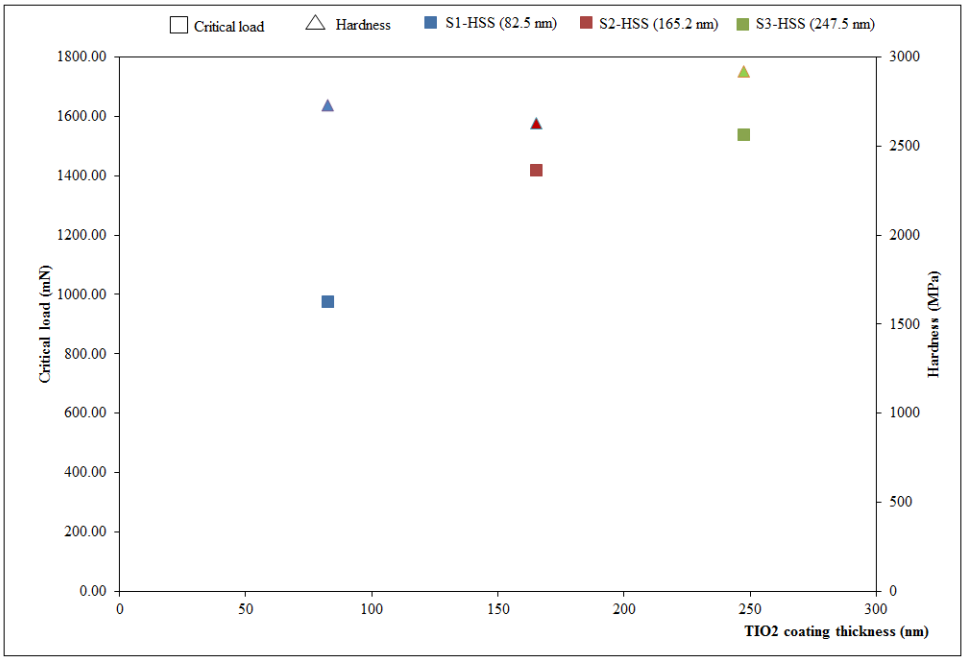

(a)

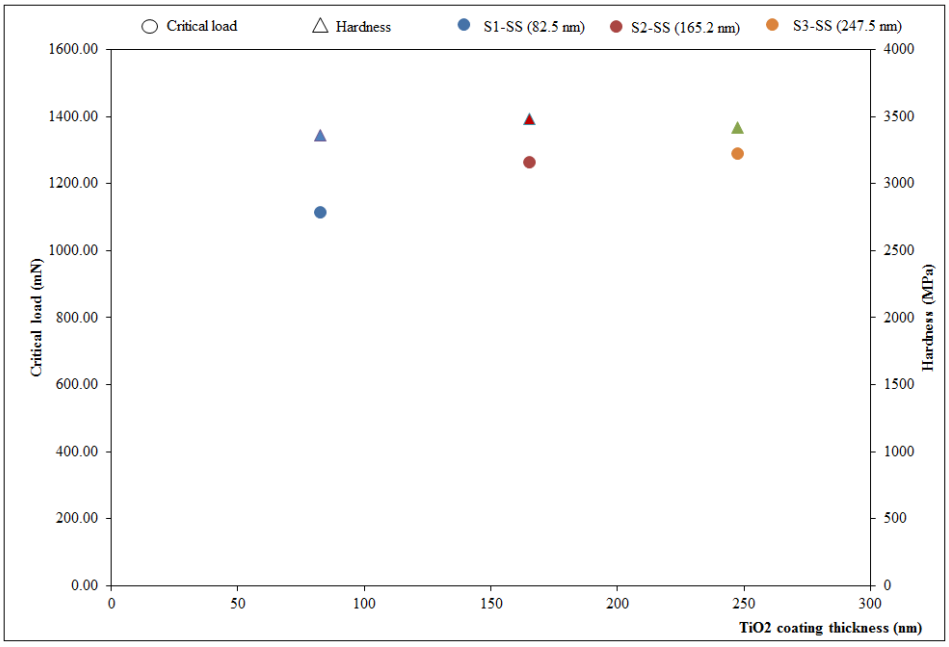

(b)

Figure 4.15: Critical loads and hardness of Ti/TiO_2/TiN coating deposited at 200 °C for different TiO_2 coating thickness; (a) HSS substrate and; (b) SS substrate.

The study on the substrate surface condition was conducted on HSS substrate with four different surface roughnesses. The measured surface roughnesses, Ra for each sample were summarized in Table 4.5.

Table 4.5: Measured surface roughness, Ra of HSS substrate.

No	**Sample**	**Roughness (Ra)**			
		Reading 1 (μm)	Reading 2 (μm)	Reading 3 (μm)	Average (μm)
1	R1-HSS	0.01	0.02	0.02	0.02
2	R2-HSS	0.02	0.03	0.03	0.03
3	R3-HSS	0.30	0.27	0.25	0.27
4	R4-HSS	1.13	1.21	1.25	1.20

Figure 4.16 shows the plot of critical load and coating hardness against substrate surface roughness. The critical load of Ti/TiO_2/TiN coating deposited on HSS decreases with the increases of substrate surface roughness, Ra. Better coating adhesion was observed for coating deposited on smooth substrate surface. The critical loads ranged from 1299.24 mN to 1417.19 mN were observed for substrate surface roughness less than 0.03 μm. For substrate surface roughness more than 0.27 μm, the value of critical load measured was less than 1000 mN. For the coating hardness, no obvious changes were observed in term of coating hardness values as the substrate surface roughness increases.

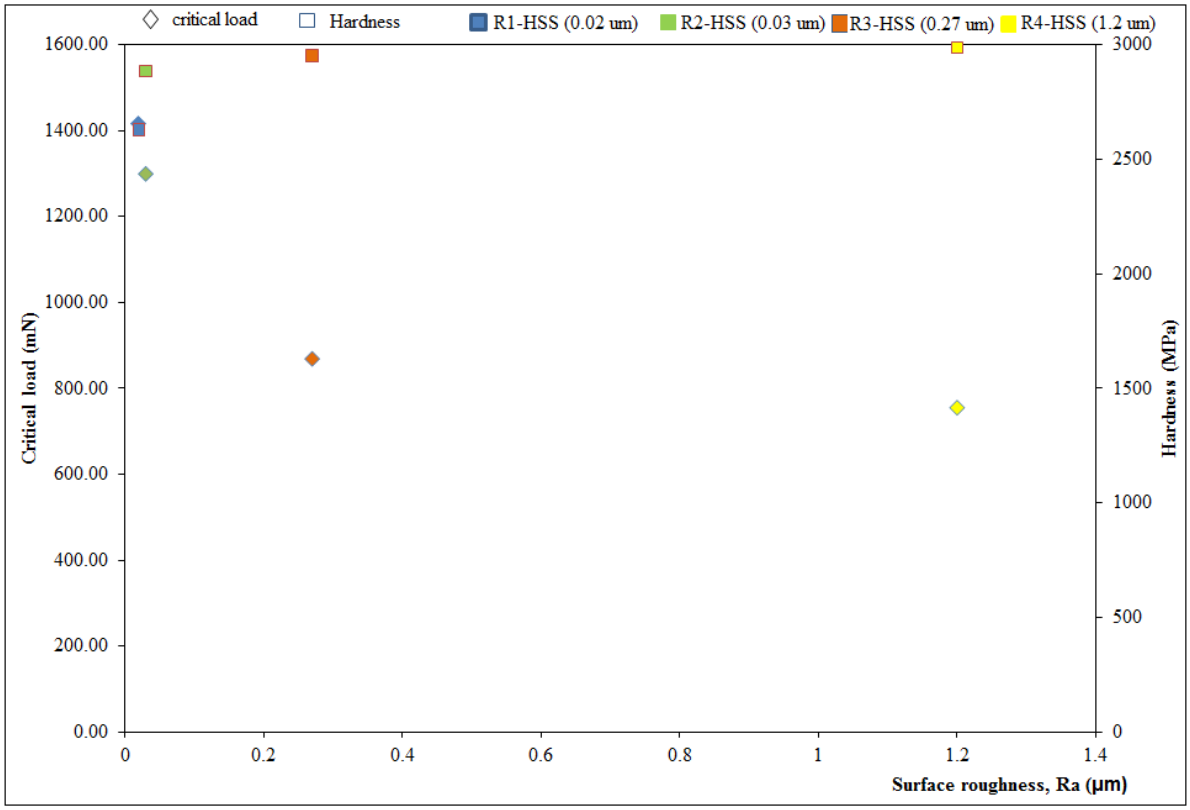

Figure 4.16: Critical loads and hardness of Ti/TiO_2/TiN coating deposited at 200 °C on HSS substrate for different substrate surface condition (surface roughness).

4.3 The effect of annealing on the mechanical properties of the substrate coating systems.

Figure 4.17 shows the FESEM images of coating surface on HSS substrates of as-deposited coating and after annealing at different temperature. The as-deposited coatings had uniformly dense film with no sign of crack or film delamination observed. The coating annealed at 400^0C also presents no sign of crack. However, the color of the coatings changed from violet-bronze to yellow-green color. For coating annealed at 500 °C, no cracks were observed but coating spallation starting to develop. Once the annealing temperature reached 600 °C, film delamination in some area of the coating surface appeared as shown in Figure 4.17 (d). For coating annealed at 500 and 600 °C, the colors of the coating seem to be darker as compared to the as-deposited coating.

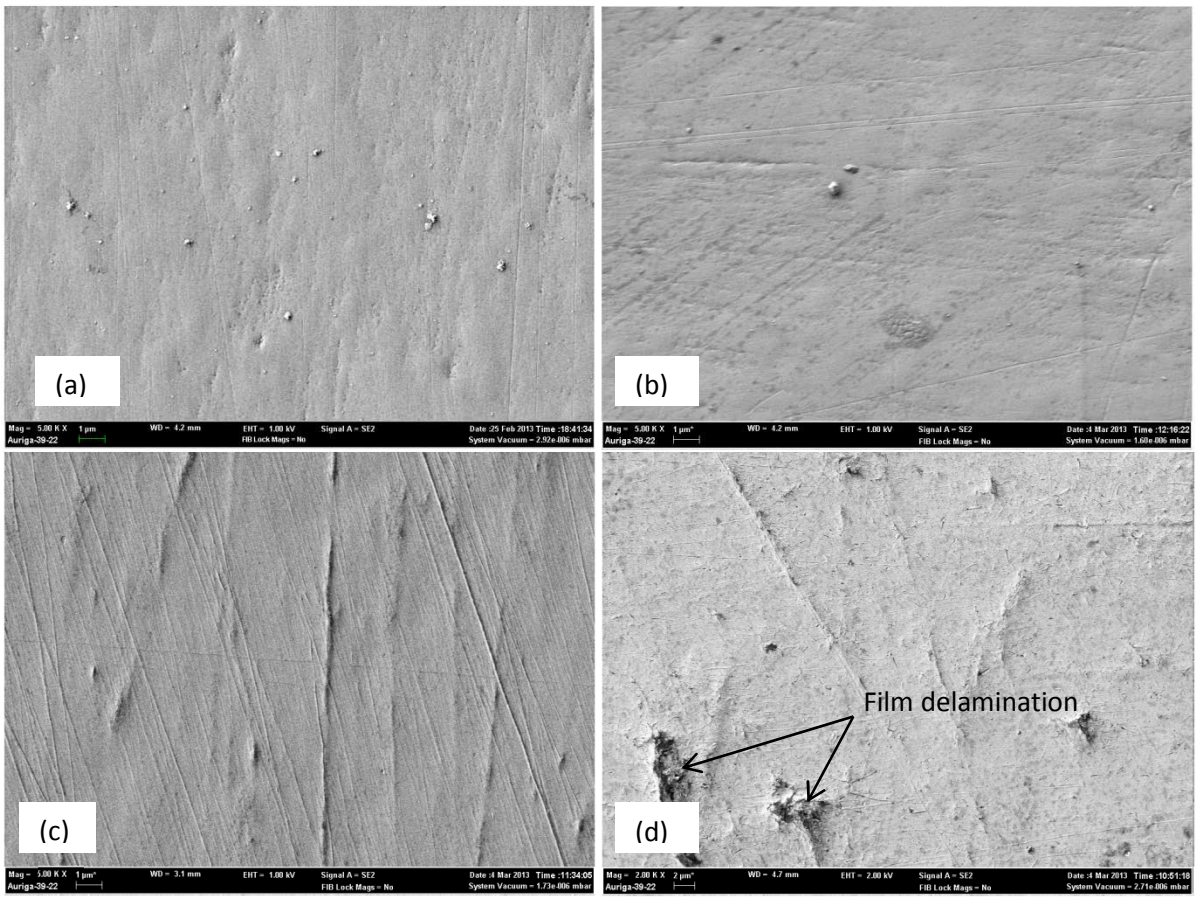

Figure 4.17: FESEM image (top view) of Ti/TiO_2/TiN coatings deposited on HSS substrate after annealing at; (a) as-deposited; (b) 400 °C; (c) 500 °C and; (d) 600 °C.

The X-ray diffraction (XRD) analysis conducted on the as-deposited and annealed samples show a number of peaks which indicates the presence of TiN, TiO_2, Ti and Fe phases (see Figure 4.18). TiN peak was observed at $2\theta = 42.5^0$ oriented along (2 0 0) plane for all samples. For as-deposited coating, TiO_2 peak was detected at $2\theta = 36.9^0$ and belong to (1 0 3) plane. For annealed samples, TiO_2 peak was detected at $2\theta = 37.1^0$ and belong to (1 0 3) plane. The intensity of TiO_2 peaks for annealed samples were lower compared to as-deposited coating. Ti peak for all samples was observed at $2\theta = 40^0$ and strongly oriented in (1 0 1) direction. Fe peak was detected at $2\theta = 44.7^0$ oriented along (1 0 1) plane belonging to the substrate which was visible to all coatings.

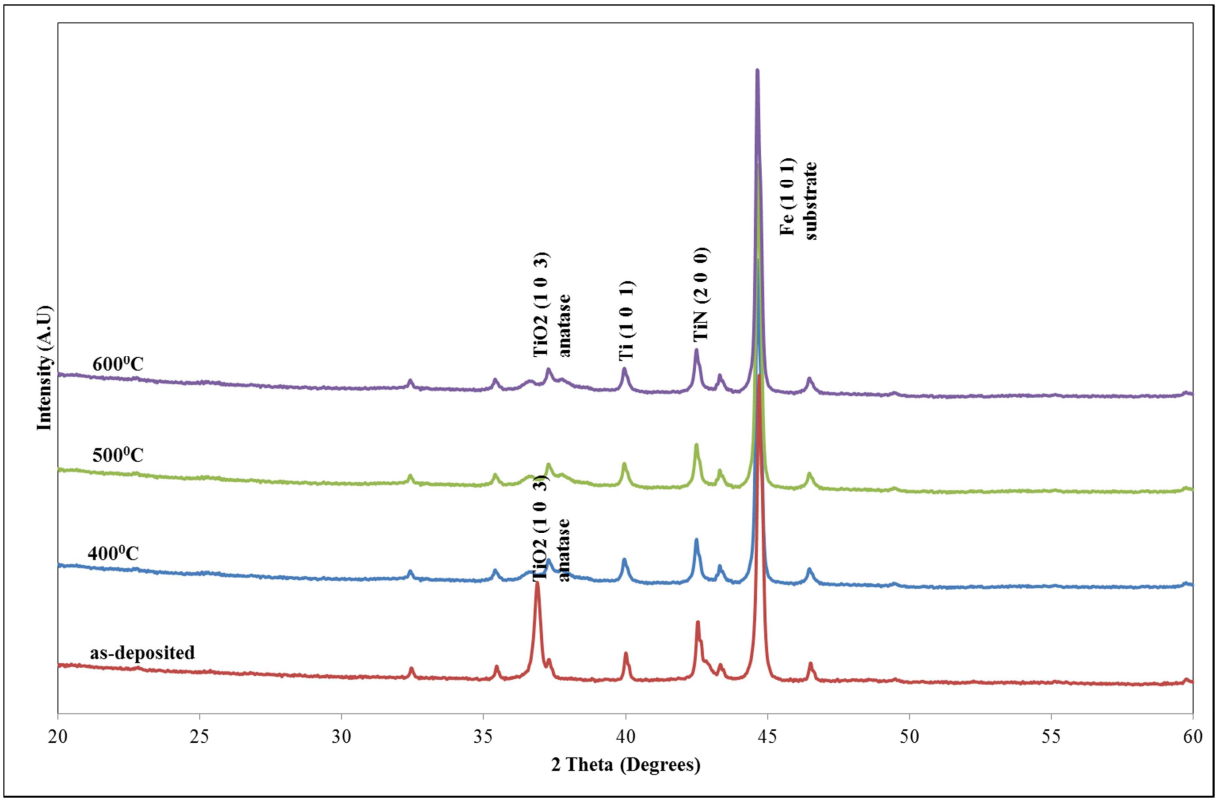

Figure 4.18: XRD patterns of as-deposited and annealed Ti/TiO_2/TiN coatings deposited on HSS substrates.

EDX analysis on the annealed samples revealed higher oxygen contents compared to as-deposited coatings. The atomic-percentage of Ti and nitrogen decreased when the annealing temperature increased. Figure 4.19 shows the summary atomic-percentage of Ti, oxygen and nitrogen in the as-deposited and annealed Ti/TiO_2/TiN coatings on HSS substrates.

Figure 4.20 summarized the critical load and coating hardness of as-deposited and annealed Ti/TiO_2/TiN coatings on HSS substrates. Maximum adhesion strength belonged to the coatings annealed at 500 °C (2154.3 mN). The coatings annealed at 600 °C exhibited lowest adhesion strength of 817.81 mN. The coating hardness increased for coatings annealed at 400 and 500 °C. The hardness values were 2730 MPa and 2700 MPa. Lowest coating hardness value was observed for coating annealed at 600 °C (2586 MPa).

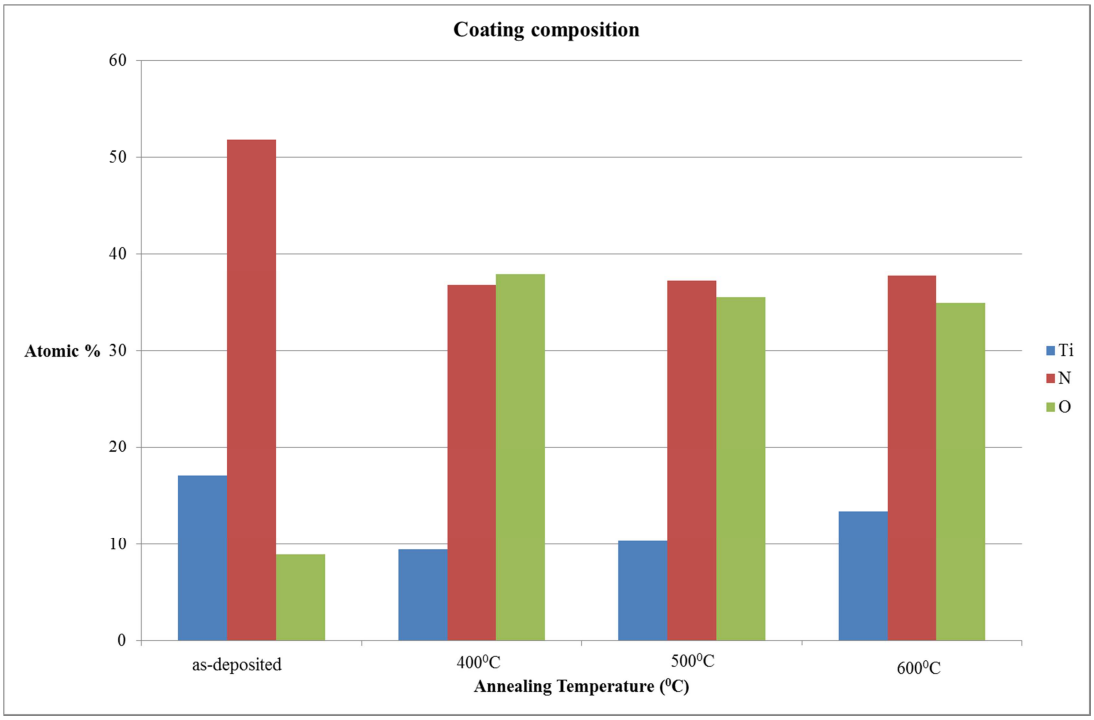

Figure 4.19: Atomic percentages of Ti, N and O in the Ti/TiO_2/TiN coatings after annealing treatment at different anneal temperatures.

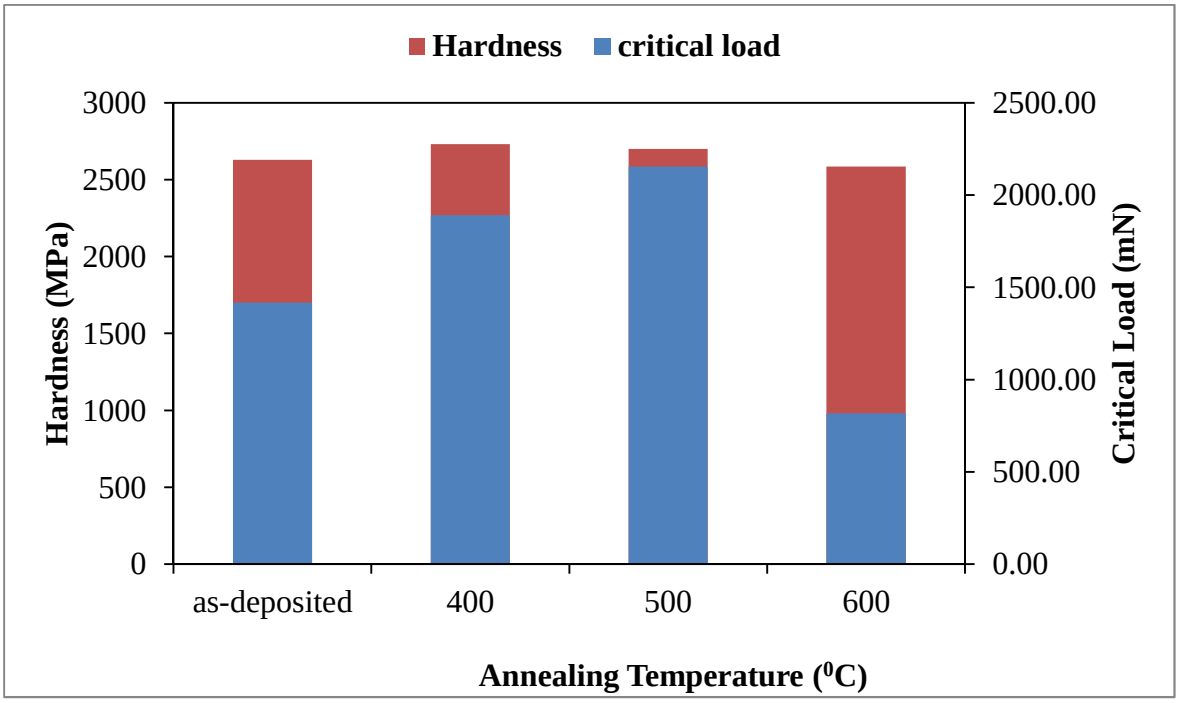

Figure 4.20: Critical loads and hardness values for as-deposited Ti/TiO_2/TiN coating and coating samples after annealing at 400, 500 and 600 °C.

CHAPTER 5

DISCUSSION

5.1 The effect of implementing Ti and TiO_2 as interlayer on adhesion strength improvement of TiN coating.

Many studies have been reported on the adhesion strength of single layer TiN (Larsson et al., 2000; Laugier, 1987; Valli et al., 1985) and Ti/TiN coating systems (Simmonds et al., 1997). In contrast, there have been a few reports on the adhesion strength of multilayer coating particularly Ti/TiO_2/TiN coating systems.

In this present study, TiO_2 films were deposited together with Ti films as interlayer for TiN coating to understand the effect of those interlayer coating on the adhesion strength improvement of commercially used TiN coating. The XRD analysis on Ti/TiO_2/TiN coating proved the present of TiO_2 on the coating. It is found that the TiO_2 coating film deposited on HSS and SS substrate at 200^0C are polycrystalline having anatase phase only. The grown film is found to be crystalline. In order for a crystalline phase to develop, the depositing atom should have sufficient energy to obtain lower energy position which leading to the formation of crystalline phases. High substrate temperature can provide the sufficient energy to develop crystalline phase (Hasan et al., 2010). This may be the reason for the growth of anatase-TiO_2 in the present study.

The results of EDX analysis indicated the present of Ti, TiN and TiO_2 coating layer. The EDX spectrum for all coatings show higher content of Ti compared to nitrogen and oxygen. The lower content of nitrogen and oxygen in the coating may be due to lower working gas pressure (gas flow rate).

The optical microscope analysis of the coating shows dense and uniform film for coating deposited on HSS substrate. The morphologies of the coating deposited on SS substrate show non-uniform film distribution. This may be due to substrate surface condition used during the deposition. Smooth substrate surface may produce uniform film distribution as well as higher adhesion between the coating and the substrate. Small surface features can only be seen at very high magnification using FESEM. The coating layer is made of small grains of hexagonal crystallite of approximately 38.7 nm size which represent TiN coating. The observation was quite differ to results obtained by Carradò et al. (2010) and Gangopadhyay et al. (2010), where the grains size of TiN was found to be 10 nm size.

Further analysis on the coating cross sections reveals compact and dense coating film. The completed growth of coating film produced flakes that are overlapped, arranged as in network which may contribute to enhancement of adhesion strength.

The average coating thickness layer of TiO_2, Ti and TiN measured was 165.2, 504.7 and 174.2 nm, respectively. The coating thicknesses obtained from the deposition were differ to thickness obtained from literature (Carradò et al., 2010; Kusano et al., 1998b) although the deposition parameters were similar. The difference is thought to be due to different size of deposition chamber used and variation in the working pressure during the deposition. Coating thickness deposited on the substrate depends on the deposition parameters which may contribute to variation in thickness for all coating samples. Working gas flow, D.C power, working pressure as well as the ratio of the gas used during deposition were some of the factors that may cause the variation in coating thickness. Higher D.C power will produce thicker coating thickness. Substrates also need to be rotate during the deposition process to ensure uniformity of the coating. In this present work, substrate holder was rotated during deposition of all coating samples to ensure coating uniformity.

In term of adhesion strength, it is generally accepted as an important property in evaluating coating integrity. In order for a coating to be functionality effective, sufficient adhesion are required to avoid coating detachment and failure. TiN coatings have been used in tooling applications to increase the mechanical properties such as wear resistance of the tools and hence increase the tool life. Thus, study on the TiN coating deposited on tool steel materials such as HSS and SS have done intensively. Most of the study concentrated on the adhesion of the coating on the substrate. Adhesion strength of coating deposited by various techniques such as plasma spraying and magnetron sputtering are well studied. Improvements on the adhesion strength of TiN coating have been done by using metallic coating as an interlayer. However, there is no standard value by which comparison can be made objectively. Different studies report different value of adhesion strengths. Most of the study report on the adhesion strength of single layer TiN coating and TiN coating with a metallic coating interlayer.

Laugier (1987) reported that single layer TiN coating produced by PVD technique with thickness of 3 μm tended to spall at critical load of 1.2 kgf. Valli et al. (1985) claimed to achieve a critical normal load of 31 N for 0.8 μm TiN coating. The adhesion strength improvement of TiN coating has been reported by Helmersson et al. (1985) with the use of titanium interlayer. However, Valli et al. reported an opposite result from Helmersson et al. They reported that 0.3 μm titanium interlayer was found to decrease the coating adhesion.

In the present study, Ti/TiO_2/TiN coatings were deposited on HSS and SS. Ti and TiO_2 interlayer were deposited between TiN coating and the substrate to enhance the adhesion strength. The adhesion strength of TiN, Ti/TiN and Ti/TiO_2/TiN coating deposited on HSS and SS substrate were determined by scratch test. Ti/TiN coatings show good adhesion compared to single layer TiN for both HSS and SS substrate. The adhesion strength improvement proved that Ti interlayer has beneficial effect on the adhesion strength of single layer TiN coating. The results were in agreement with the findings by Helmersson et al.

(1985) on the adhesion of the films increased with the use of an intermediate layer of pure titanium in between TiN coating and substrates.

$Ti/TiO_2/TiN$ coating exhibited higher adhesion compared to Ti/TiN and single layer TiN coating, thus suggesting the beneficial effect of TiO_2 intermediate coating layer on the adhesion strength. Similar observation was obtained by Kusano et al. (1998b) where the adhesion of TiO_2 /Ti/TiN coating exhibit superior adhesion compared to TiN coating.

The improved of the adhesion strength with the presence of Ti interlayer can be explained on the basis of better bonding between the titanium interlayer and the substrate and also better bonding between the titanium layer and the TiN coating. It is also suggested that the Ti interlayer acts as a graded interface that can evades the abrupt change in composition at the sharp interface between a coating and metal substrate. Better adhesion strength of $Ti/TiO_2/TiN$ can be explained by the basis that by making a compositional change in the interface transition region gradient and smooth, both chemical and mechanical bonding are expected to be improved.

Analysis on the internal stress of TiN, Ti/TiN and $Ti/TiO_2/TiN$ coating revealed compressive internal stress for all coatings. The internal stress of $Ti/TiO_2/TiN$ was found to be smaller compared to TiN and Ti/TiN coatings. A lower internal stress of $Ti/TiO_2/TiN$ coating is thought to cause a better adhesion in addition to stronger chemical bonding.

Evaluation on the hardness of the $Ti/TiO_2/TiN$ coating shows a decrease in value compared to hardness of TiN coating. The lower hardness of $Ti/TiO_2/TiN$ coating is thought to be due to inter-diffusion between oxide and nitride layers.

5.2 The effect of sputtering parameter on the $Ti/TiO_2/TiN$ adhesion strength.

The effects of sputtering parameters have been reported to influence the adhesion strength of the coatings. The substrate temperature, coating thickness and substrate surface condition are the parameters which affect the adhesion of the coating. Helmersson et al. (1985) reported on the increased of TiN coating adhesion with increased in substrate temperature. Perry (1983) reported on the critical load increased with increased coating thickness. Steinmann et al. (1987) suggested that the critical load of the coating depends on the substrate roughness.

In this study, $Ti/TiO_2/TiN$ coatings deposited at higher deposition temperature exhibits higher value of critical load. The critical load increases as the deposition temperature increases from 50 to 200 °C. At deposition temperature 250 °C, it is notice that the value of critical load slightly decrease compared to deposition at 250 °C. The optimum adhesion strength of $Ti/TiO_2/TiN$ coatings can be obtained at temperature of 200 °C. The reason for higher adhesion strength at high deposition temperature is thought due to an increase in strength of both chemical and mechanical bonding of coatings to substrate. The hardness of $Ti/TiO_2/TiN$ coating increases as the deposition temperature increases from 200 to 250 °C. The hardness was higher compared to single layer TiN coating.

The study on the effect of TiO_2 coating thickness on the $Ti/TiO_2/TiN$ coating adhesion strength shows an increase in the critical load as the TiO_2 coating thickness increases. The value of critical load kept increasing as the TiO_2 coating thickness increase. No optimum value of TiO_2 coating thickness was observed. Thus, the study on the optimum TiO_2 coating thickness can be done in future to obtain the maximum adhesion strength of $Ti/TiO_2/TiN$ coating systems. A similar pattern was also observed for the measured coating hardness. The hardness of the coating increases as the TiO_2 coating thickness increases.

The study on the substrate surface condition was conducted by varying the surface roughness of the substrate used. The critical load of Ti/TiO_2/TiN coating deposited on HSS decreases with the increases of substrate surface roughness, Ra. Better coating adhesion was observed for coating deposited on smooth substrate surface. The critical load clearly dependence on the substrate surface roughness. It is believed that although all the substrates were coated during the same treatment prior to deposition process, the adhesive properties can vary since the efficiency of the cleaning operation is influence by the surface roughness.

5.3 The effect of annealing on the mechanical properties of the substrate coating systems.

The results on the annealing treatment of Ti/TiO_2/TiN coating show that the mechanical properties of the coating improved significantly up to certain annealing temperature. It is noticed that highest critical load and hardness were obtained for coatings annealed at 500 °C. The lowest critical load was observed for coating annealed at 600 °C. It is believed that during annealing, the coating interacted with oxygen in air environment and forming denser TiO_2 coating films. It can be noticed that from the EDX analysis, the atomic percentages of oxygen increase for annealed coating samples. However, annealing the coatings at higher temperature (600 °C) yielded to partial film detachment which is the reason of decreasing in adhesion strength. Therefore, the overall results in the present study suggest that 500 °C is probably the optimum annealing temperature to achieve the best adhesion strength and coating hardness.

CHAPTER 6

CONCLUSIONS AND RECOMMENDATIONS

6.1 Conclusions

The introduction of TiO_2 coating layer as an intermediate layer has great influence on the adhesion strength of the TiN coating systems. Deposition temperature, coating thickness, substrate surface condition and post-heat treatment of the coating does affect the adhesion strength of the coating. The results and findings in this thesis are concluded as follows;

1. TiO_2 coating film deposited D.C magnetron sputtering on HSS and SS substrate at 200 °C and discharge power of 150 W was polycrystalline having anatase phase.
2. Ti/TiO_2/TiN coating exhibits higher adhesion strength compared to Ti/TiN and single layer TiN coating, thus suggesting the beneficial effect of TiO_2 intermediate coating layer on the adhesion strength.
3. The hardness of the Ti/TiO_2/TiN coating shows a decrease in value compared to hardness of TiN coating.
4. Ti/TiO_2/TiN coatings deposited at higher deposition temperature exhibits higher value of critical load. The optimum adhesion strength of Ti/TiO_2/TiN coatings can be obtained at temperature of 200 °C.
5. The adhesion strength of Ti/TiO_2/TiN coating increases as the TiO_2 coating thickness increases.
6. The adhesion strength of Ti/TiO_2/TiN coating deposited on HSS decreases with the increases of substrate surface roughness. Better coating adhesion was observed for coating deposited on smooth substrate surface.

7. It was found that annealing Ti/TiO_2/TiN coating at 500 °C yielded highest adhesion strength and coating hardness. The annealed coating at 600 °C revealed film delamination and exhibited lowest adhesion strength.

6.2 Recommendations

1. The mechanical properties of Ti/TiO_2/TiN coating in the present study were defined in terms of adhesion strength evaluation using scratch test and coating hardness using micro-hardness tester. Investigation of the mechanical properties of the coating by using other mechanical characterizations such as sliding tests may help in further understanding of mechanical behavior of the coating systems.
2. The study on the effect of TiO_2 coating thickness can be extended to evaluate the optimum coating thickness for maximum adhesion strength.

REFERENCES

A

Adachi, S., & Nakata, K. (2007). Improvement of adhesive strength of Ti–Al plasma sprayed coating. *Surface and Coatings Technology, 201*(9–11), 5617-5620.

al., V. G. e. (1994). Recent development in the laser spallation technique to measure the interface strength and its relationship to interface toughness with application to metal/ceramics, ceramic/ceramic and ceramic/polymer interface. *Adhesion Measurement of Films and Coatings*, 367 - 401.

Arai, T., Fujita, H., & Watanabe, M. (1987). Evaluation of adhesion strength of thin hard coatings. *Thin Solid Films, 154*(1–2), 387-401.

B

Bergmann, E., Vogel, J., & Simmen, L. (1987). Failure mode analysis of coated tools. *Thin Solid Films, 153*(1–3), 219-231.

Bishop, C. A. (2011). 9 - Adhesion and Adhesion Tests *Vacuum Deposition onto Webs, Films and Foils (Second Edition)* (pp. 177-185). Oxford: William Andrew Publishing.

Boustie, M., Auroux, E., & Romain, J.-P. (2000). Application of the laser spallation technique to the measurement of the adhesion strength of tungsten carbide coatings on superalloy substrates. *The European Physical Journal - Applied Physics, 12*(01), 47-53.

Bull, S. J. (1991). Failure modes in scratch adhesion testing. *Surface and Coatings Technology, 50*(1), 25-32.

Burnett, P. J., & Rickerby, D. S. (1988). The scratch adhesion test: An elastic-plastic indentation analysis. *Thin Solid Films, 157*(2), 233-254.

Bushroa, A. R., Masjuki, H. H., & Muhamad, M. R. (2011). Parameter Optimization of Sputtered Ti Interlayer Using Taguchi Method. *International Journal of Mechanical and Materials Engineering (IJMME), Vol.6 (2011)*(2), 140-146.

C

Carradò, A., Schmerber, G., & Pelletier, H. (2010). Structural and mechanical investigations of magnetron sputtering TiO_2/Ti/TiN multilayer films on Si(100) substrate. *Journal of Coatings Technology and Research, 7*(6), 821-829.

Chalker, P. R., Bull, S. J., & Rickerby, D. S. (1991). A review of the methods for the evaluation of coating-substrate adhesion. *Materials Science and Engineering: A, 140*(0), 583-592.

Chopra, K. L. (1969). Thin Film Phenomena (pp. 319): McGraw-Hill, New York.

D

Diao, D. F., Kato, K., Hokkirigawa, K. (1994). Fracture mechanisms of ceramic coatings in indentation. *Journal of Tribology, 116*(4), 860-869.

F

Fella, R., & Holleck, H. (1991). Preparation and properties of metastable TiC/SiC PVD coatings for wear protection. *Materials Science and Engineering: A, 140*(0), 676-681.

G

Gangopadhyay, Acharya, S., Chattopadhyay, R., & Paul, S. (2010). Effect of Substrate Bias Voltage on Structural and Mechanical Properties of Pulse DC Magnetron Sputtered TiN-MoS_x Composite Coatings. *Vacuum, 84*(6), 843-850.

Gerth, J., & Wiklund, U. (2008). The influence of metallic interlayers on the adhesion of PVD TiN coatings on high-speed steel. *Wear, 264*, 885-892.

Gupta, V., Argon, A. S., Parks, D. M., & Cornie, J. A. (1992). Measurement of interface strength by a laser spallation technique. *Journal of the Mechanics and Physics of Solids, 40*(1), 141-180.

H

Hagerman, E., Shim, J., Gupta, V., & Wu, B. (2007). Evaluation of laser spallation as a technique for measurement of cell adhesion strength. *J Biomed Mater Res A 82*(4), 852-860.

Hasan, M. M., Haseeb, A. S. M. A., Masjuki, H. H., & Saidur, R. (2010). Adhesion and Wear Behavior Of Nanostructured Titanium Oxide Thin Films. *International Journal of Mechanical and Materials Engineering (IJMME), 5*(1), 5-10.

Hedenqvist, P., Olsson, M., Jacobson, S., & Söderberg, S. (1990). Failure mode analysis of TiN-coated high speed steel: In situ scratch adhesion testing in the scanning electron microscope. *Surface and Coatings Technology, 41*(1), 31-49.

Helmersson, U., Johansson, B. O., Sundgren, J.-E., Hentzell, H. T. G., & Billgren, P. (1985). Adhesion of titanium nitride coatings on high-speed steels. *Journal of Vacuum Science & Technology A: Vacuum, Surfaces, and Films, 3*(2), 308-315.

I

Ikeda, R., Uchiyama, T., Cho, H., Ogawa, T., & Takemoto, M. (2006). An advanced method for measuring the residual stress of deposited film utilizing laser spallation technique. *Science and Technology of Advanced Materials, 7*(1), 90.

J

Jacobsson, R., & Kruse, B. (1973). Measurement of adhesion of thin evaporated films on glass substrates by means of the direct pull method. *Thin Solid Films, 15*(1), 71-77.

Jaworski, R., Pawlowski, L., Roudet, F., Kozerski, S., & Petit, F. (2008). Characterization of mechanical properties of suspension plasma sprayed TiO_2 coatings using scratch test. *Surface and Coatings Technology, 202*(12), 2644-2653.

Je, J. H., Gyarmati, E., & Naoumidis, A. (1986). Scratch adhesion test of reactively sputtered TiN coatings on a soft substrate. *Thin Solid Films, 136*(1), 57-67.

Jindal, P. C., Quinto, D. T., & Wolfe, G. J. (1987). Adhesion measurements of chemically vapor deposited and physically vapor deposited hard coatings on WC-Co substrates. *Thin Solid Films, 154*(1–2), 361-375.

K

Kasetsart, J. (2008). Phase Characterization of TiO_2 Powder by XRD and TEM. *Nat. Sci.* (42), 357-361.

Kobayashi, A., Jain, A., Gupta, V., & Kireev, V. (2004). Study on the interface strength of zirconia coatings by a laser spallation technique. *Vacuum, 73*(3–4), 533-539.

Kusano, E., Kitagawa, M., Kuroda, Y., Nanto, H., & Kinbara, A. (1998a). Adhesion and hardness of compositionally gradient TiO_2/Ti/TiN, ZrO_2/Zr/ZrN, and TiO_2/Ti/Zr/ZrN coatings. *Thin Solid Films, 334*, 151-155.

Kusano, E., Kitagawa, M., Kuroda, Y., Nanto, H., & Kinbara, A. (1998b). Adhesion and hardness of compositionally gradient TiO_2/Ti/TiN, ZrO_2/Zr/ZrN, and TiO_2/Ti/Zr/ZrN coatings. *Thin Solid Films, 334*(1–2), 151-155.

L

Larsson, M., Olsson, M., Hedenqvist, P., & Hogmark, S. (2000). Mechanisms of coating failure as demonstrated by scratch and indentation testing of TiN coated HSS. *Surface Engineering, 16*(5), 436-444.

Laugier, M. (1981). The development of the scratch test technique for the determination of the adhesion of coatings. *Thin Solid Films, 76*(3), 289-294.

Laugier, M. T. (1984). An energy approach to the adhesion of coatings using the scratch test. *Thin Solid Films, 117*(4), 243-249.

Laugier, M. T. (1987). Adhesion and toughness of protective coatings. *Journal of Vacuum Science & Technology A: Vacuum, Surfaces, and Films, 5*(1), 67-69.

M

Marco, J. F., Cuesta, A., Gracia, M., Gancedo, J. R., Panjan, P., & Hanžel, D. (2005). Influence of a deposited TiO_2 thin layer on the corrosion behaviour of TiN-based coatings on iron. *Thin Solid Films, 492*(1–2), 158-165.

Marshall, D. B., & Evans, A. G. (1984). Measurement of adherence of residually stressed thin films by indentation. I. Mechanics of interface delamination. *Journal of Applied Physics, 56*(10), 2632-2638.

Mattox, D. M. (2010). *Handbook of Physical Vapor Deposition (PVD) Processing*: William Andrew.

N

Niemi, E., Korhonen, A. S., Harju, E., & Kauppinen, V. (1986). Comparison of wear characteristics and properties of TiN-coated gear cutting hobs. *Journal of Vacuum Science & Technology A: Vacuum, Surfaces, and Films, 4*(6), 2763-2767.

Nsongo, T., & Gillet, M. (1995). Adhesion characterization of titanium and titanium nitride thin coatings on metals using the scratch test. *International Journal of Adhesion and Adhesives, 15*(3), 191-196.

O

Ollendorf, H., Schneider, D., Schwarz, T., Kirchhoff, G., & Mucha, A. (1996). A comparative study of the mechanical properties of TiN coatings using the non-destructive surface acoustic wave method, scratch test and four-point bending test. *Surface and Coatings Technology, 84*(1–3), 458-464.

P

Park, J. H., & Sudarshan, T. S. (2001). *Chemical Vapor Deposition*: Asm International.

Perry, A. J. (1981). Adhesion studies of ion-plated TiN on steel. *Thin Solid Films, 81*(4), 357-366.

Perry, A. J. (1983). Scratch adhesion testing of hard coatings. *Thin Solid Films, 107*(2), 167-180.

S

Schulz, A., Stock, H. R., & Mayr, P. (1991). Physical vapour deposition of TiN hard coatings with additional electron beam heat treatment. *Materials Science and Engineering: A, 140*(0), 639-646.

Simmonds, M. C., Van Swygenhoven, H., Pflüger, E., Savan, A., Hauert, R., Knoblauch, L., & Mikhailov, S. (1997). Magnetron sputter deposition and characterisation of Ti/TiN, Au/TiN and MoSX/Pb multilayers. *Surface and Coatings Technology, 94–95*(0), 490-494.

Steinmann, P. A., & Hintermann, H. E. (1985). Adhesion of TiC and Ti(C,N) coatings on steel. *Journal of Vacuum Science & Technology A: Vacuum, Surfaces, and Films, 3*(6), 2394-2400.

Steinmann, P. A., Tardy, Y., & Hintermann, H. E. (1987). Adhesion testing by the scratch test method: The influence of intrinsic and extrinsic parameters on the critical load. *Thin Solid Films, 154*(1–2), 333-349.

Szalkowska, E., Gluszek, J., Masalski, J., & Tylus, W. (2001). Structure and protective properties of TiO_2 coatings obtained using the sol-gel technique. *Journal of Materials Science Letters, 20*(6), 495-497.

V

Valli, J., & Mäkelä, U. (1987). Applications of the scratch test method for coating adhesion assessment. *Wear, 115*(1–2), 215-221.

Valli, J., Makela, U., Matthews, A., & Murawa, V. (1985). TiN coating adhesion studies using the scratch test method. *Journal of Vacuum Science & Technology A: Vacuum, Surfaces, and Films, 3*(6), 2411-2414.

von Stebut, J., Rezakhanlou, R., Anoun, K., Michel, H., & Gantois, M. (1989). Major damage mechanisms during scratch and wear testing of hard coatings on hard substrates. *Thin Solid Films, 181*(1–2), 555-564.

W

Wang J., Nancy R. Sottos and Richard L. Weaver. (2004). Tensile and mixed-mode strength of a thin film-substrate interface under laser induced pulse loading. *Journal of the Mechanics and Physics of Solids, 52*(5), 999-1022.

Wang, Y. K., Cheng, X. Y., Wang, W. M., Gu, X. H., Xia, L. F., Lei, T. C., & Liu, W. H. (1995). Microstructure and properties of (Ti, Al) N coating on high speed steel. *Surface and Coatings Technology, 72*(1–2), 71-77.

Weaver, C. (1975). Adhesion of thin films. *Journal of Vacuum Science and Technology, 12*(1), 18-25.

Wen Jun Chou, G. P. Y. a. J. H. H. (2002). Mechanical properties of TiN thin film coatings on 304 stainless steel substrates. *Surface and Coatings Technology*, *149*, 7-13.

Westergård, R., Axén, N., Wiklund, U., & Hogmark, S. (2000). An evaluation of plasma sprayed ceramic coatings by erosion, abrasion and bend testing. *Wear*, *246*(1–2), 12-19.

Y

Yamamoto, Shuji, Ichimura, & Hiroshi. (1992). Effects of intrinsic properties of TiN coatings on acoustic emission behavior at scratch test. *Journal of Materials Research, 7*(8), 2240-2247.

Z

Zhang, S., & Zhu, W. (1993). TiN coating of tool steels: A review. *Journal of Materials Processing Technology*, *39*, 165-177.